

Marc-André Delsuc

- Aujourd'hui à l'IGBMC de Strasbourg (9 ans)
 - ▶ après Gif-sur-Yvette (10 ans) et Montpellier (15 ans)
 - ▶ chimie-orga - peptides - protéines - IDP
- Intérêts:
 - ▶ IDP - PolyProlines - Récepteur Androgène
- Méthodes
 - RMN
 - méthodologie - processing
 - FT-MS *depuis peu*
 - 2D FT-ICR - processing - top-down
 - processing / analyse *depuis toujours*
 - Analyse de Fourier
 - Compressed Sensing
 - Analyse statistique



NMR Principles

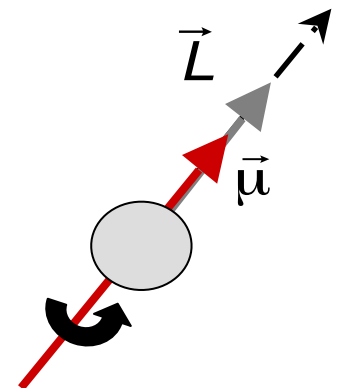
*from observation to
structural information*

*Marc-André Delsuc
Renafobis - 2018*



Nuclear Magnetic Resonance

- Spectroscopy of the magnetic properties of the nuclei of atoms



Nuclear Magnetic Resonance

- Spectroscopy of the magnetic properties of the nuclei of atoms

- Some atom nucleus have a spin $\neq 0$

- | | |
|---|--------------------------------------|
| ▶ ^1H spin $\frac{1}{2}$ \equiv the proton | ▶ ^{19}F spin $\frac{1}{2}$ |
| ▶ ^2H spin 1 low abund. | ▶ ^{31}P spin $\frac{1}{2}$ |
| ▶ ^{13}C spin $\frac{1}{2}$ low abund. | ... |
| ▶ ^{15}N spin $\frac{1}{2}$ low abund. | |

the most interesting
to the biologist

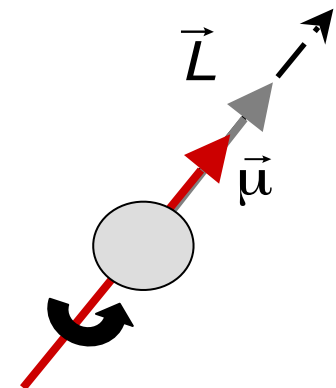
- What is the spin ???

$$\left(\beta mc^2 + \sum_{k=1}^3 \alpha_k p_k c \right) \psi(\mathbf{x}, t) = i\hbar \frac{\partial \psi(\mathbf{x}, t)}{\partial t}$$

- appears as the solution of the Dirac equation
 - ▶ Schrödinger + Relativity
- an intrinsic property of particles (*and black holes*)
 - ▶ as the mass or the charge
- carries a momentum
 - ▶ magnetic momentum - angular momentum

$\vec{\mu}$

\vec{L}

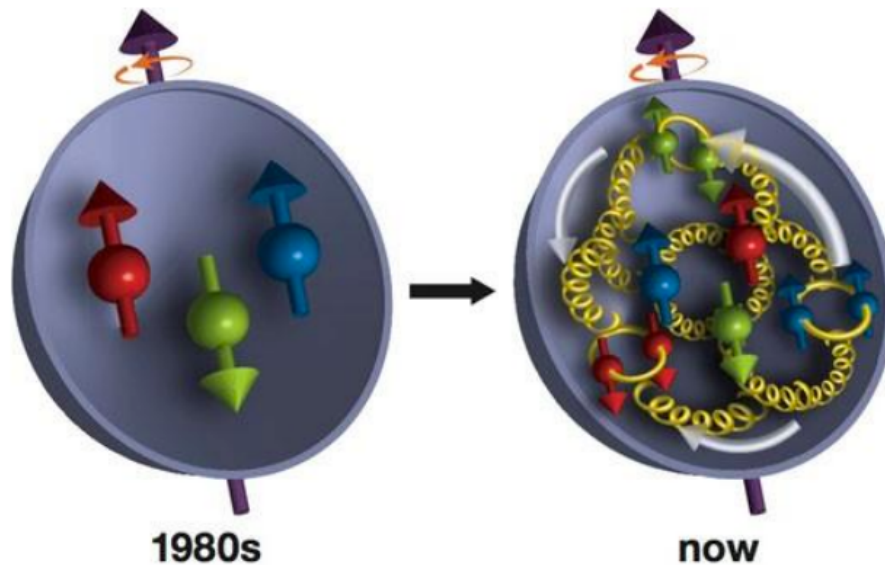


Nuclear Magnetic Resonance

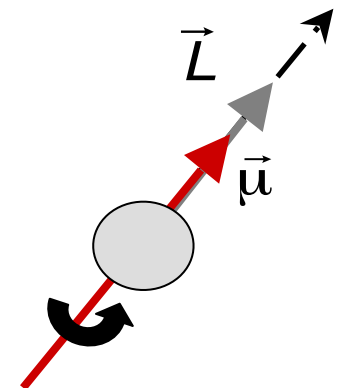
- Spectroscopy of the magnetic properties of the nuclei of atoms

How Did The Proton Get Its Spin?

Mon, 04/03/2017 - 11:01am Comments by Department of Energy, Office of Science

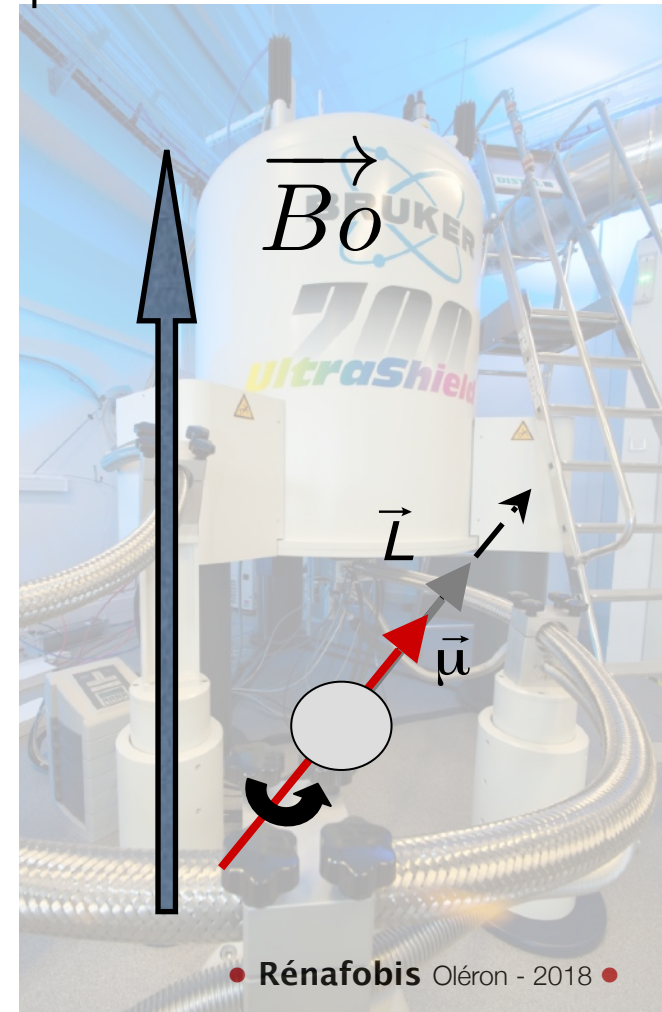
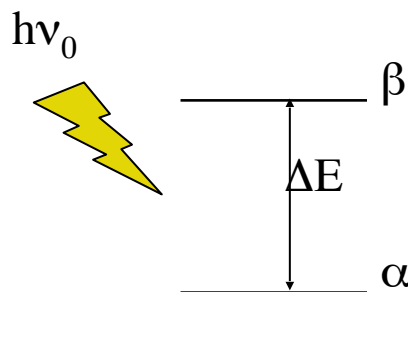
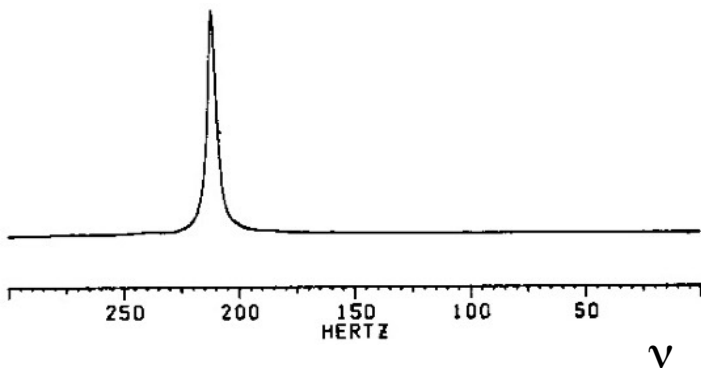


In the 1980s, scientists discovered that a proton's three valence quarks (red, green, blue) account for only a fraction of the proton's overall spin. More recent measurements have revealed that gluons (yellow corkscrews) contribute as much as or possibly more than the quarks. Photo courtesy of Brookhaven National Laboratory



Nuclear **Magnetic** Resonance

- Spectroscopy of the magnetic properties of the nuclei of atoms
 - In presence of a strong magnetic field B_0 , a spin n presents $2n+1$ different energy states, so a spin $\frac{1}{2} \Rightarrow 2$ states
 - Energy difference ΔE
 - ▶ determines the transition frequency
 - ▶ is proportional to B_0



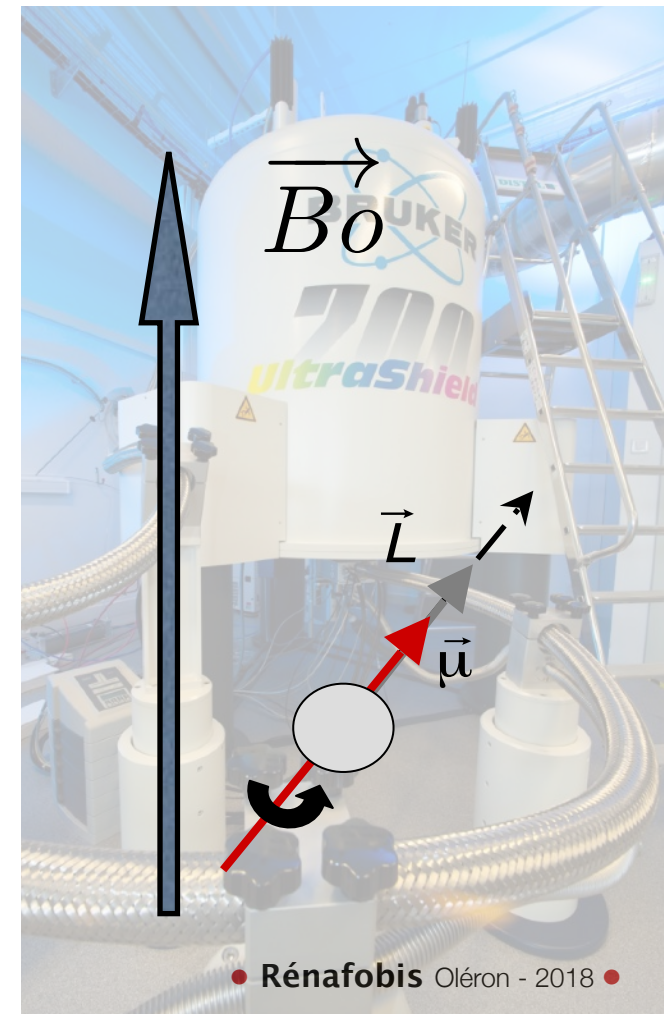
Nuclear **Magnetic** Resonance

- Spectroscopy of the magnetic properties of the nuclei of atoms

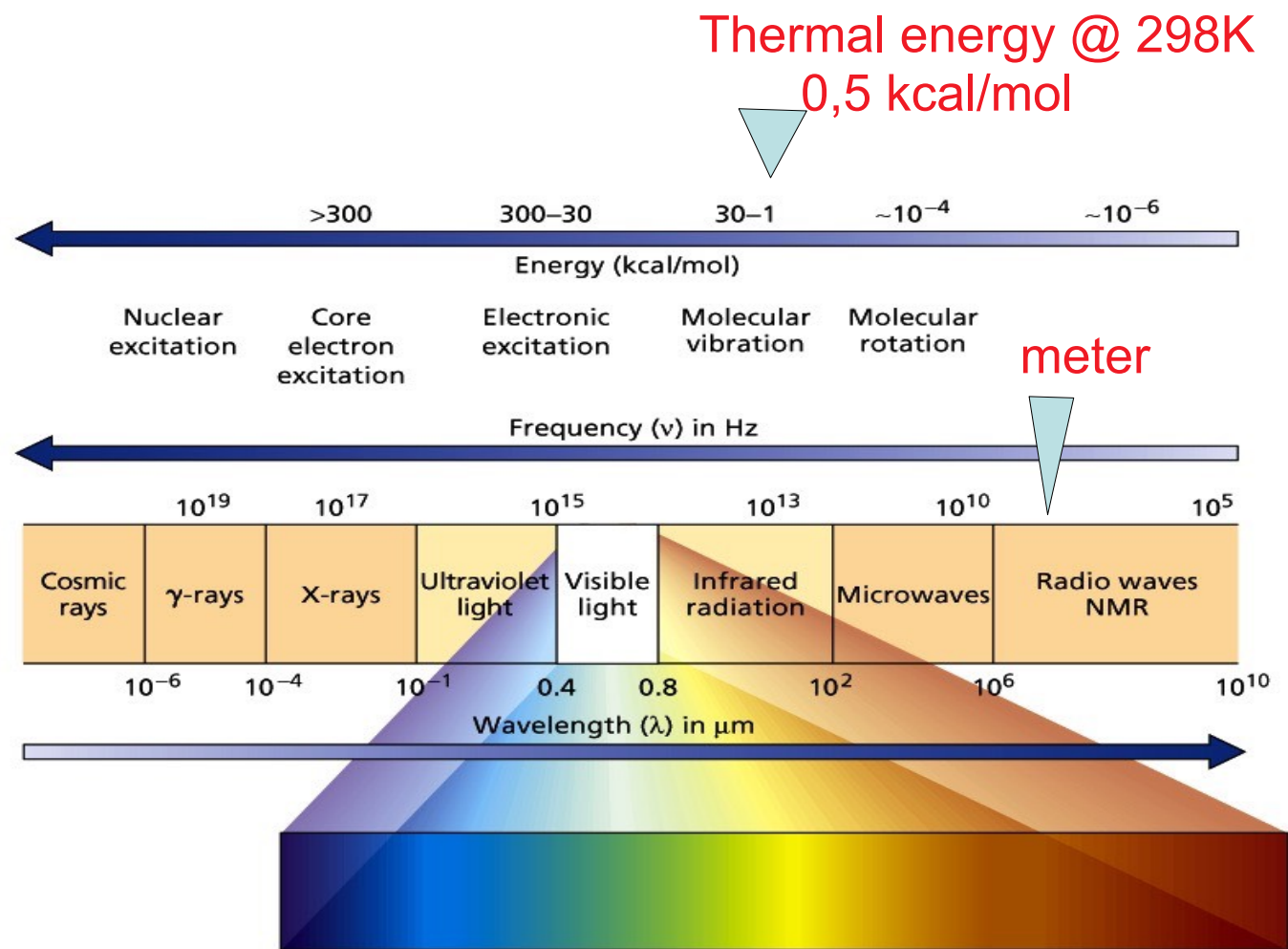
$$E = \hbar\nu \quad \nu = \gamma|B_0|$$

- with γ depending on nucleus type

- ▶ ^1H spin $\frac{1}{2}$ 800 MHz
- ▶ ^2H spin 1 low abund. 123 MHz
- ▶ ^{13}C spin $\frac{1}{2}$ low abund. 200 MHz
- ▶ ^{15}N spin $\frac{1}{2}$ low abund. 80 MHz
- ▶



NMR is a very low energy spectroscopy



Energy

$$E = \hbar \gamma B_0$$

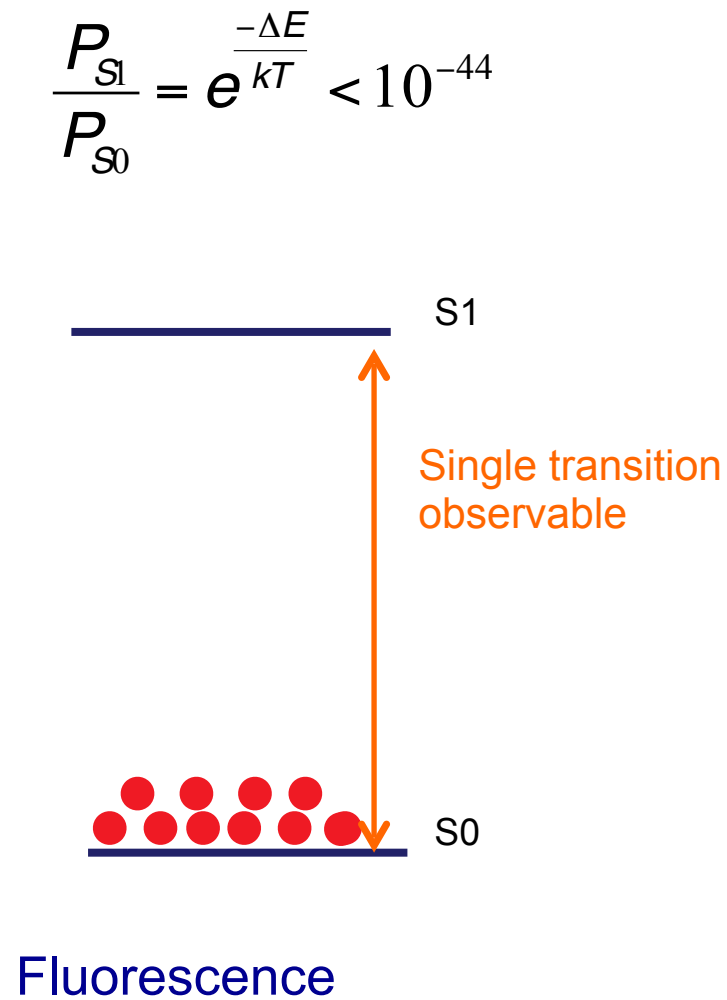
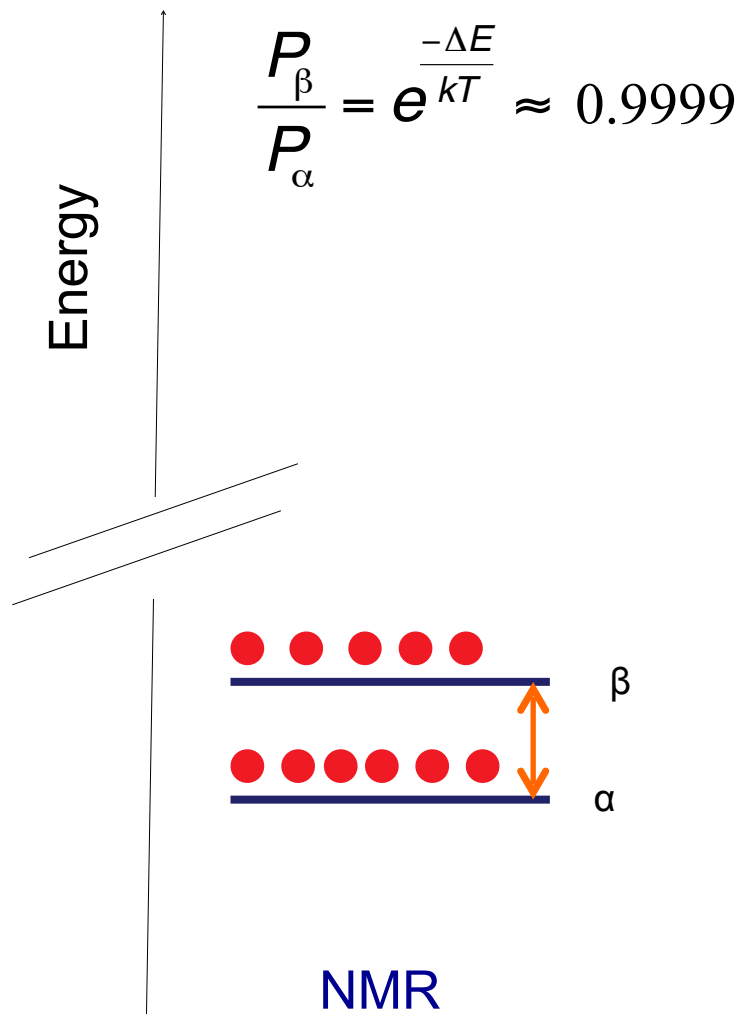
Frequency

$$\nu = 2\pi^{-1} \gamma B_0$$

Wavelength

$$\lambda = \frac{2\pi c}{\gamma B_0}$$

Low-energy = low sensitivity

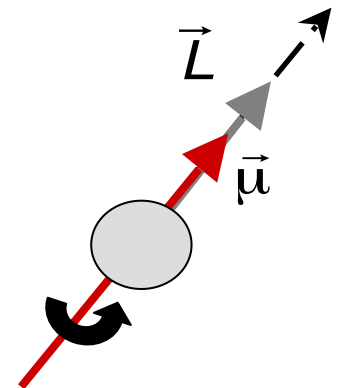


From B Kieffer

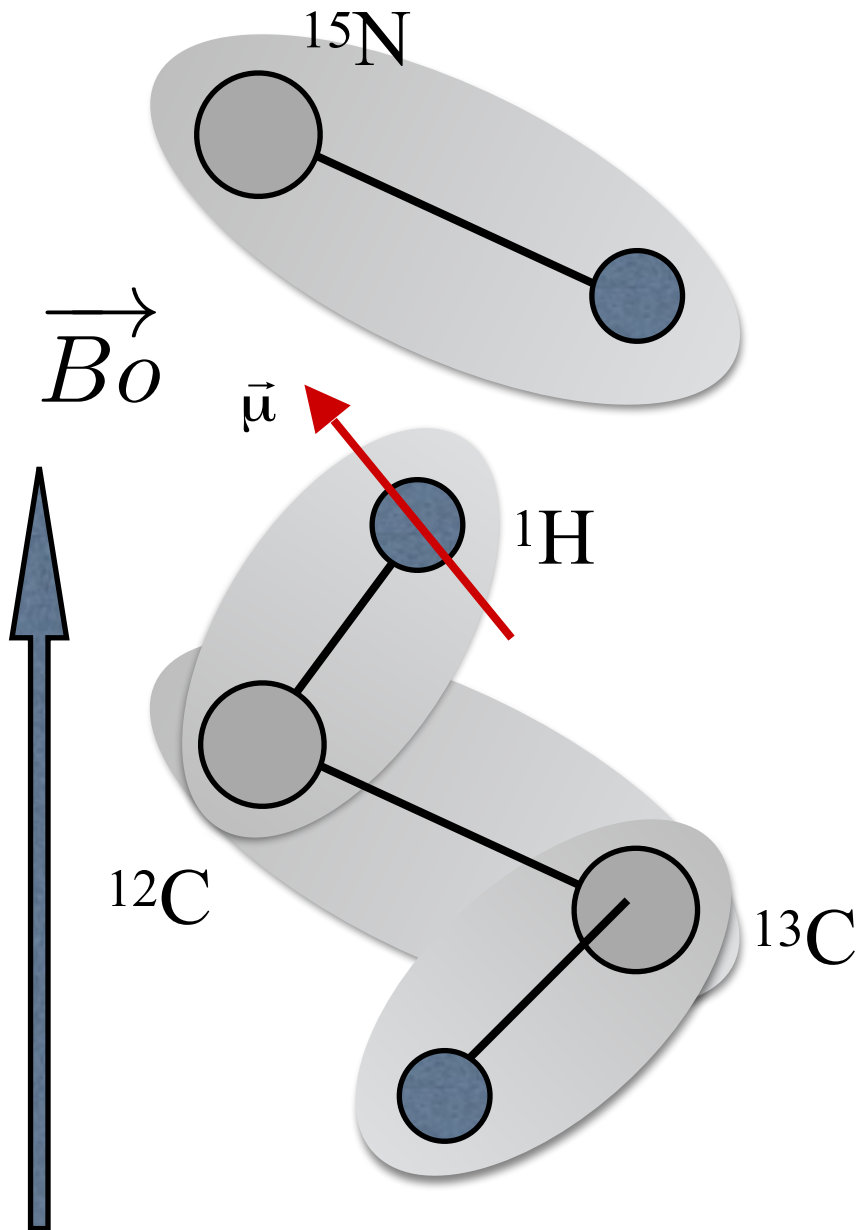
Nuclear Magnetic **Resonance**

- Spectroscopy of the magnetic properties of the nuclei of atoms
- The Quantum Resonance
 - ▶ phase **coherence** of the wave functions of the different particules
- observed / used in
 - ▶ LASERS
 - ▶ Quantum Computers
 - ▶ NMR
- characterized by
 - ▶ strange quantum effects
 - ▶ coherence transfers
 - ▶ decoherence limits life time
 - ▶ enhanced sensitivity

carry home message:
NMR effect is an intrinsic Quantum effect
it is complicated!



Spins in the Field...



- nuclear spins interact with
 - other nuclear spins
 - molecular orbitals
 - ▶ local
 - ▶ nearby
 - electronic spins
 - ...
- act as perfect spies
 - no impact on molecular phenomenon
- and perfect reporters
 - will react to anything

Spins in the Field...



- In NMR EVERYTHING is rotating
 - in physical space
 - in quantum space
 - rotating in a rotating frame
⇒ Precession
- + ALL interactions are depending strongly on orientation
 - molecular axis vs B_0
 - spin-spin axis vs B_0
⇒ Tensor algebra

Phenomenon

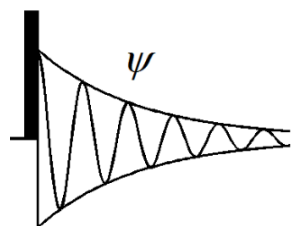
- Chemical-Shift
 - resonance frequency
- Spin-Spin interaction
 - many effects J, D, RDC, NOE...
- Relaxation
 - *decoherence* of the quantum states
 - TWO main effects
 - decoherence of resonance: loss of signal: T_2
 - return to initial steady state: recovery: T_1
 - ...
- Measure by impulse response

The NMR observables... on a simple molecule

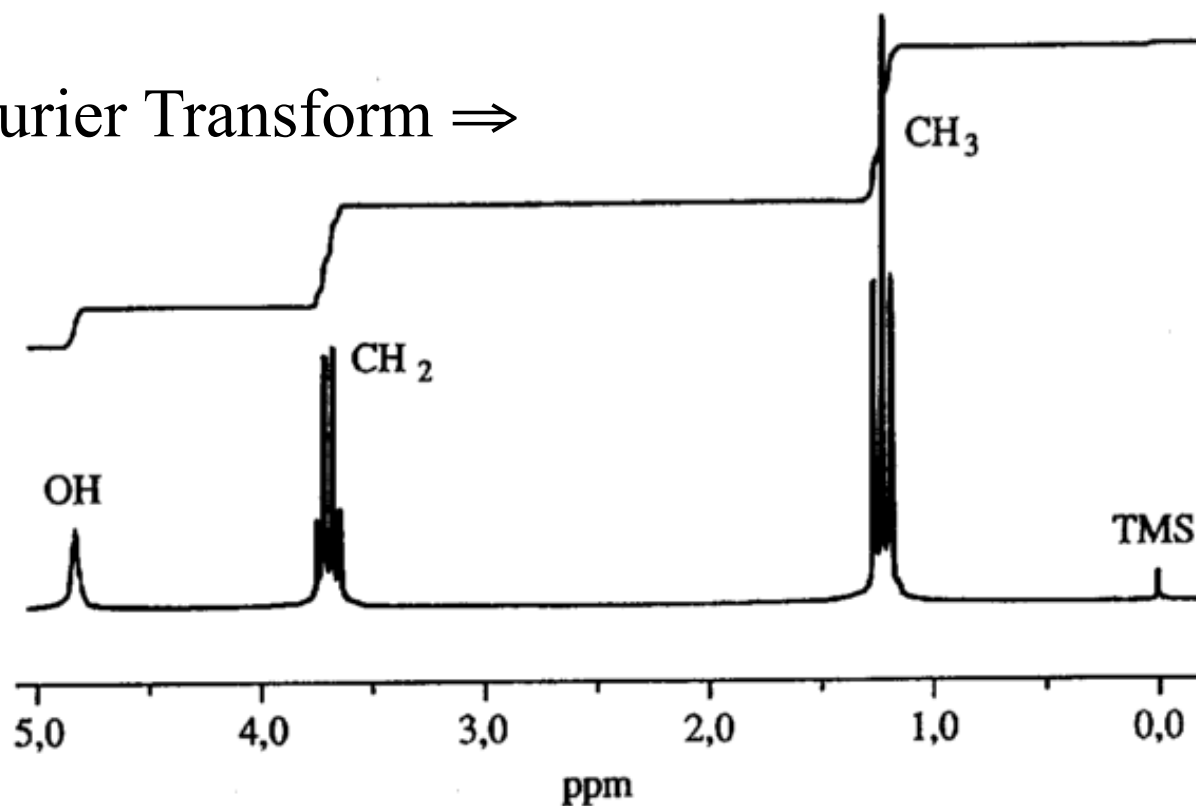
- Ethanol ^1H spectrum



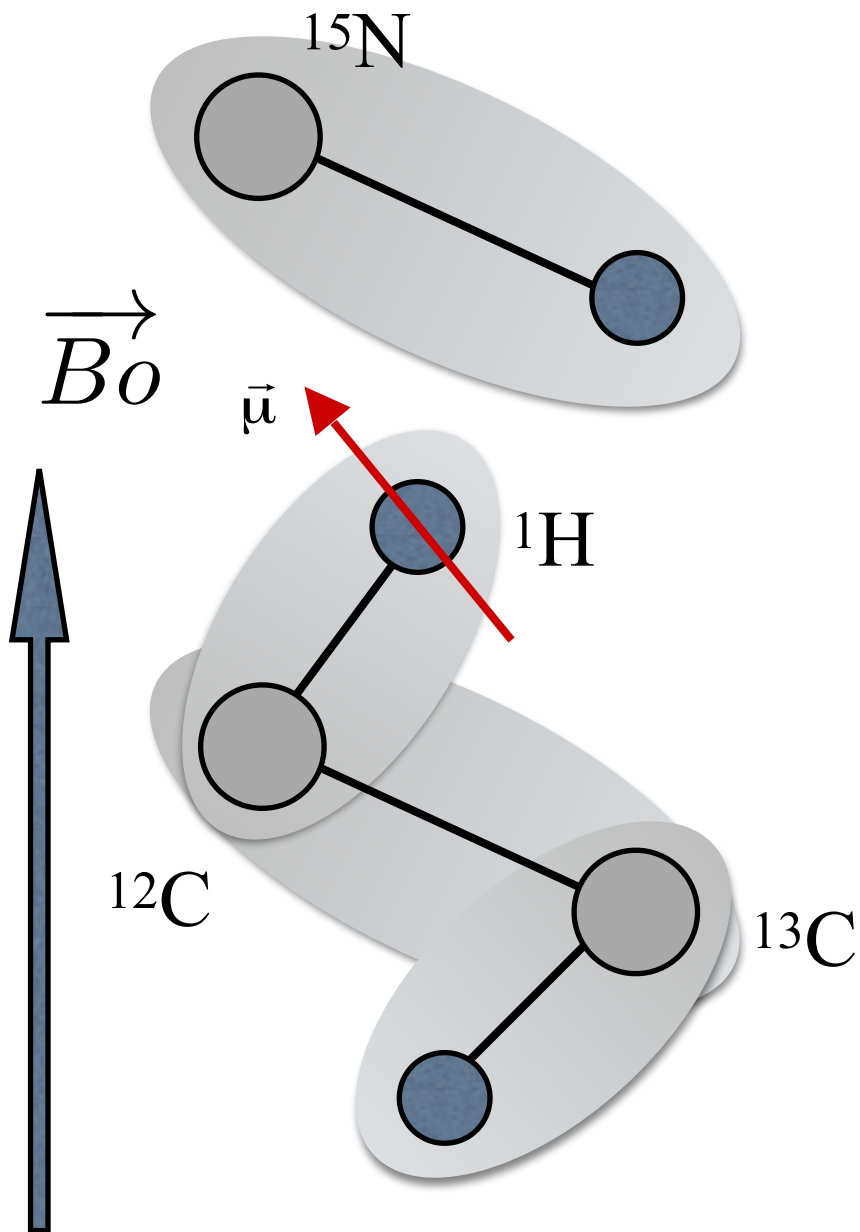
Record spin impulse response *aka* resonance



Apply Fourier Transform \Rightarrow



Chemical Shift



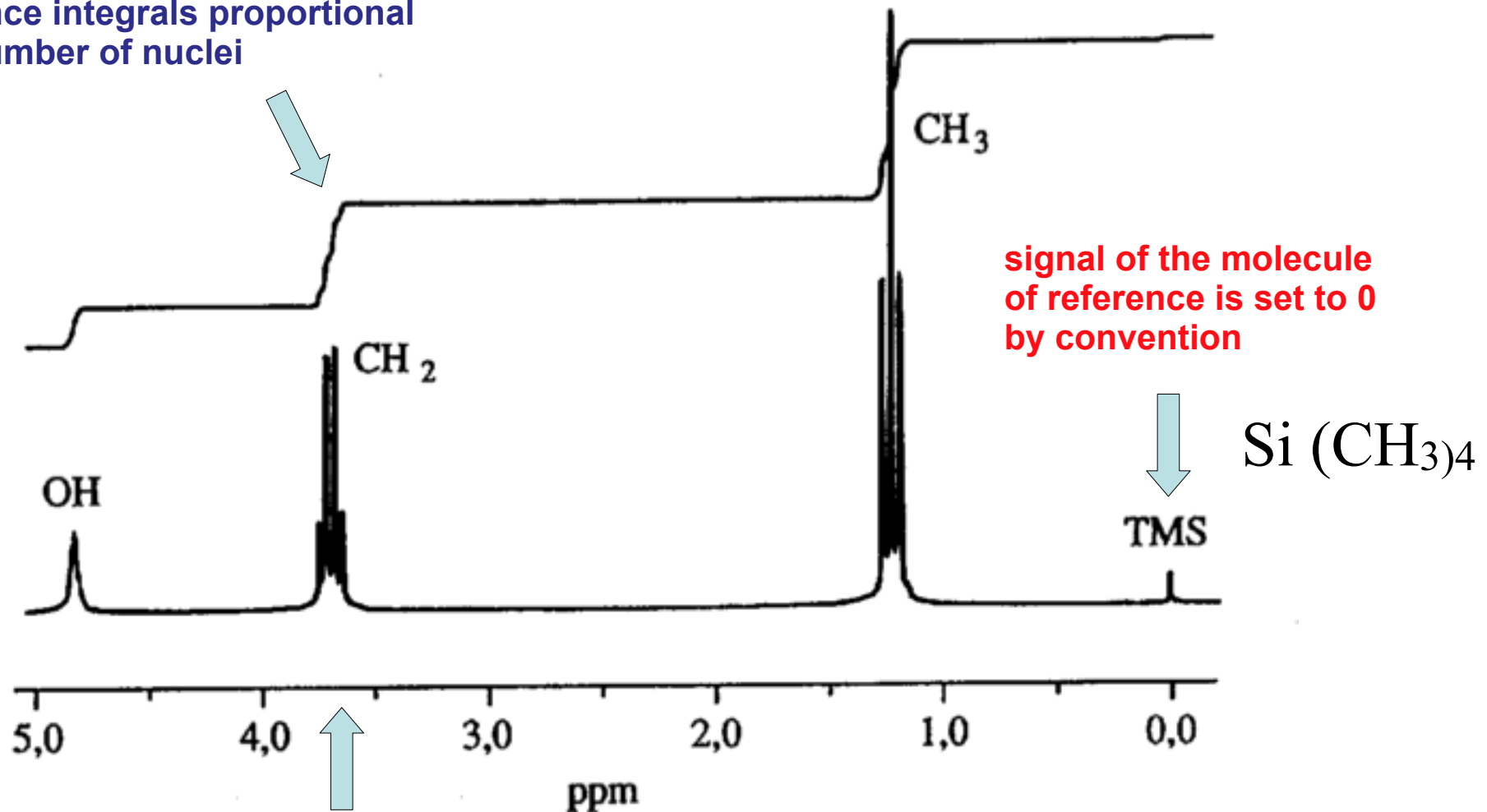
- CS depends strongly on molecular orientation vs B_0
- in liquids all values are averaged
 - only mean value is observed
 - in solids \Rightarrow wide lines
- isotropic CS is affected by shielding of the orbitals
 \Rightarrow *chemical shift*
- effect proportional to B_0
 \Rightarrow ratio (ppm) indep. of B_0

The NMR observables... on a simple molecule

- Ethanol ^1H spectrum

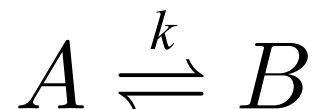


Resonance integrals proportional
to the number of nuclei



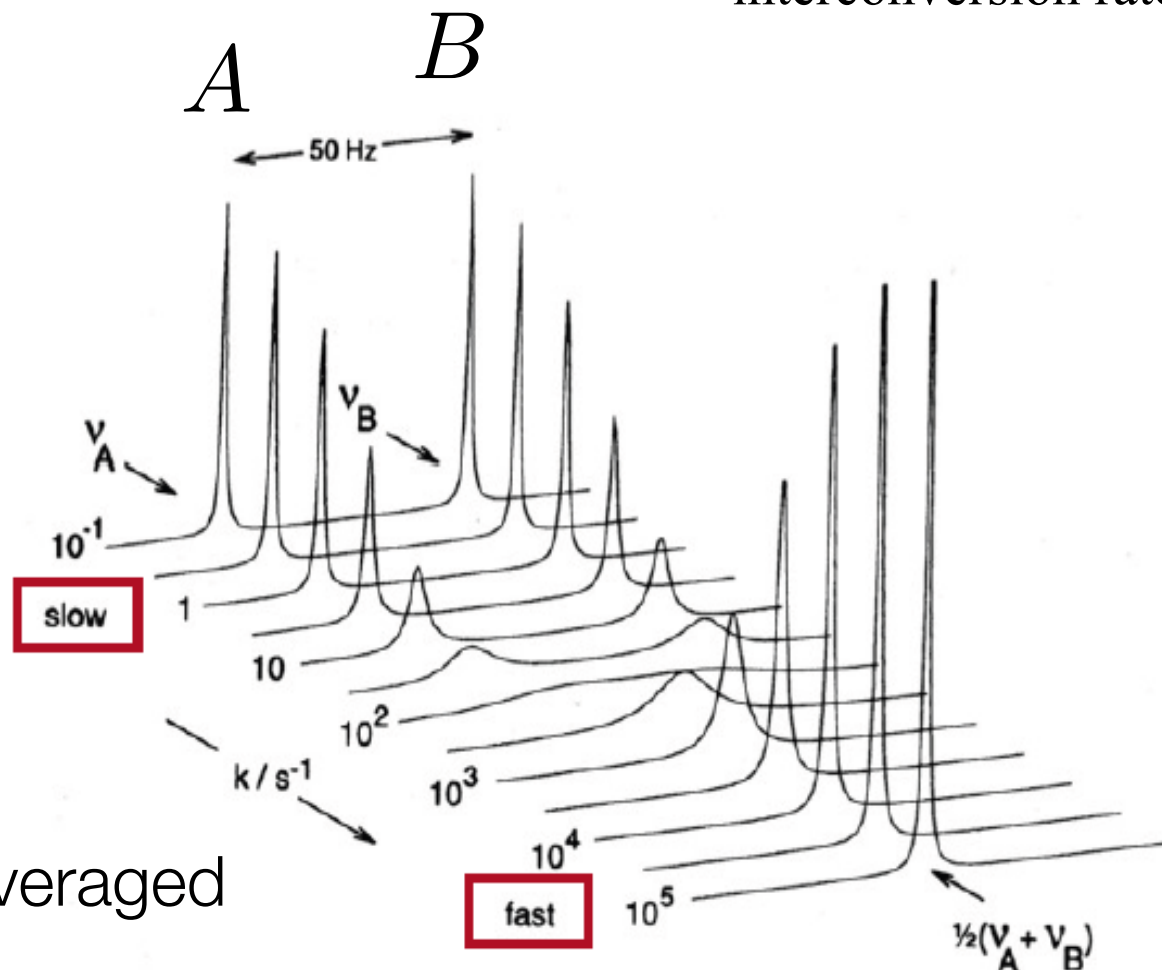
frequency depends on chemical environment
=> Chemical shifts

Averaging properties of NMR



k : characteristic
interconversion rate

- True for *any* NMR observable
- coalescence depends *very much* on observable
 - \neq life-time
 - \neq frequency difference
 - \neq interconversion rate



- in NMR EVERYTHING is averaged

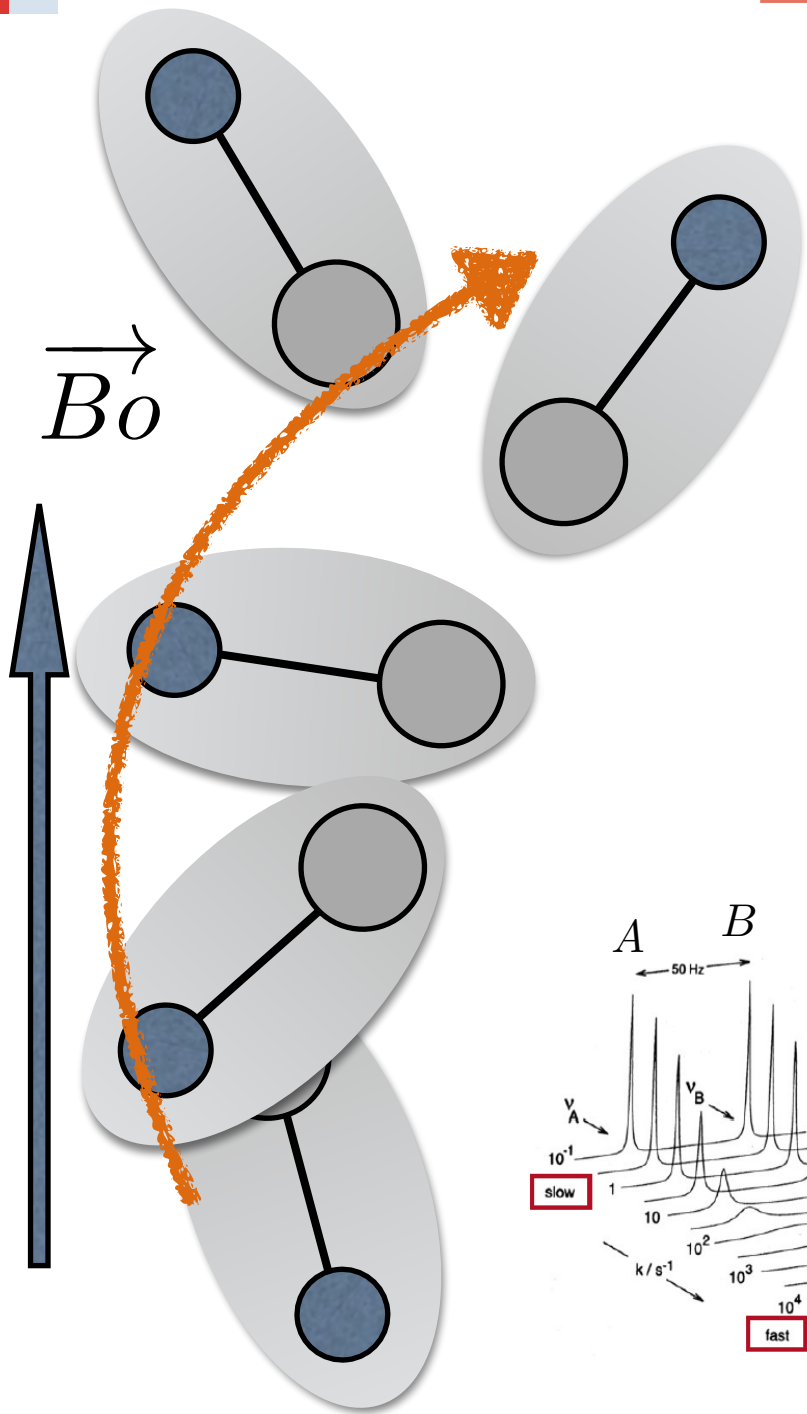
- over time

- over molecules

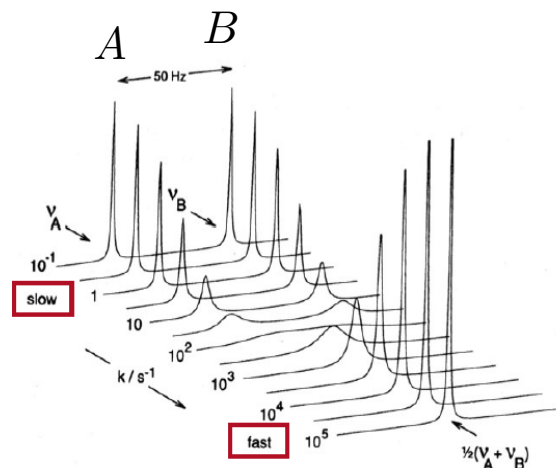
double averaging

$$\frac{c_A \nu_A + c_B \nu_B}{c_A + c_B}$$

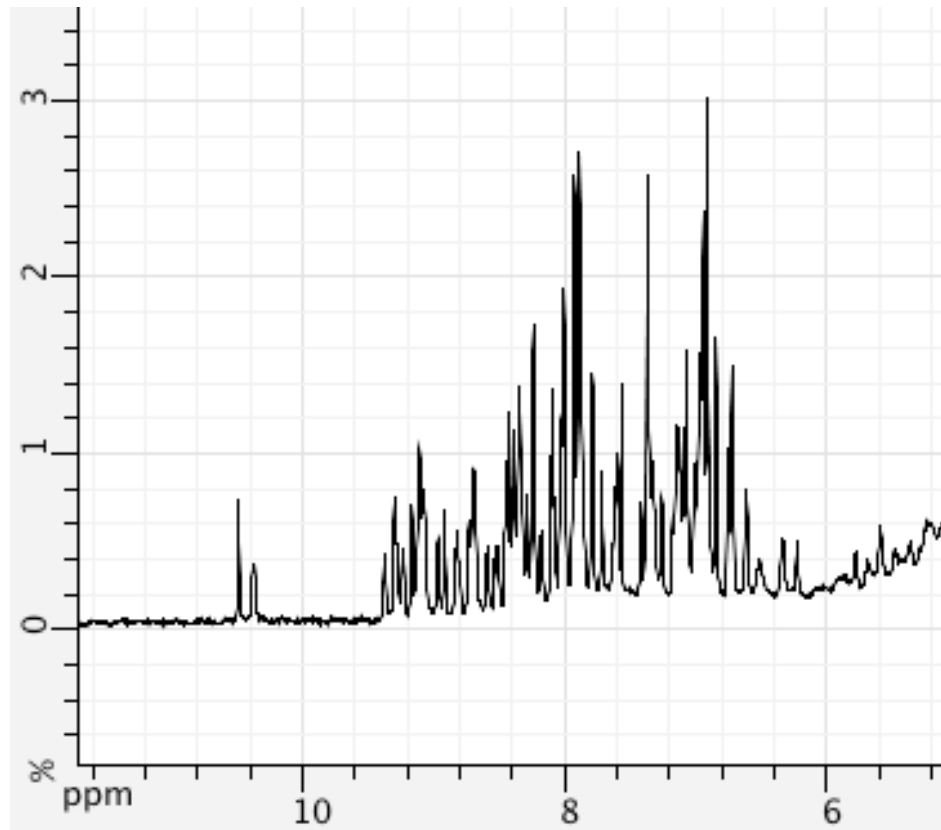
Chemical Shift



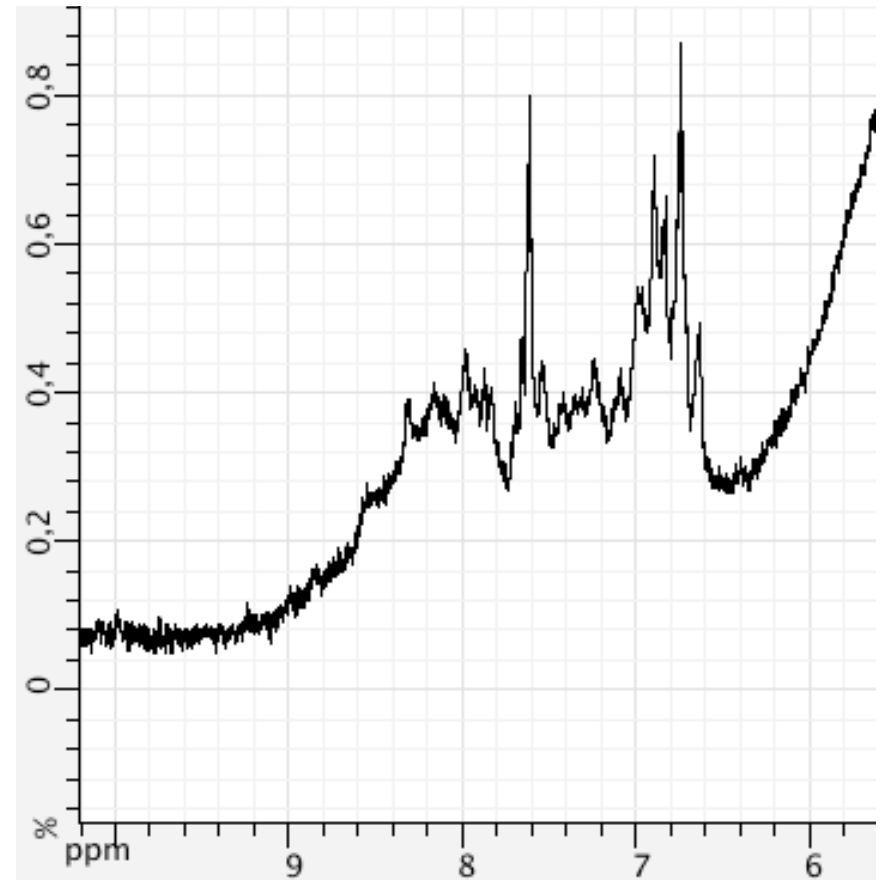
- In **liquids** during the measure, the molecules *tumble* and take successively the CS value of each orientation
- if *tumbling* is fast (small molecules) a sharp line is observed at mean CS value
- if *tumbling* is not so fast, the lines widen
- if in **solid** all CS appear \Rightarrow wide lines



effect of molecular size

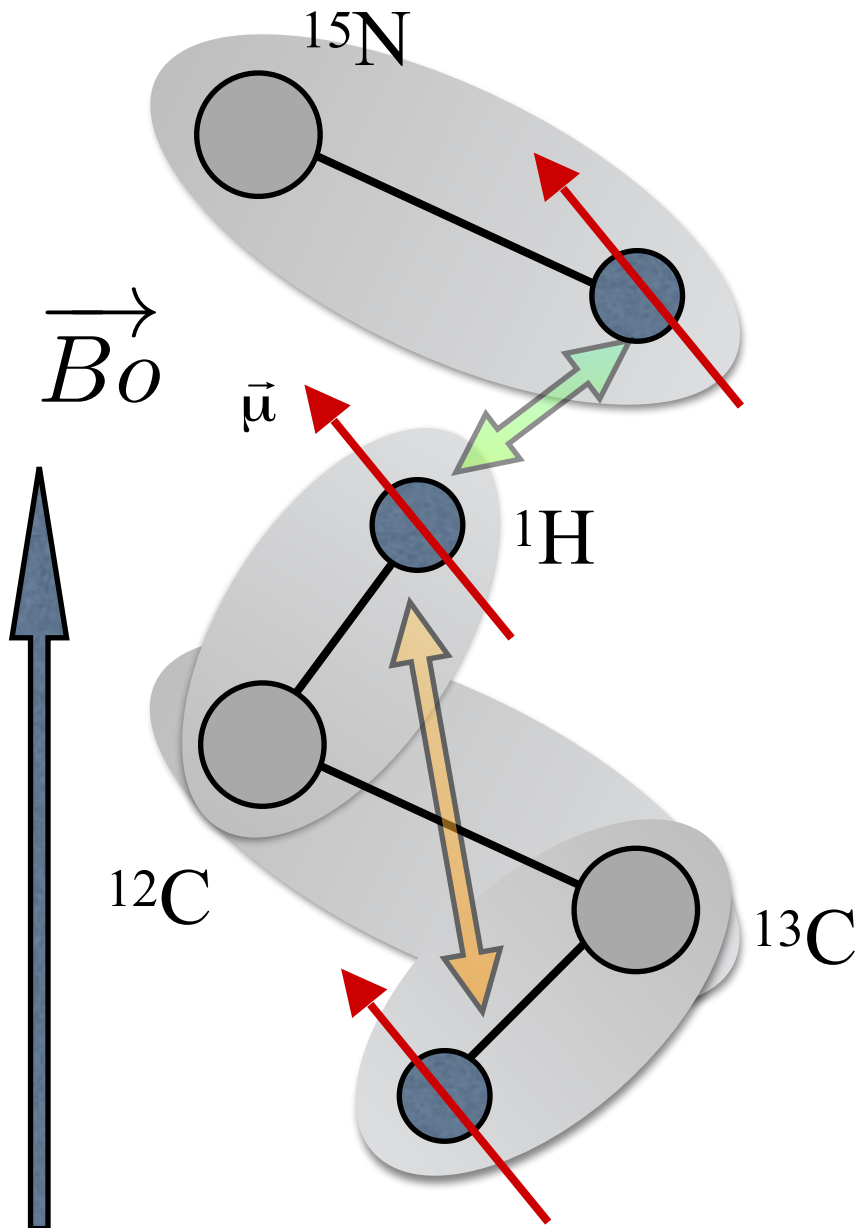




GB1 (~6 kDa)



LBD RXR Dimer (~50 kDa)

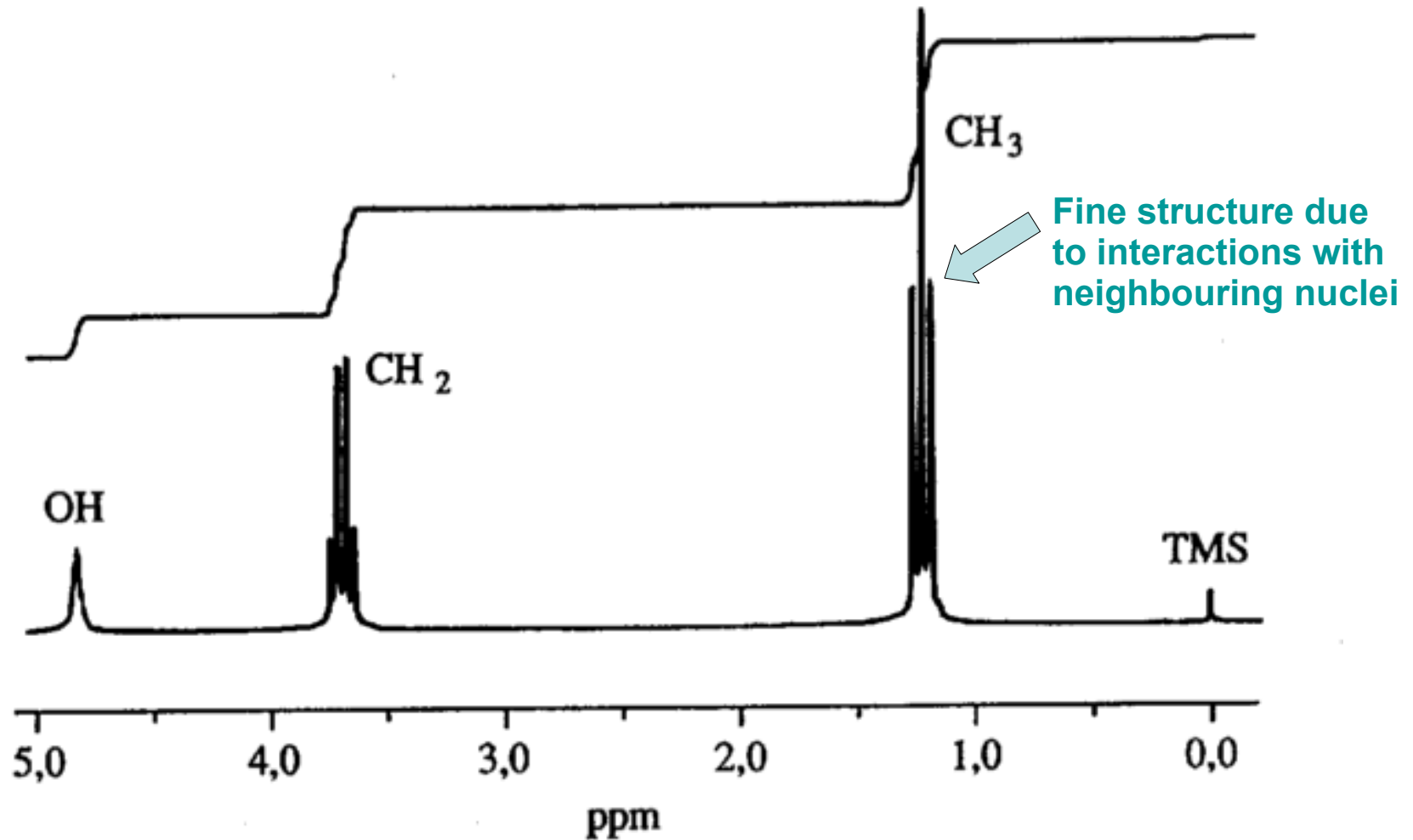
Spin-Spin interactions



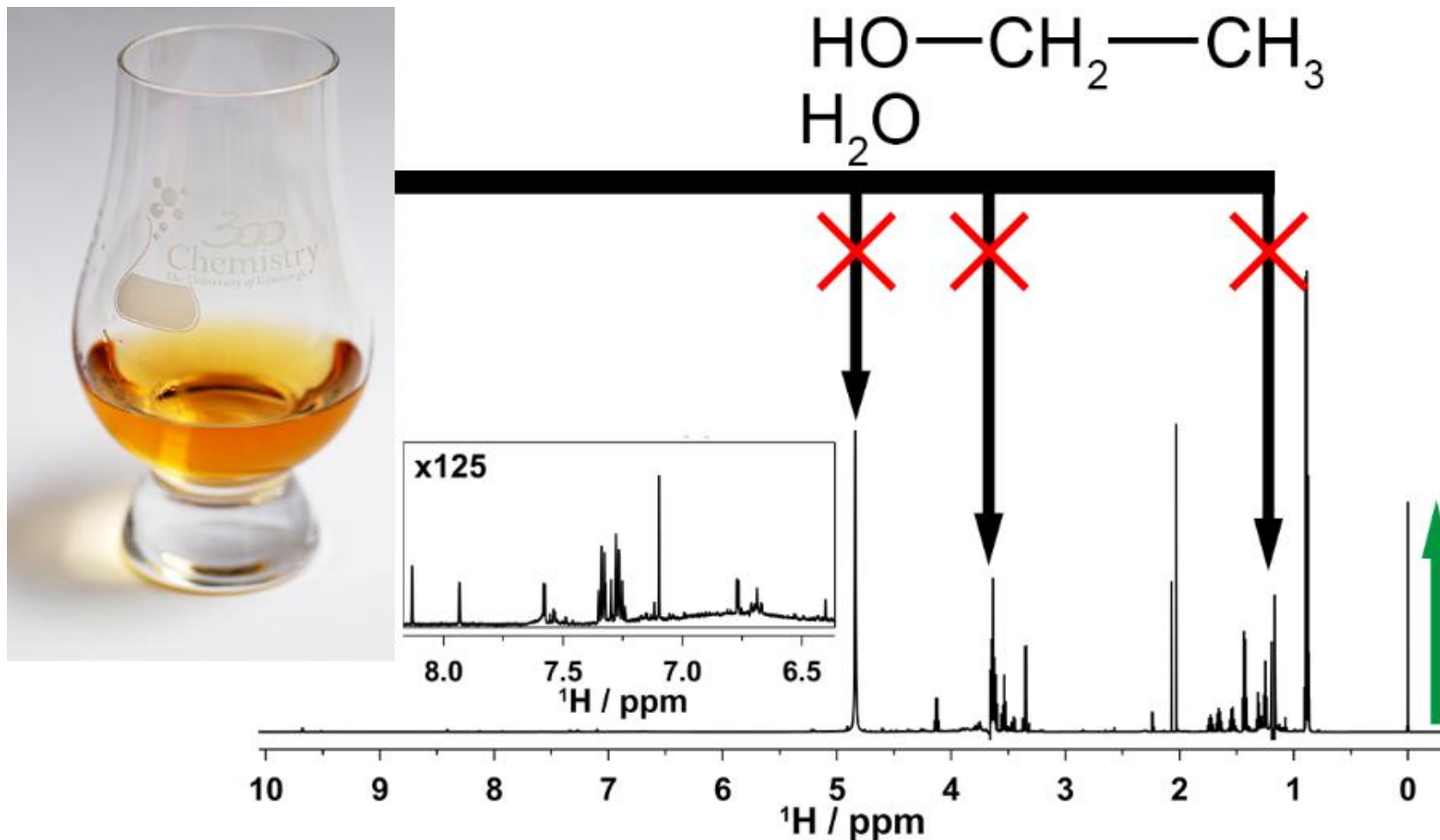
- Dipolar coupling **D** 
 - Through space
 - depends on distance
 - ▶ and of course on orientation
 - averaged to zero in isotropic liquids
 - relaxation effect
- Scalar coupling **J** 
 - isotropic part of D
 - mediated by molecular orbitals
 - depends on molecular topology
 - ▶ and also on dihedral angles

J-Coupling

- Ethanol ^1H spectrum

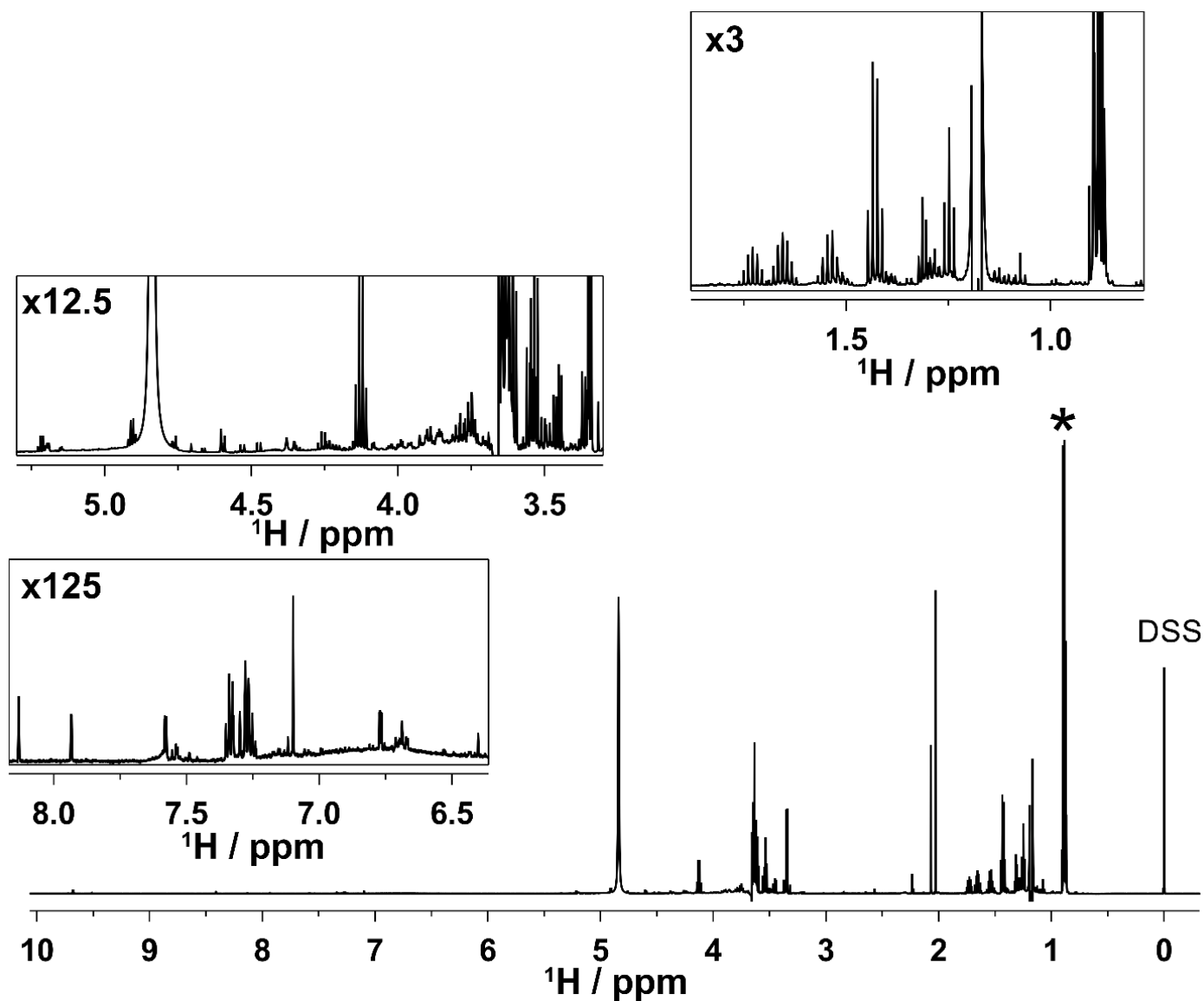


NMR Spectra of Scotch Whisky



Will Kew, Nicholle G. A. Bell, Ian Goodall, Dušan Uhrín
(2017) *Magn Reson Chem* DOI: 10.1002/mrc.4621

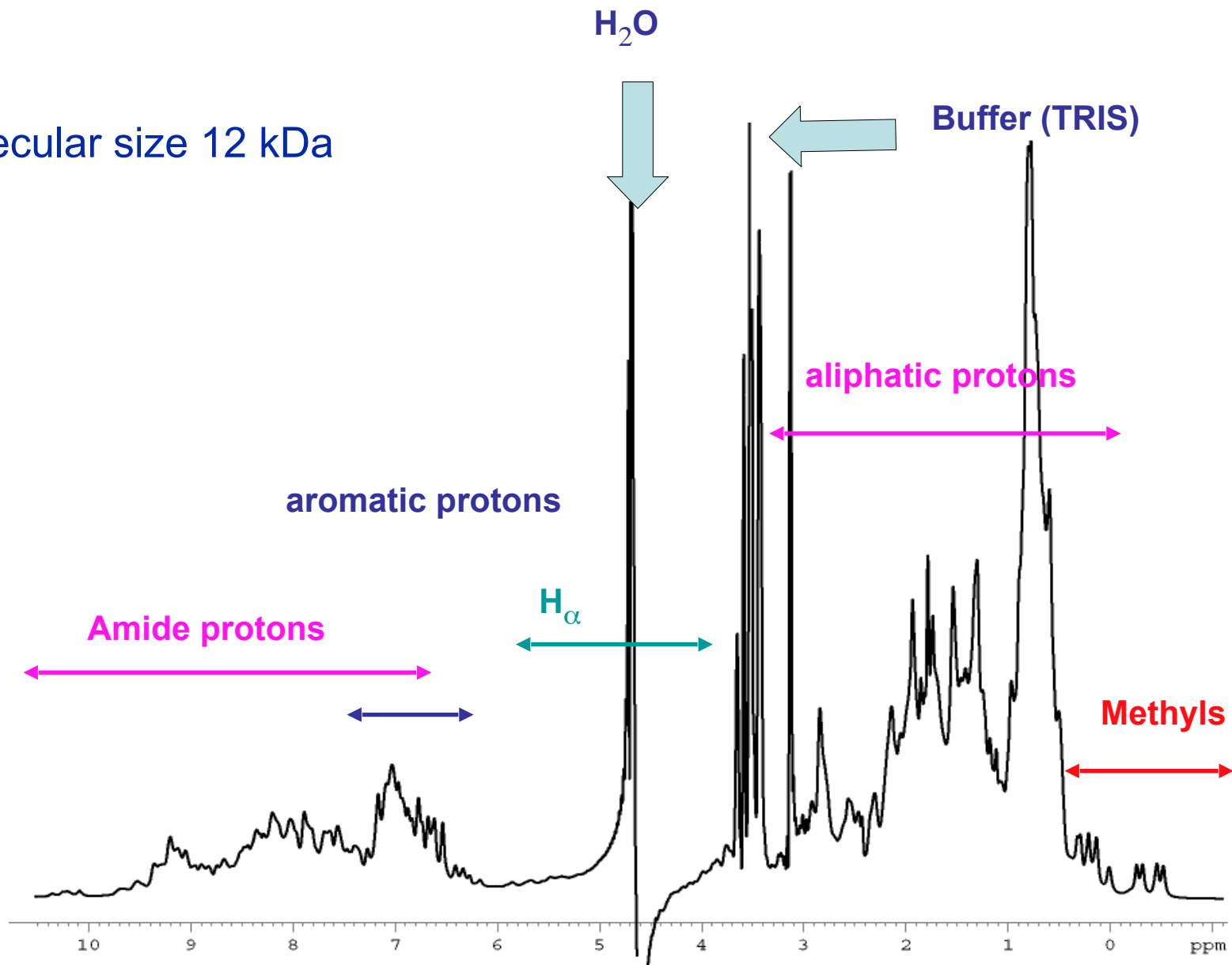
NMR Spectra of Scotch Whisky



Will Kew, Nicholle G. A. Bell, Ian Goodall, Dušan Uhrín
(2017) *Magn Reson Chem* DOI: 10.1002/mrc.4621

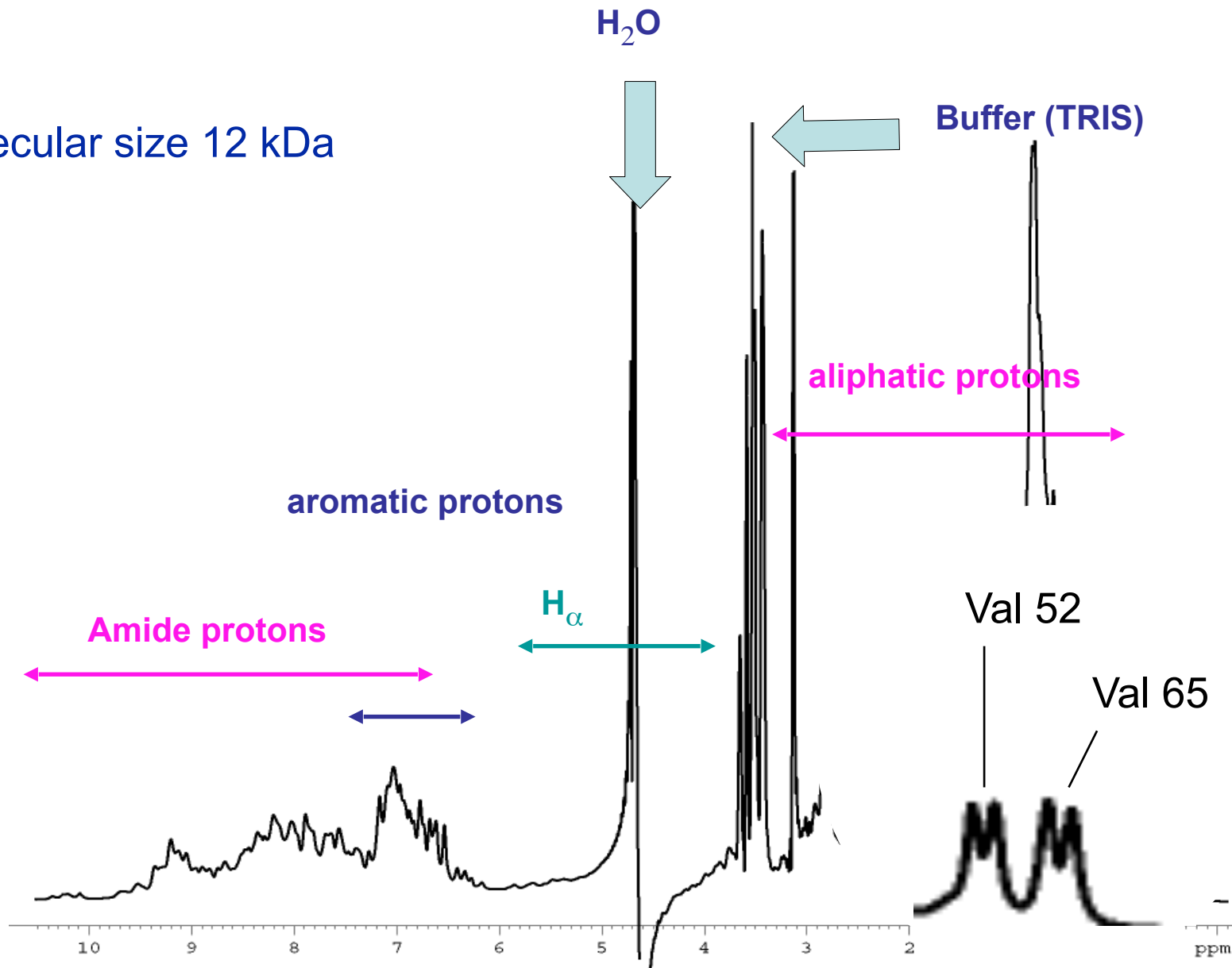
^1H NMR spectrum of a folded protein

Molecular size 12 kDa



^1H NMR spectrum of a folded protein

Molecular size 12 kDa

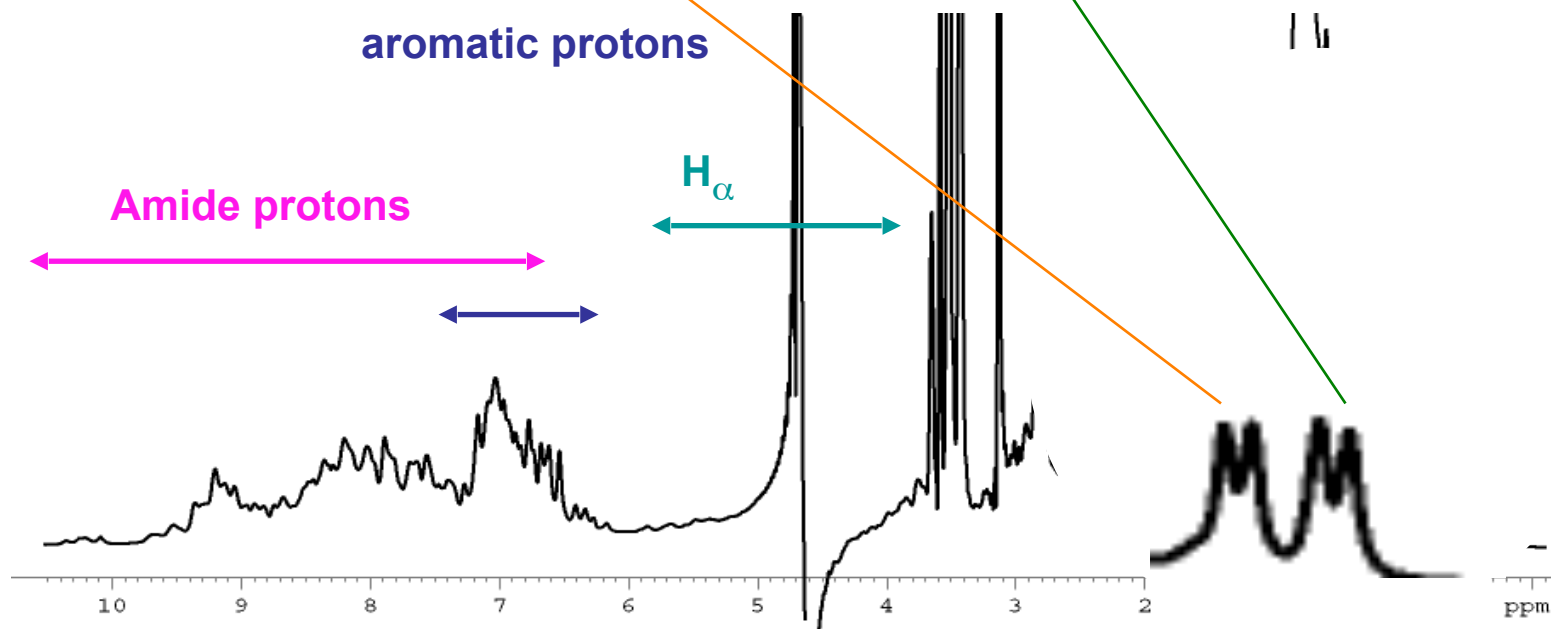


^1H NMR spectrum of a folded protein

MVKQIESKTA FQEALDAAGD KLVVVD⁵²FSAT WCGPCKMIKP
FFHSLSEKYS NVIFLEVDVD DCQDV⁶⁵ASECE VKCMPTFQFF
KKGQKVGEFS GANKEKLEAT INELV

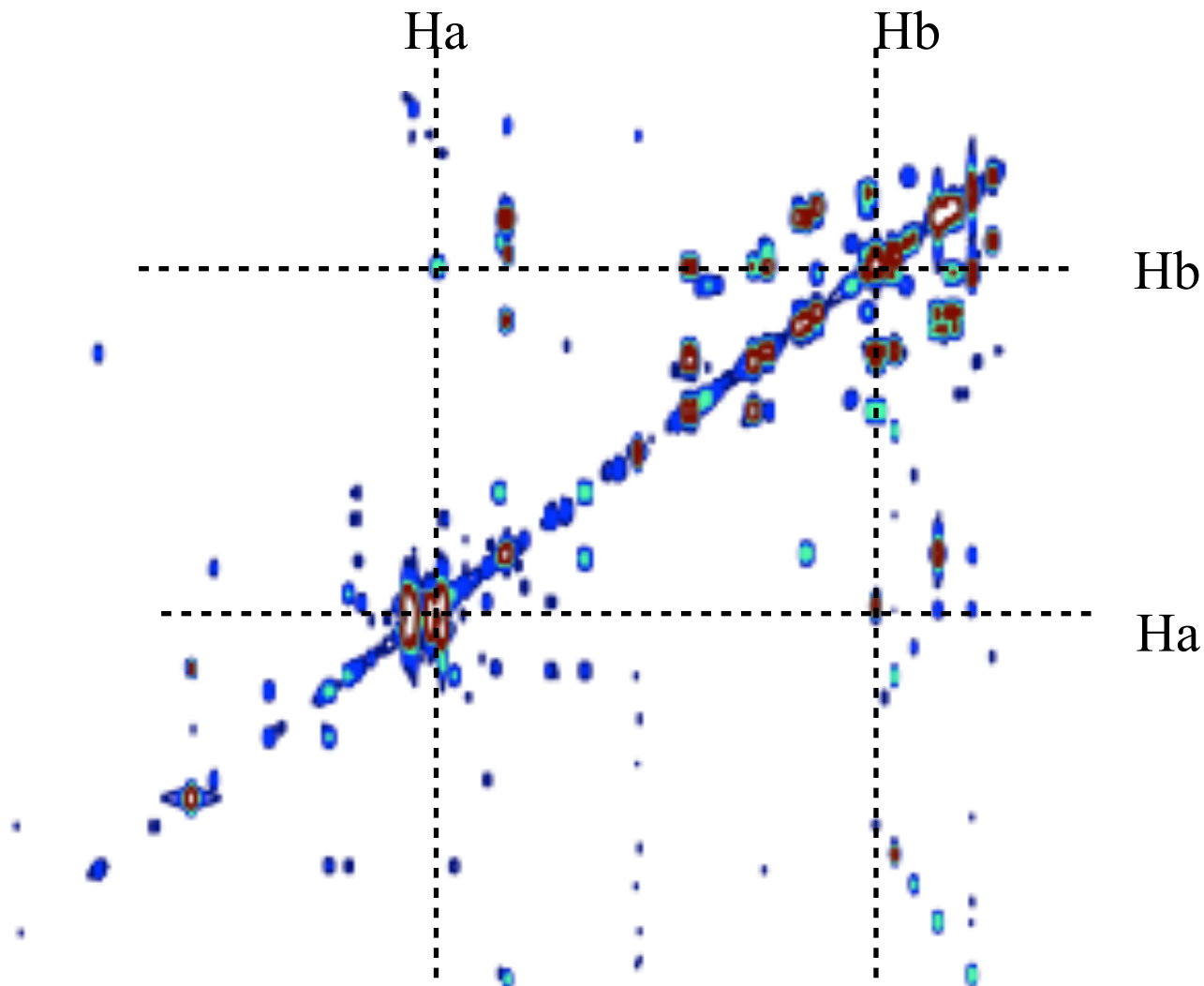
Valine 52

Valine 65

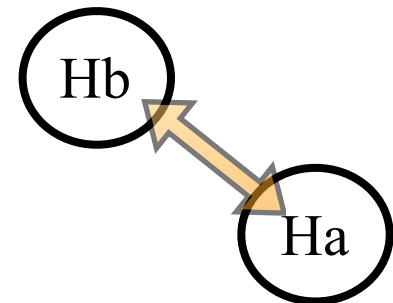


2D experiment

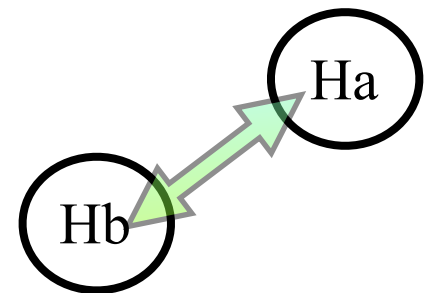
- using spin-spin interaction to transfer coherence from one spin to another



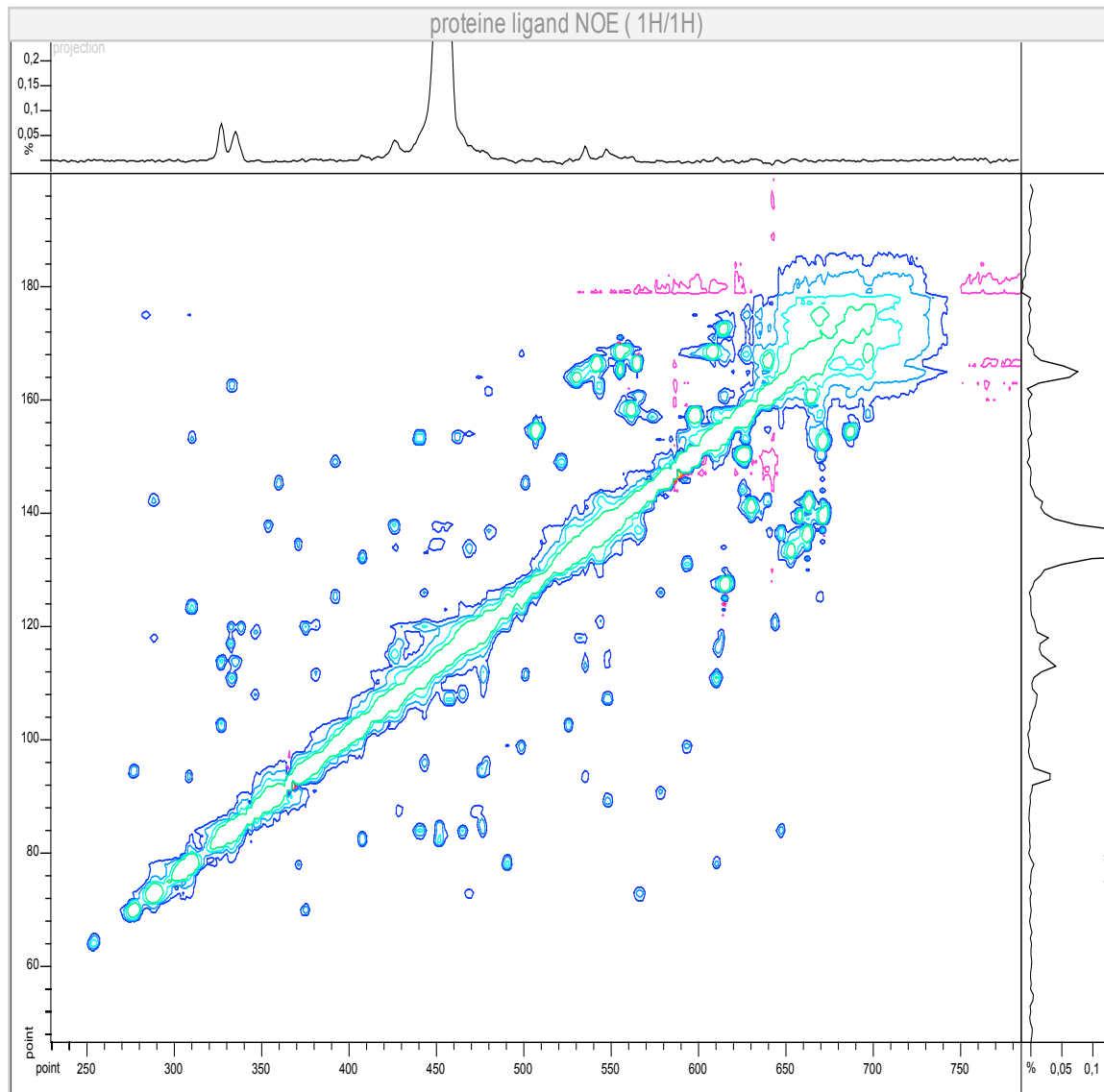
J: COSY / TOCSY



D: NOESY



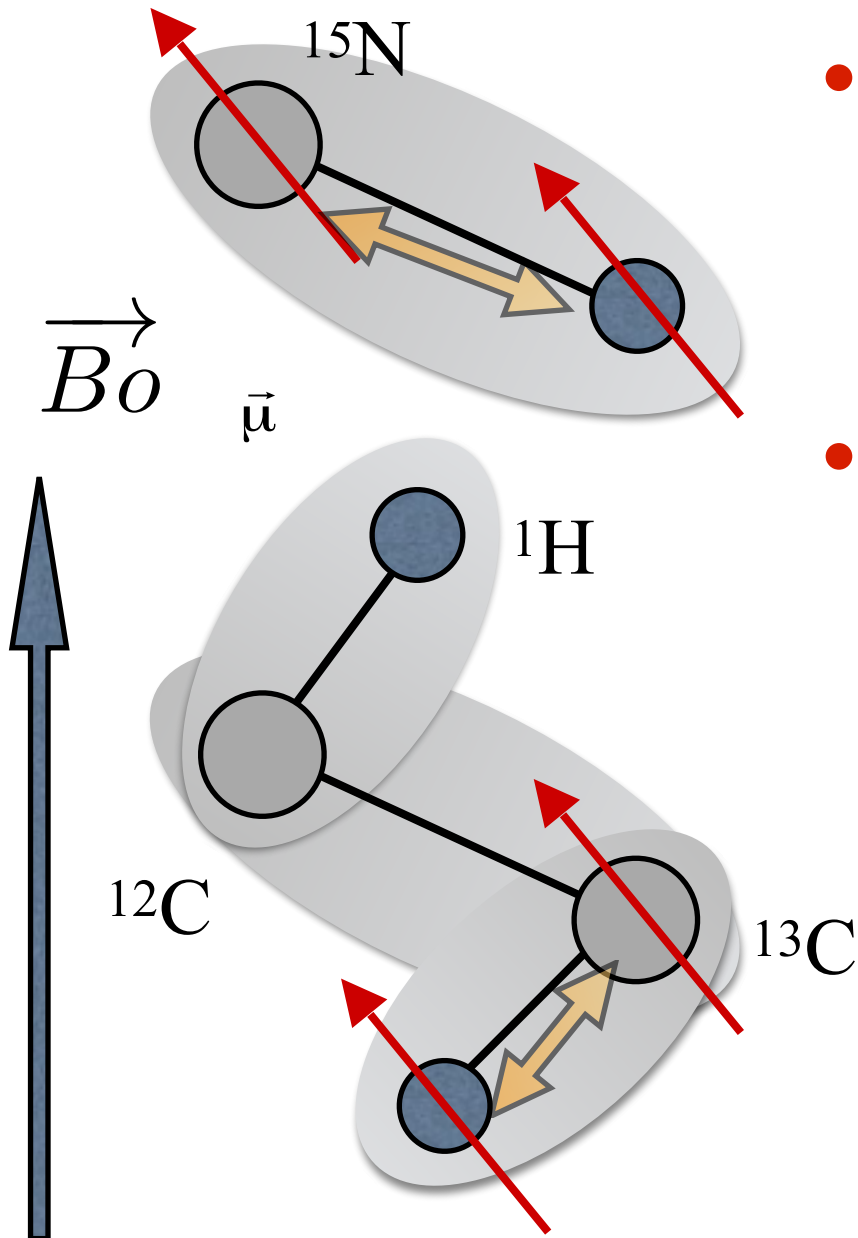
2D experiment - NOESY



Each correlation corresponds to a spatial proximity.

Here amide protons proximity
(for instance $i-i+3$ and $i-i+4$ in α -helices)

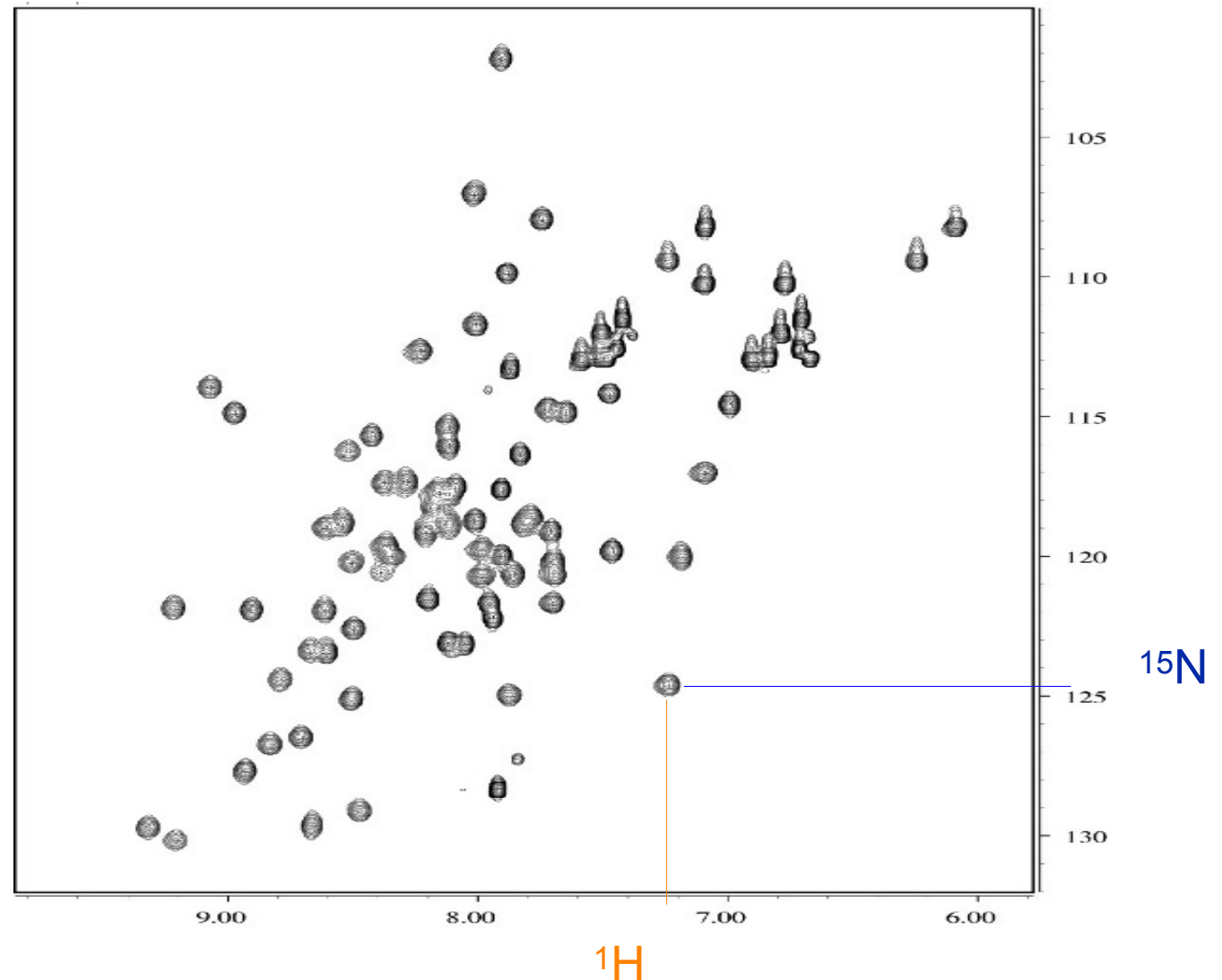
Heteronuclear interactions



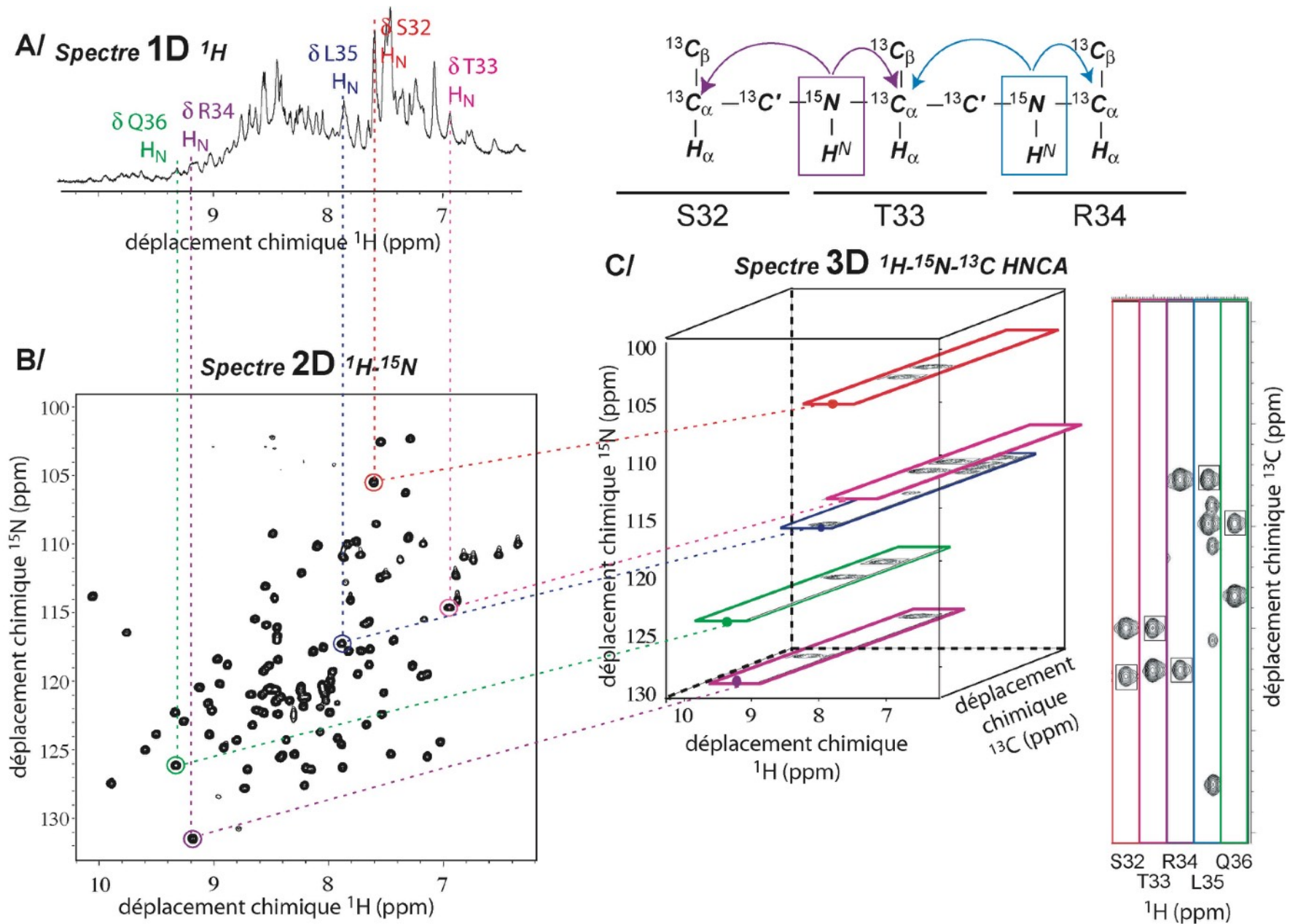
- HSQC
 - **H**eteronuclear **S**ingle **Q**uantum **C**orr.
 - 1 bound ^{13}C - ^1H or ^{15}N - ^1H
- Requires isotopic labelling (*usually*)
 - *E.coli* in minimum media
 - (^{15}N cheaper than ^{13}C)

2D HSQC

- here ^1H - ^{15}N HSQC



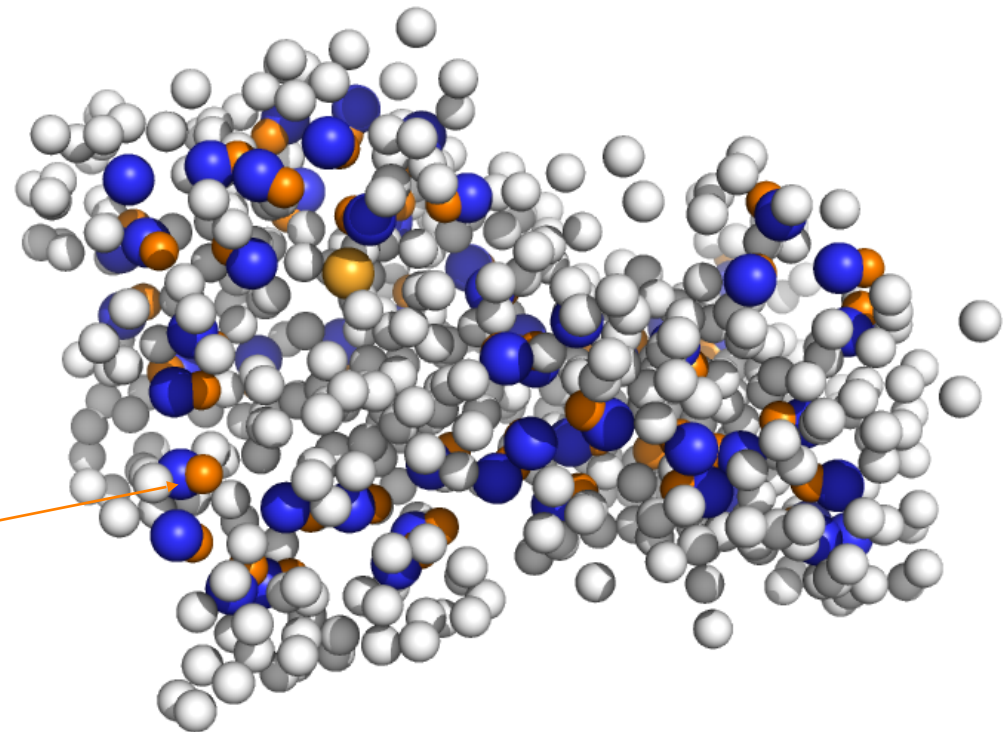
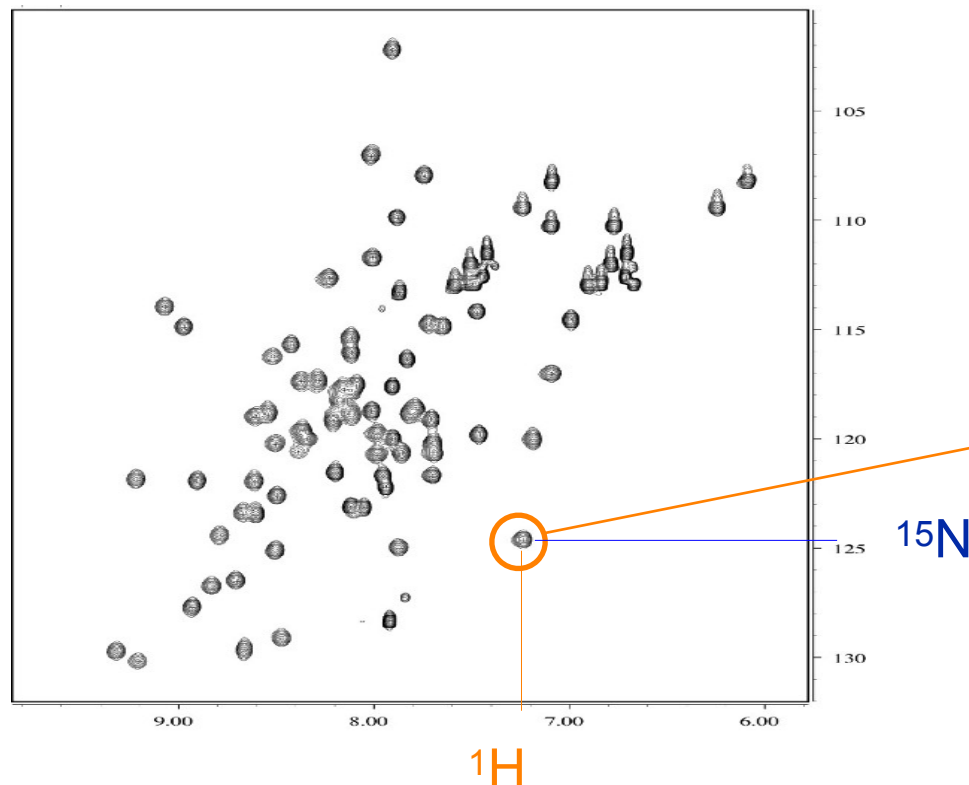
Study of large molecules requires ^{15}N - ^{13}C labeling



Isotopic labeling

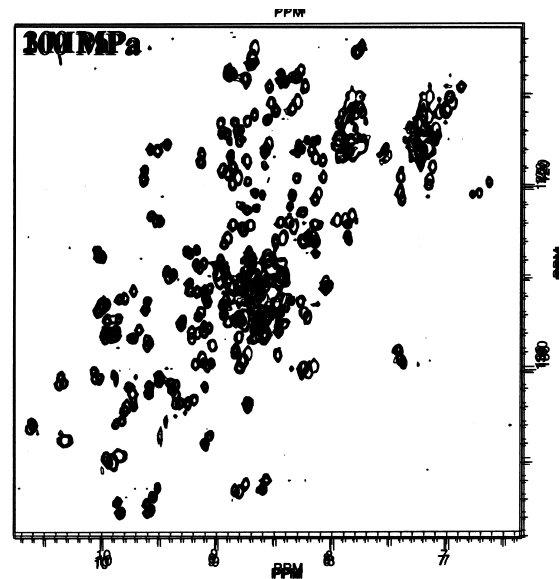
- ◆ Partial view =>
a tool to address the complexity of protein NMR spectra

^1H - ^{15}N HSQC 2D spectrum



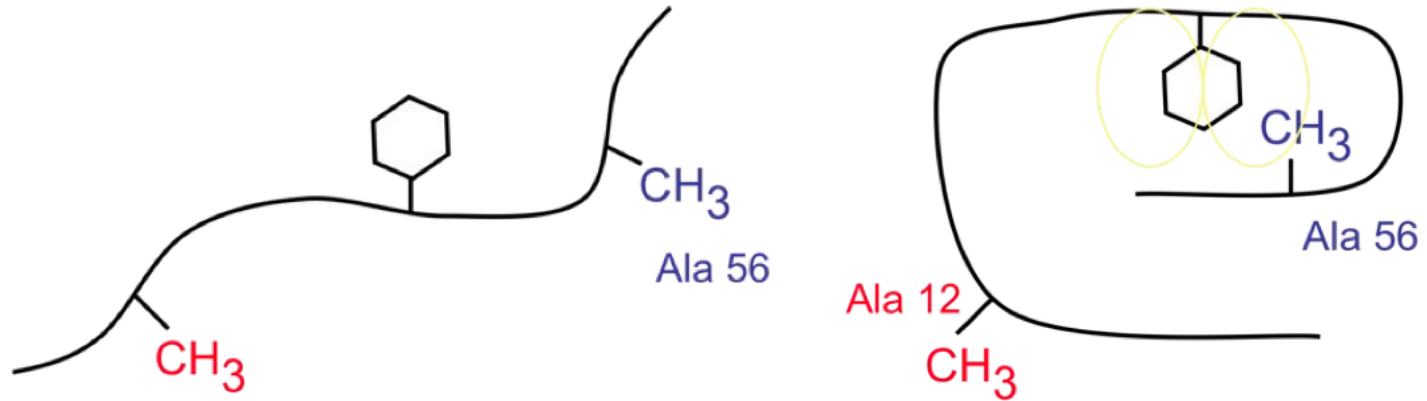
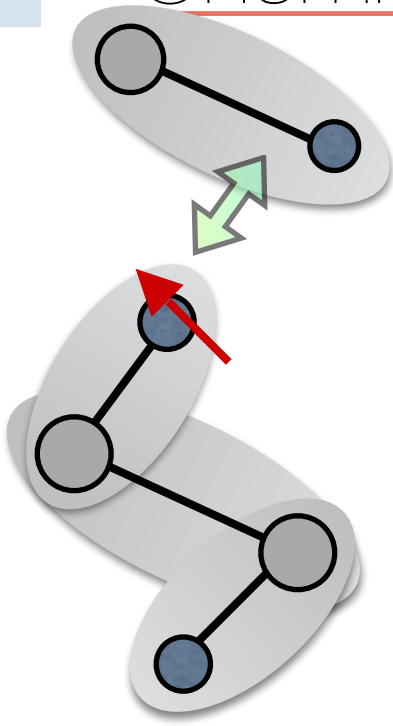
CS is sensitive to protein conformation

R. Kitahara, C. Royer, H. Yamada, M. Boyer, J-L. Saldana, K. Akasaka, C. Roumestand
Pressure-jump fluorescence and $^{15}\text{N}/^1\text{H}$ 2-D NMR studies of the unfolding of the beta-barrel protein, P13MTCP1.
J Mol Biol, 320, 3, (2002), pp 609-628



complete protein denaturation

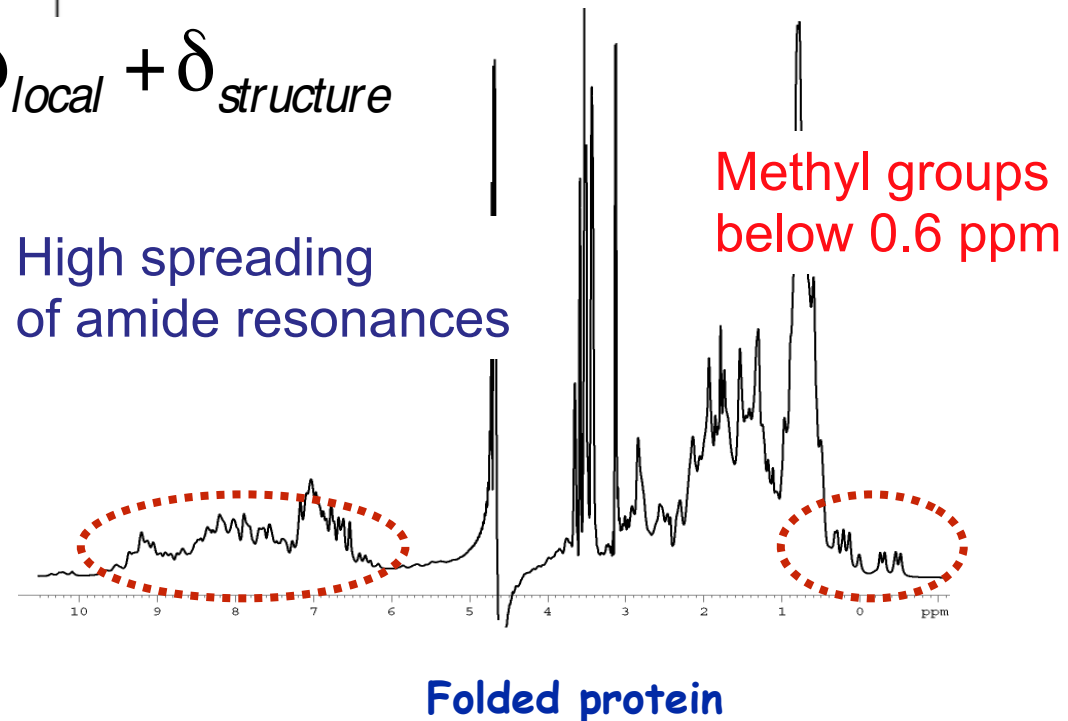
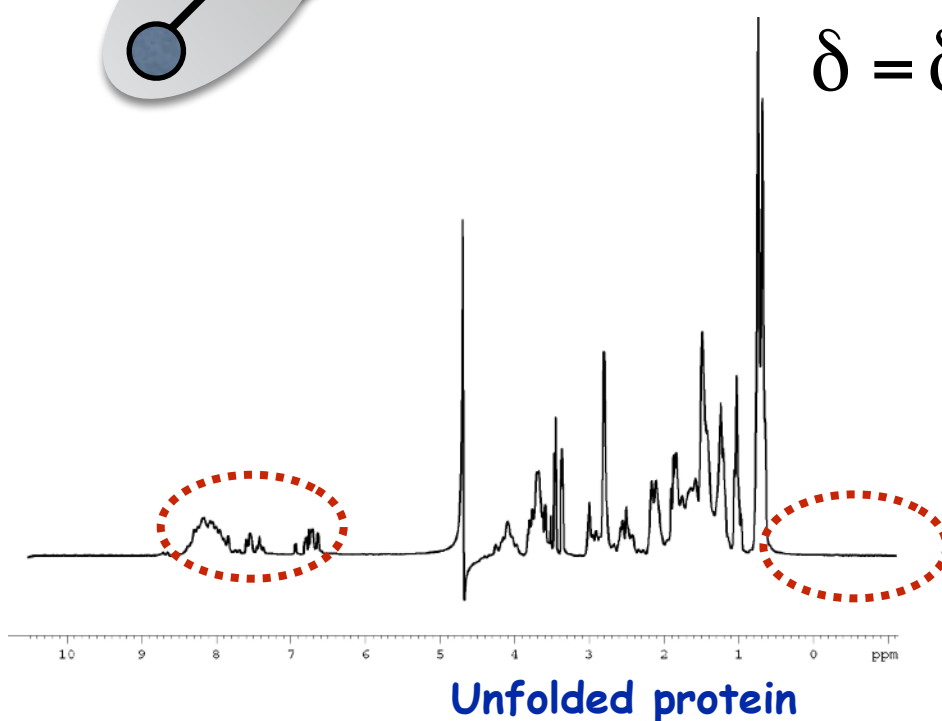
Chemical shifts contain a structural information



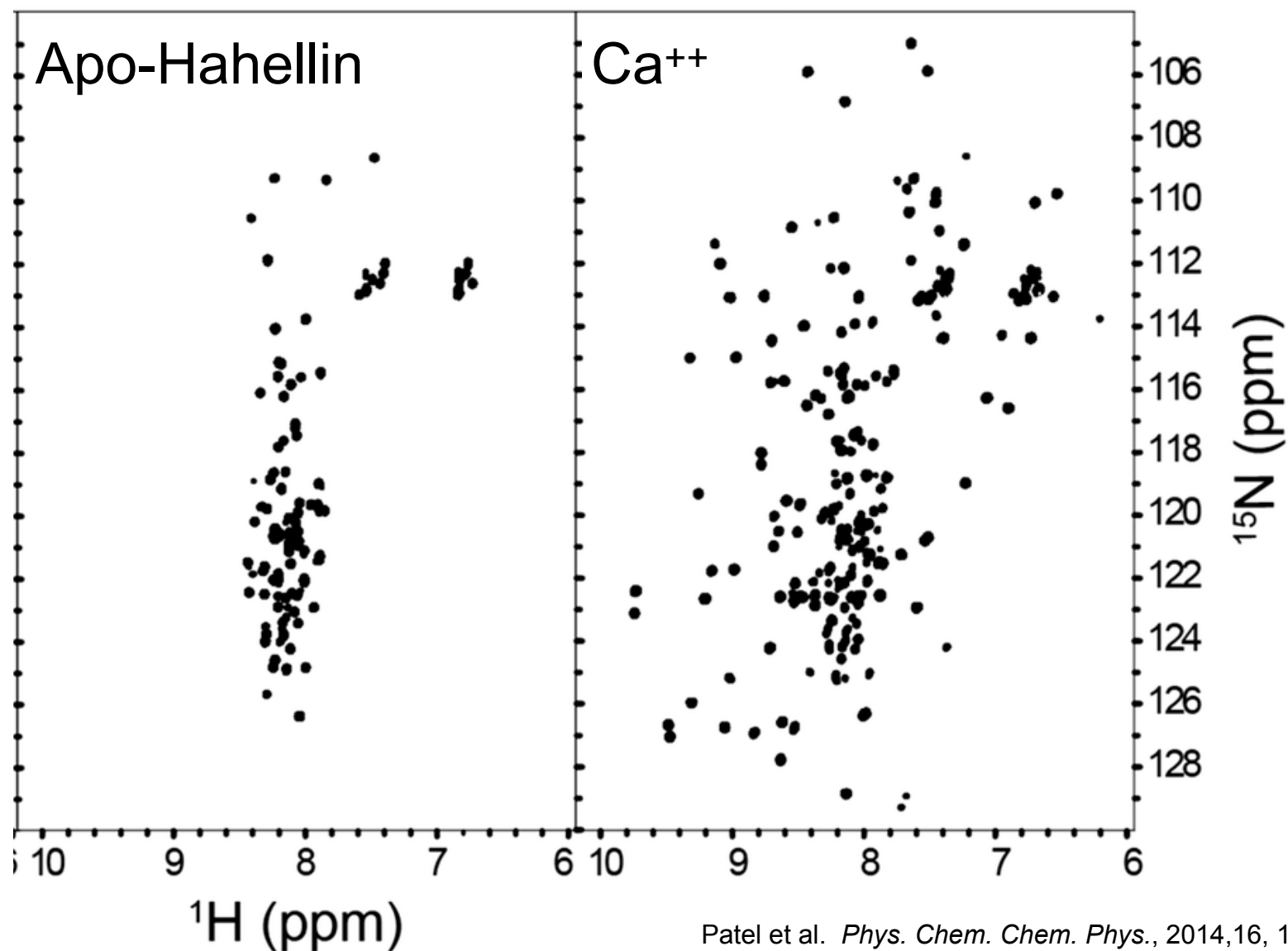
$$\delta = \delta_{local} + \delta_{structure}$$

High spreading
of amide resonances

Methyl groups
below 0.6 ppm



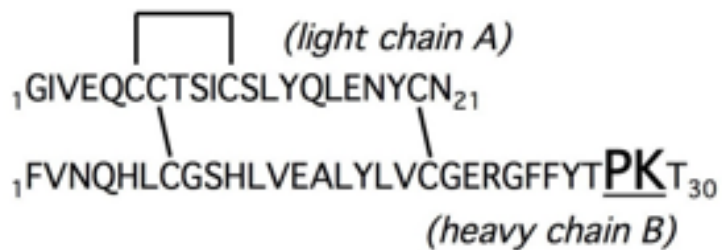
Specific methods for IDP



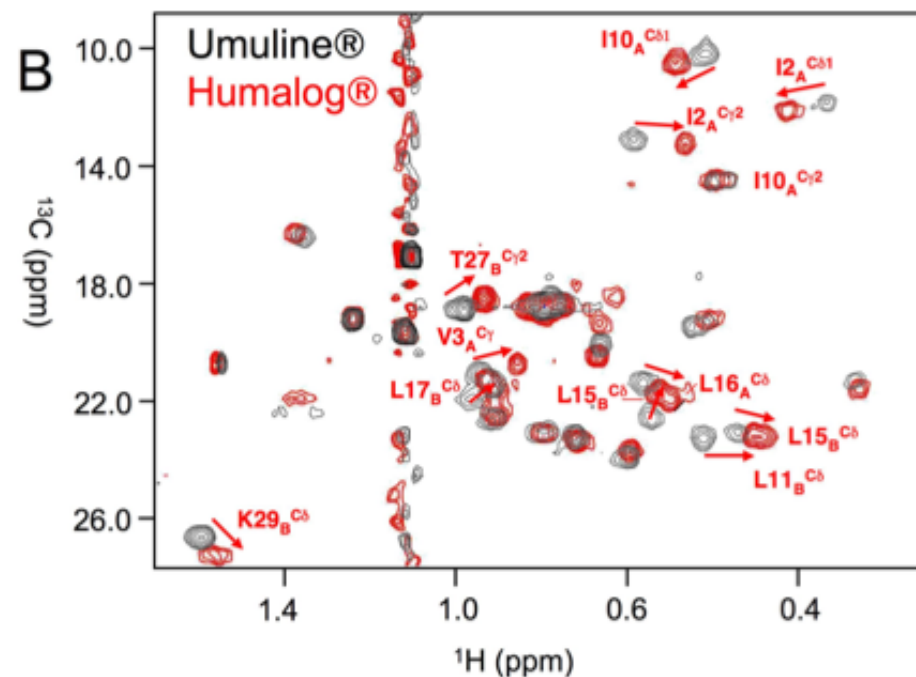
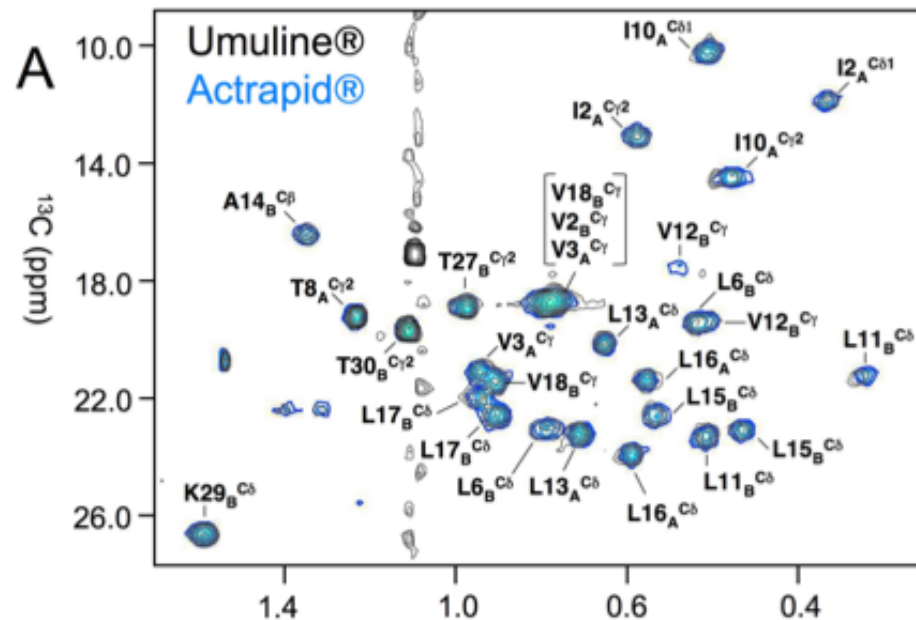
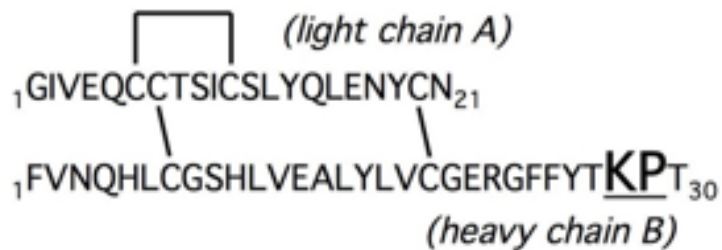
Patel et al. *Phys. Chem. Chem. Phys.*, 2014,16, 12703-12718

Bio-drug control quality

Human insulin



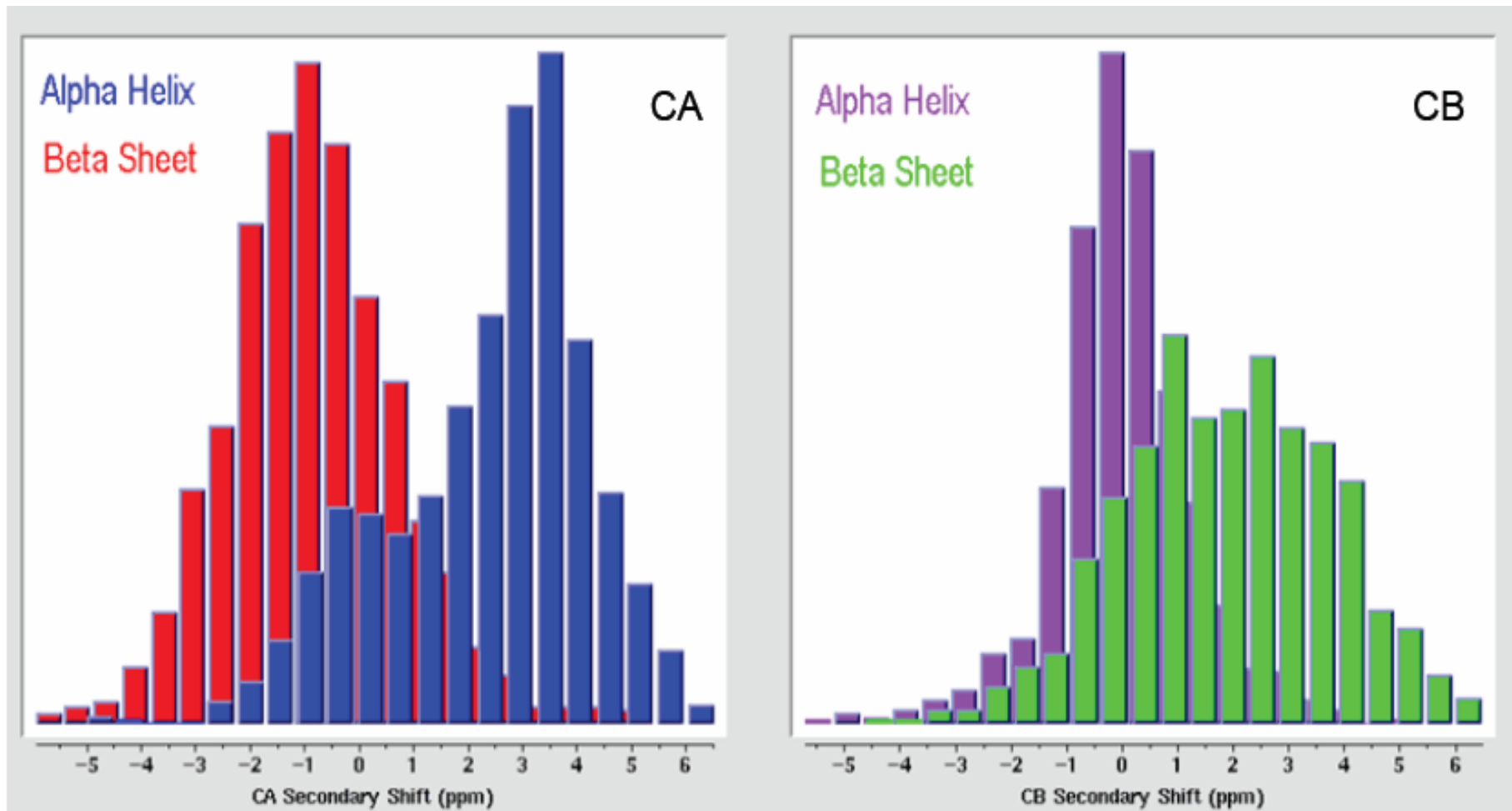
Lispro insulin

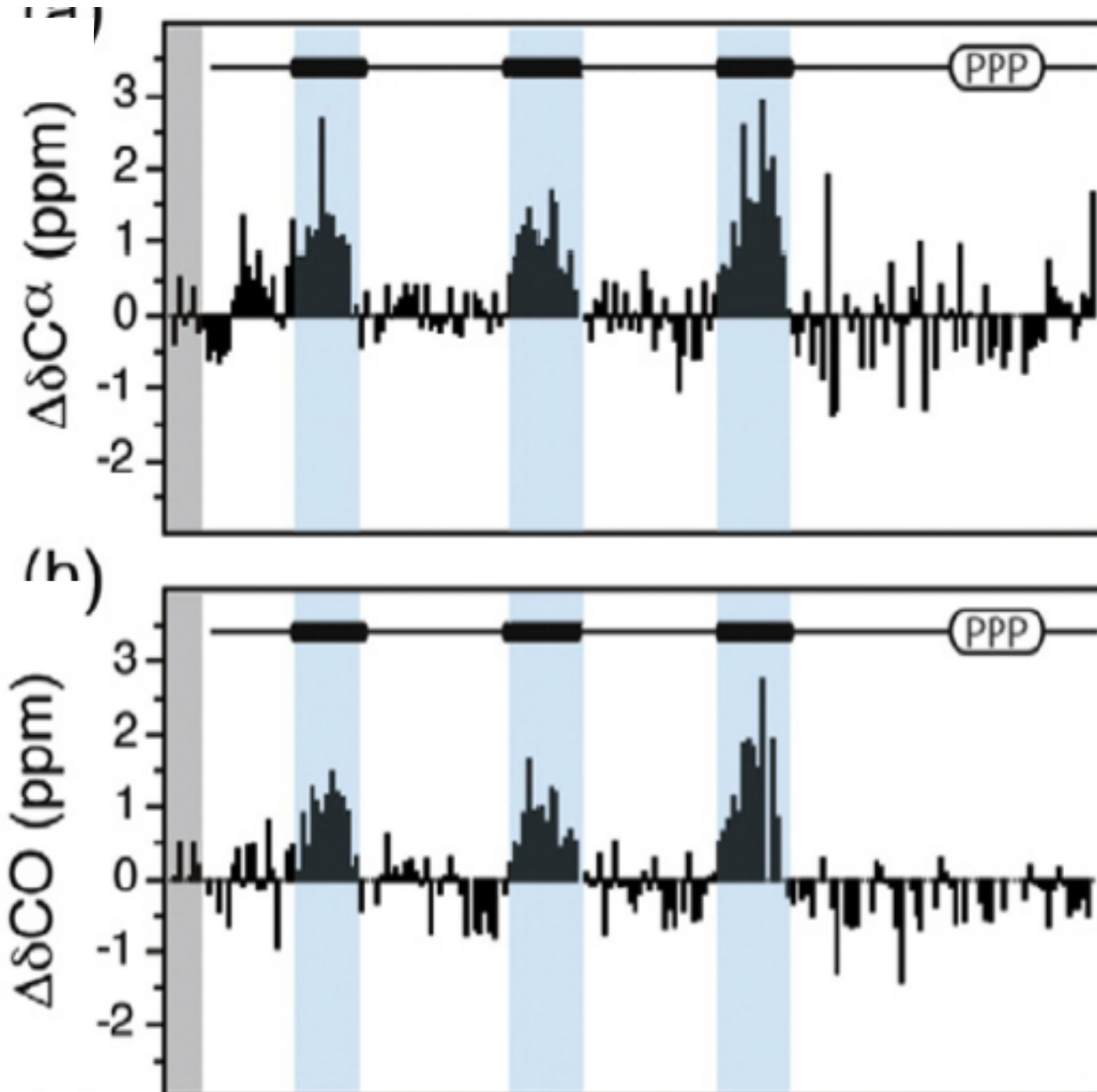


Quinternet, M., Starck, J.-P., Delsuc, M.-A., & Kieffer, B. (2013). J.Pharm. Biomed. Analysis, 78-79, 252–254.
<http://doi.org/10.1016/j.jpba.2013.02.016>

CS of backbone provide structure information

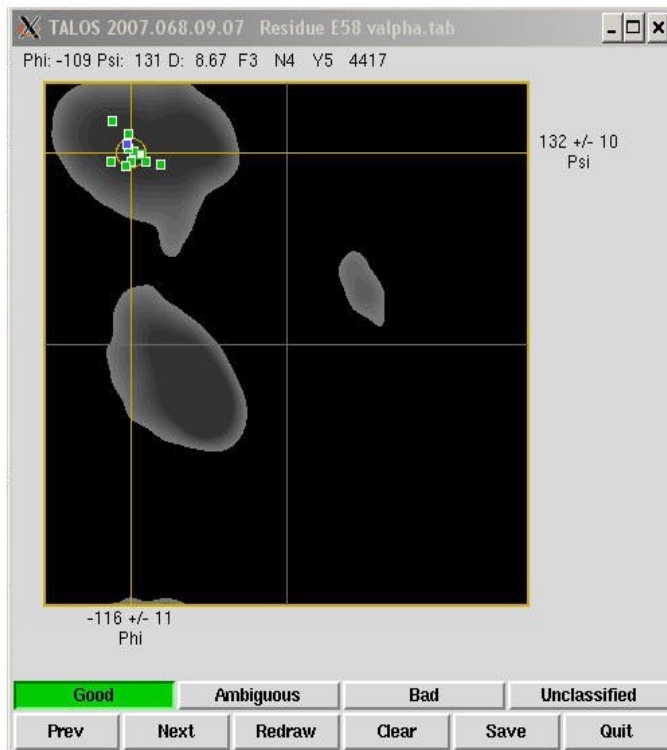
$$\text{CSI} = \delta_{\text{measured}} - \delta_{\text{randomcoil}}$$





CS interpretation as ϕ - ψ angles

Talos+ : <http://spin.niddk.nih.gov/NMRPipe>

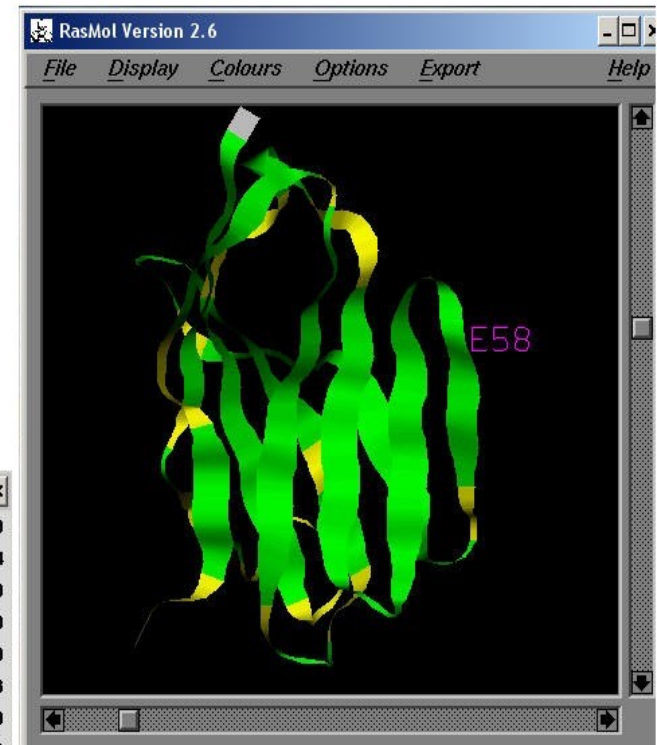
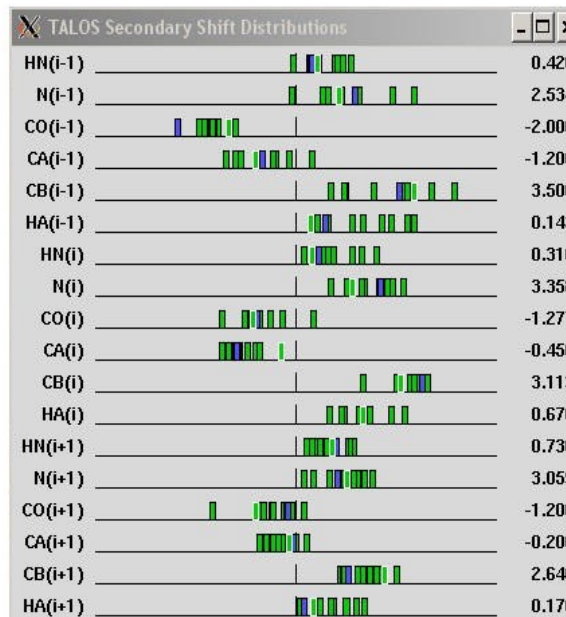


Residue E58, Triplet K57 E58 D59

Phi: -109 Psi: 131 D: 8.67 F3 N4 Y5 4417
Phi: -131 Psi: 126 D: 9.31 N107 E108 K109 4340
Phi: -130 Psi: 154 D: 11.25 C35 E36 I37 5792
Phi: -118 Psi: 145 D: 11.36 V164 K165 E166 ospA
Phi: -94 Psi: 124 D: 11.80 M71 R72 I73 vegf
Phi: -114 Psi: 133 D: 11.94 I75 Q76 S77 hav
Phi: -116 Psi: 126 D: 13.09 T102 E103 F104 apo_1fabp
Phi: -120 Psi: 123 D: 13.10 L117 E118 M119 5579
Phi: -118 Psi: 135 D: 13.25 E58 I59 I60 gyraseB
Phi: -105 Psi: 126 D: 13.39 T55 I56 Y57 4267
Phi: -116 Psi: 132 D: 11.72 Average

TALOS valpha.tab Residues 1 to 114

M1	Q2	Q3	V4	R5	Q6	S7	P8	Q9	S10
L11	T12	V13	W14	E15	G16	E17	T18	A19	I20
L21	N22	C23	S24	Y25	E26	N27	S28	A29	F30
D31	Y32	F33	P34	W35	Y36	Q37	Q38	F39	P40
G41	E42	G43	P44	A45	L46	L47	I48	S49	I50
L51	S52	V53	S54	N55	K56	K57	E58	D59	G60
R61	F62	T63	I64	F65	F66	N67	K68	R69	E70
K71	K72	L73	S74	L75	H76	I77	A78	D79	S80
Q81	P82	G83	D84	S85	A86	T87	Y88	F89	C90
A91	A92	S93	A94	S95	F96	G97	D98	N99	S100
K101	L102	I103	W104	G105	L106	G107	T108	S109	L110
V111	V112	N113	P114						



Full structure calculations: CS ROSETTA

Consistent blind protein structure generation from NMR chemical shift data

Yang Shen^{*}, Oliver Lange[†], Frank Delaglio^{*}, Paolo Rossi[‡], James M. Aramini[‡], Gaohua Liu[‡], Alexander Eletsky[§], Yibing Wu[§], Kiran K. Singarapu[§], Alexander Lemak[¶], Alexandr Ignatchenko[¶], Cheryl H. Arrowsmith[¶], Thomas Szyperski[§], Gaetano T. Montelione[‡], David Baker[¶], and Ad Bax^{*‡}

^{*}Laboratory of Chemical Physics, National Institute of Diabetes and Digestive and Kidney Diseases, National Institutes of Health, Bethesda, MD 20892; [†]Department of Biochemistry and Howard Hughes Medical Institute, University of Washington, Seattle, WA 98195; [‡]Center for Advanced Biotechnology and Medicine, Department of Molecular Biology and Biochemistry, and Northeast Structural Genomics Consortium, Rutgers, The State University of New Jersey, and Robert Wood Johnson Medical School, Piscataway, NJ 08854; [§]Departments of Chemistry and Structural Biology and Northeast Structural Genomics Consortium, University at Buffalo, State University of New York, Buffalo, NY 14260; and [¶]Ontario Cancer Institute, Department of Medical Biophysics, and Northeast Structural Genomics Consortium, University of Toronto, Toronto, ON, Canada M5G 1L5

www.pnas.org/cgi/dol/10.1073/pnas.0800256105

PNAS | March 25, 2008 | vol. 105 | no. 12 | 4685–4690

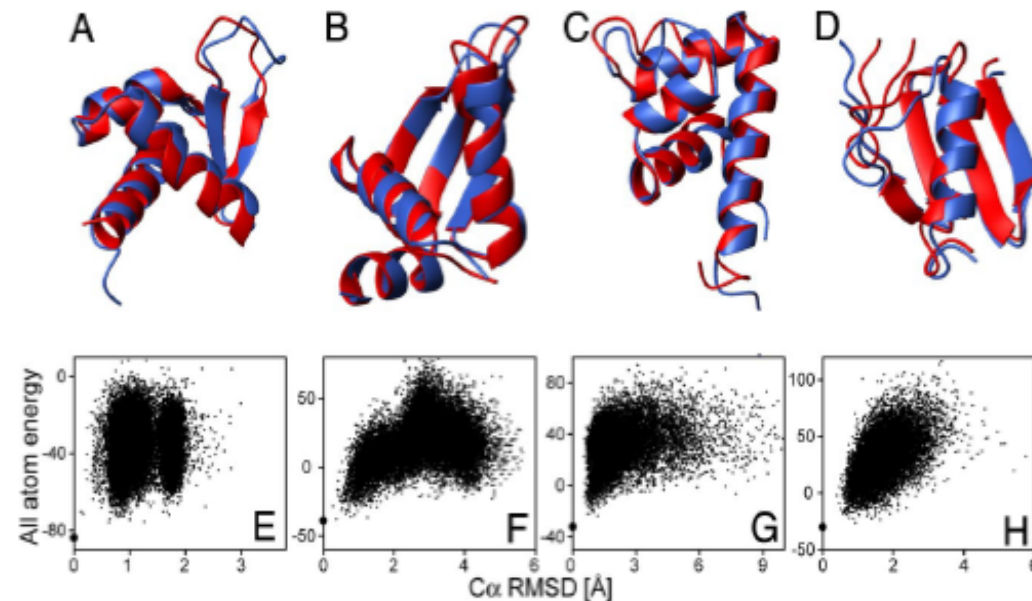
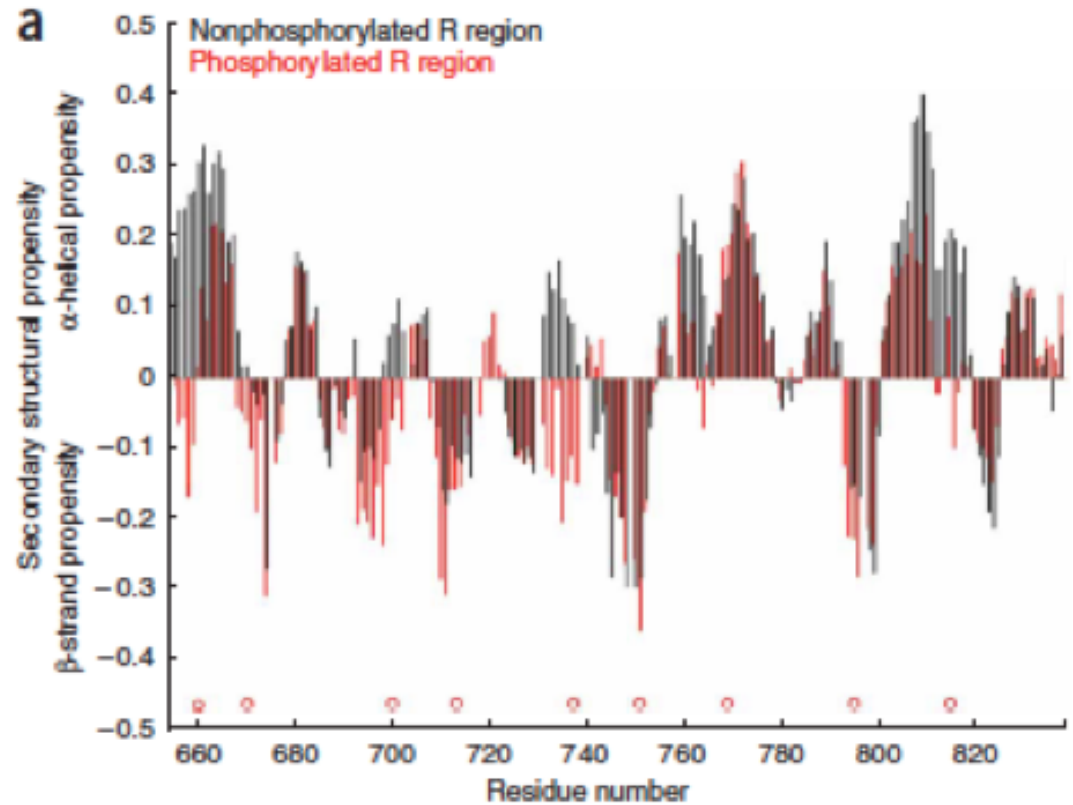
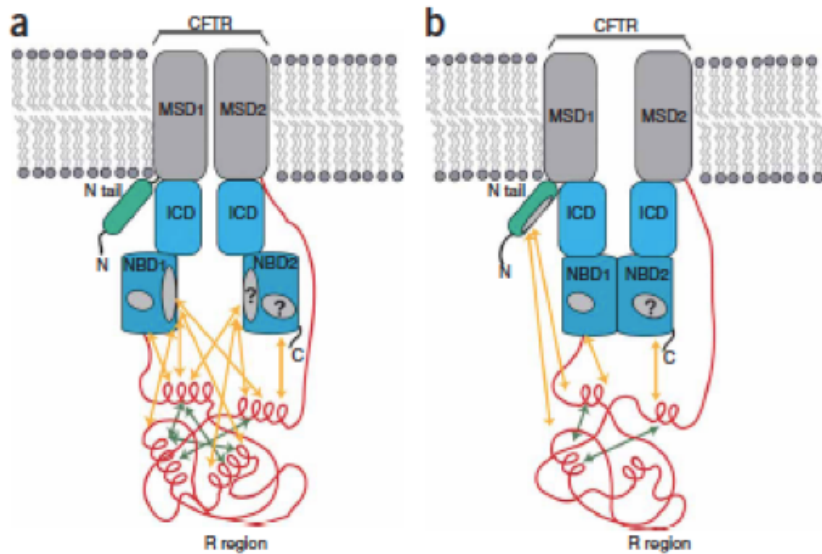


Fig. 4. Results from blind CS-ROSETTA structure generation for four structural genomics targets (Table 2). The remaining five are in SI Fig. 12. (A–D) Superposition of lowest-energy CS-ROSETTA models (red) with experimental NMR structures (blue), with superposition optimized for ordered residues, as defined in the footnote to SI Table 5. (E–H) Plots of rescored (Eq. 1) ROSETTA all-atom energy versus C α rmsd relative to the lowest-energy model (bold dot on vertical axis). (A and E) StR82. (B and F) Rpt7. (C and G) Vfr117. (D and H) NeT4.

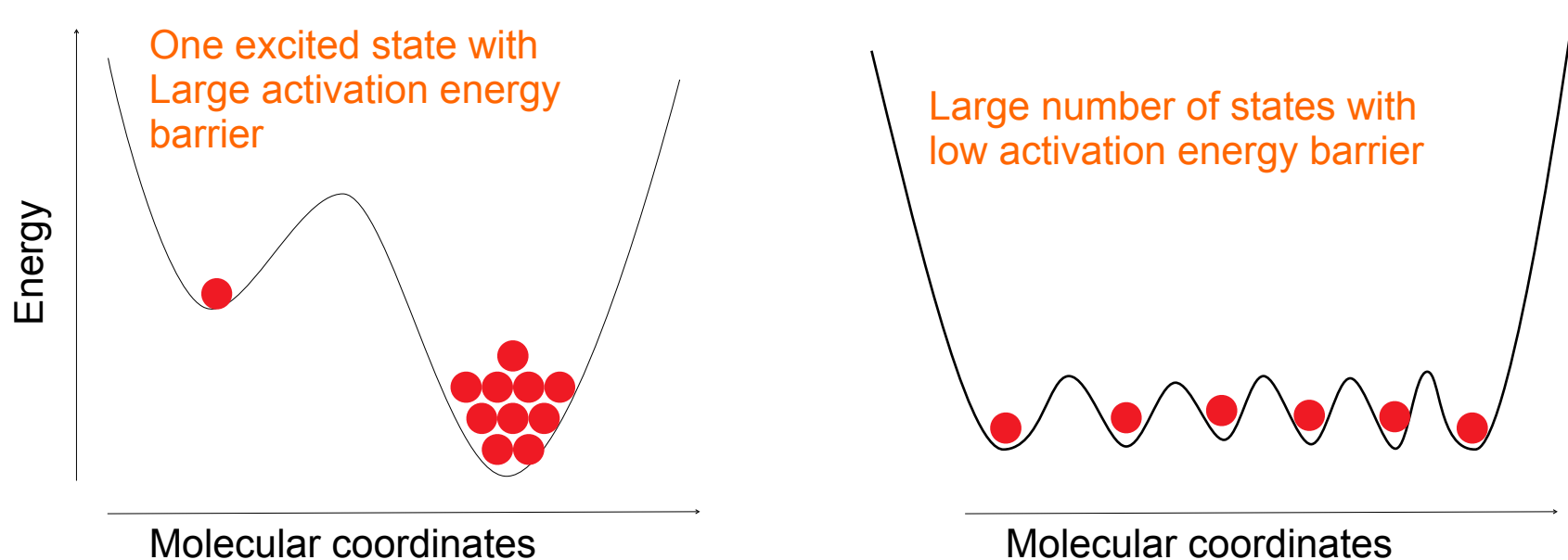
Local structure propensity from chemical shifts analysis



Baker et al 2007 *Nat. Struct. Mol. Biol.* **14**(8), 738

Large number of molecules

- Molecules will be distributed between the different states available for the observed molecular system



- NMR observables will result from an average over all these states

sensitive to all interactions

F. de Lamotte et al. / C. R. Acad. Sci. Paris, Chimie / Chemistry 4 (2001) 839–843

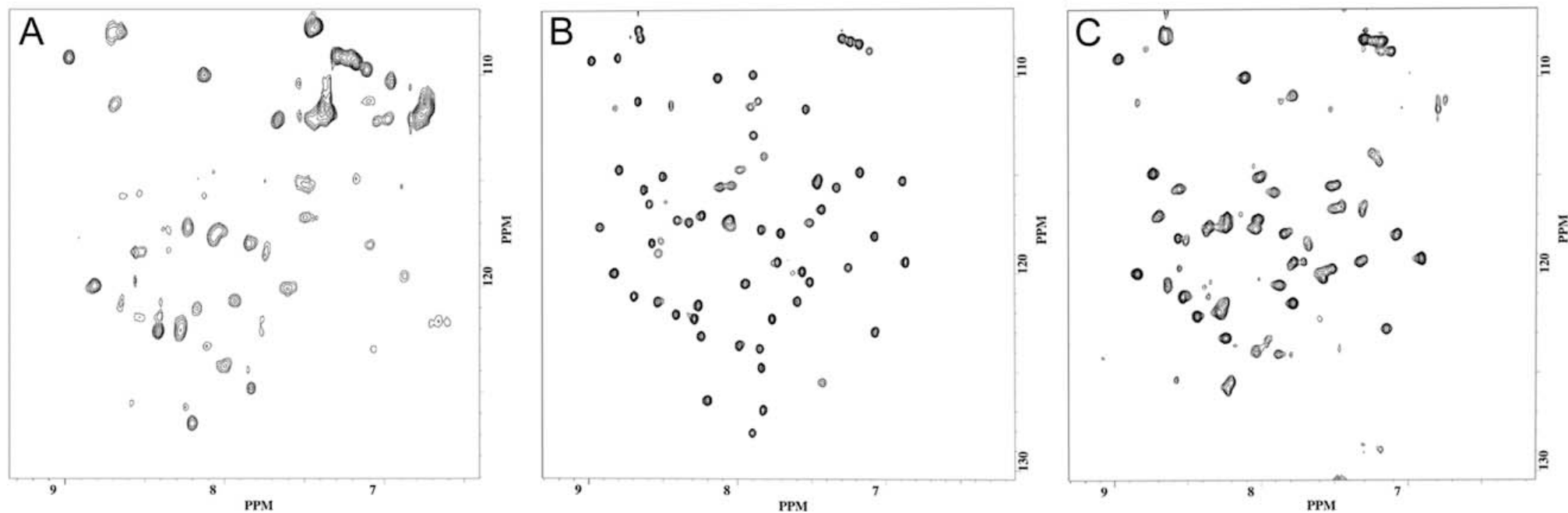
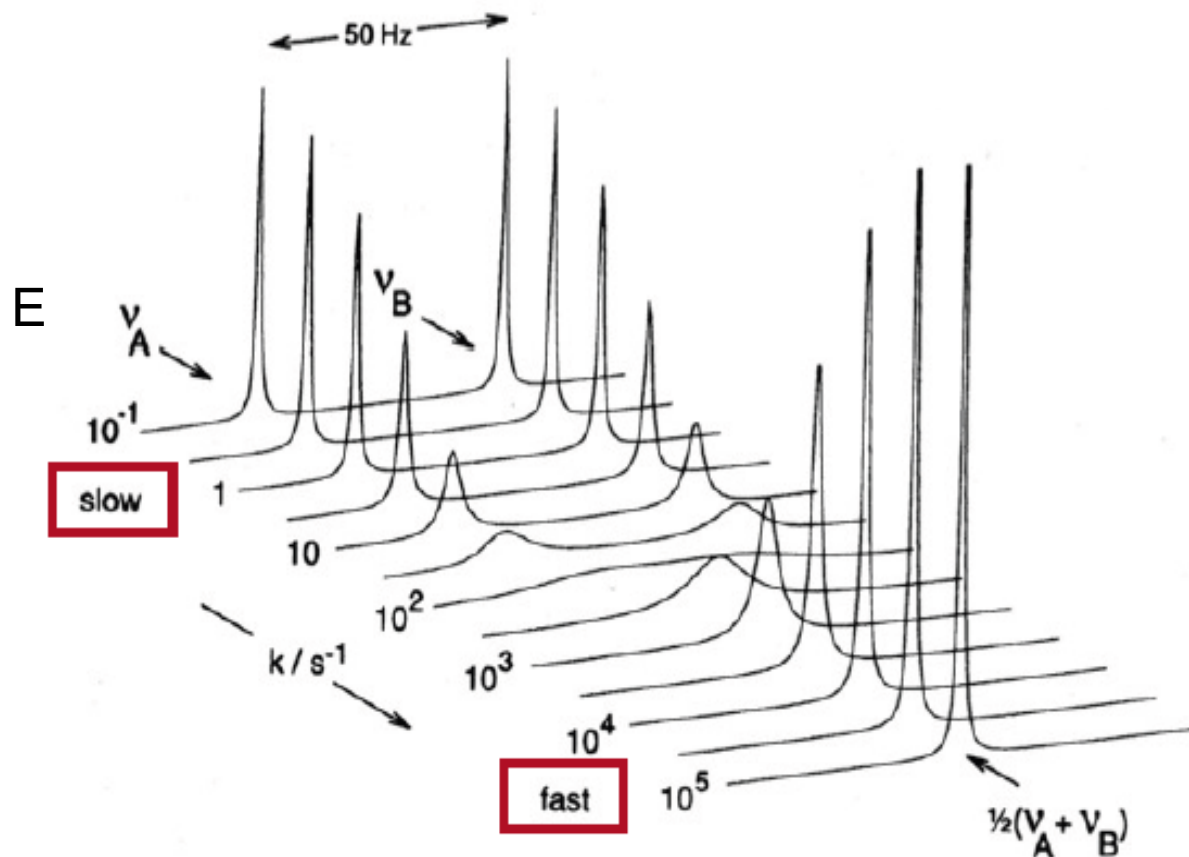
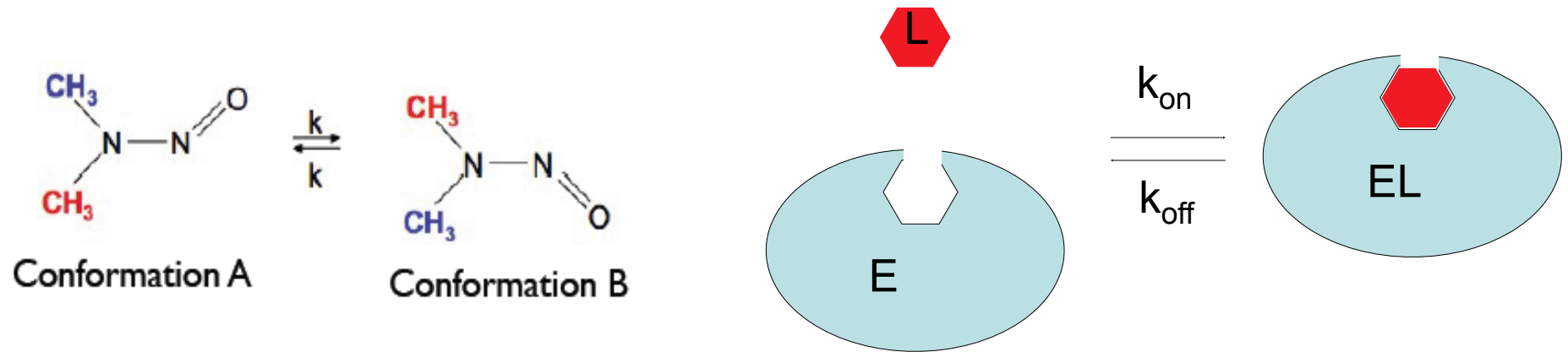
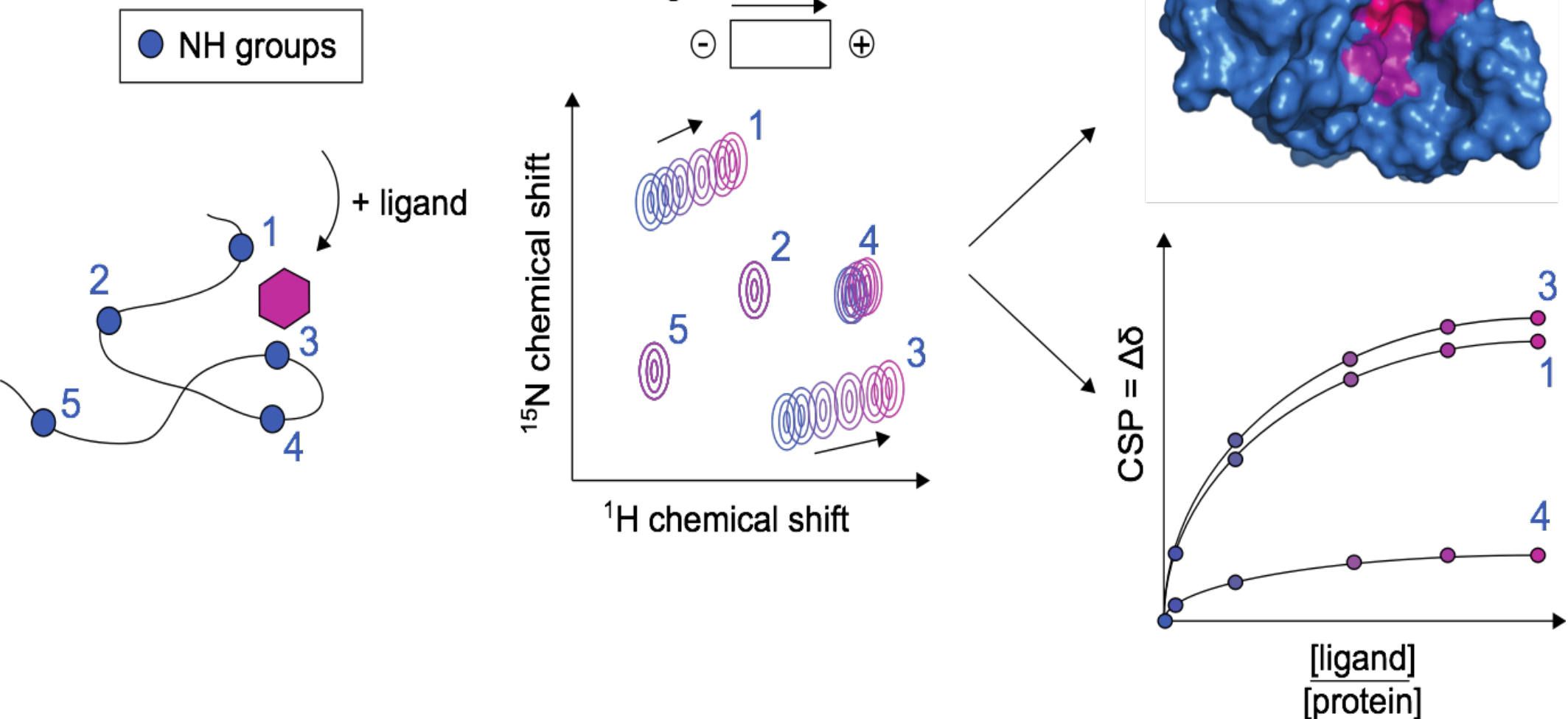


Figure 1. HSQC spectra of type 2 LTP. **A.** Unliganded. **B.** Liganded with 1.5 equiv of LPG. **C.** Liganded with 1.5 equiv of DPC.

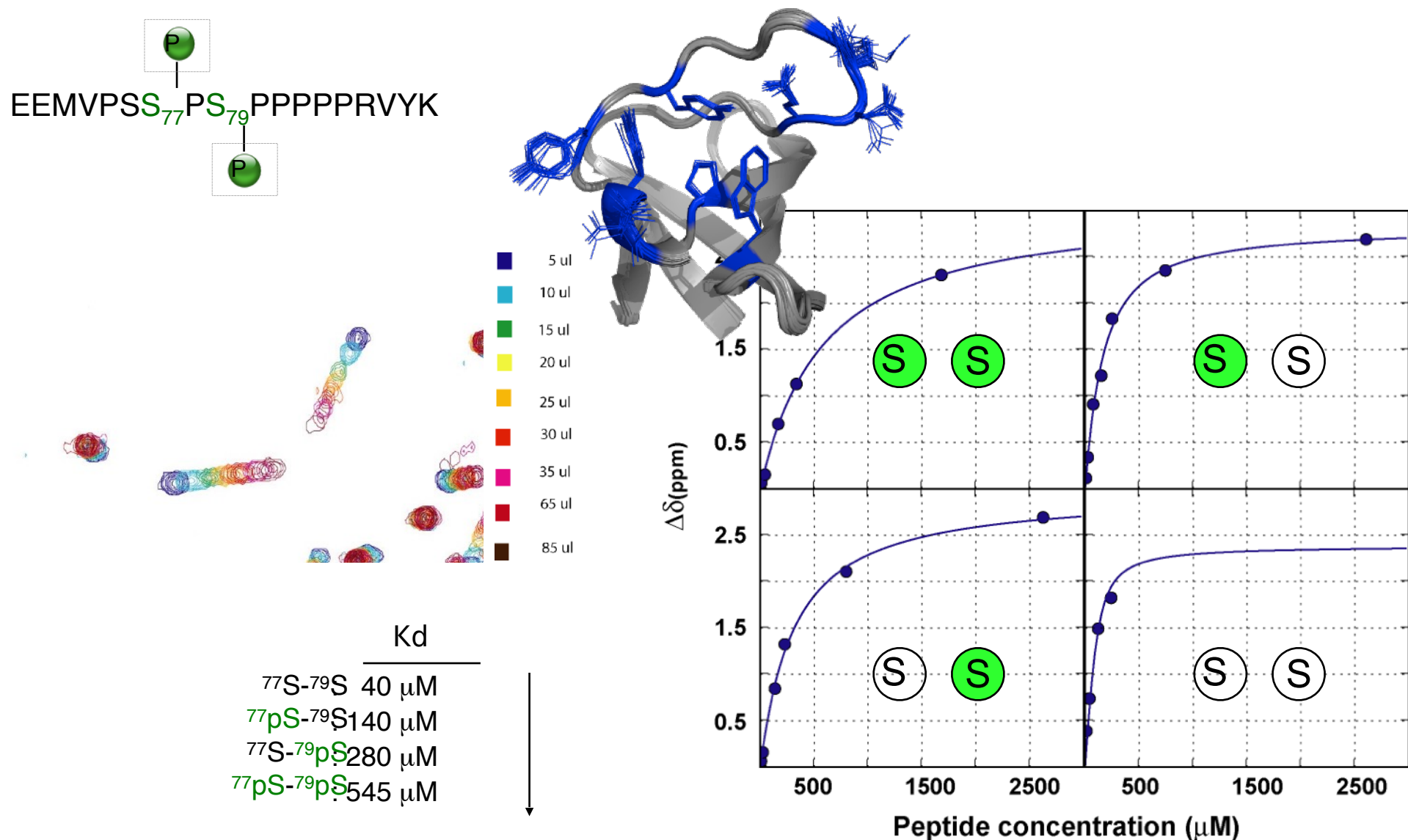
Chemical shift averaging



Using chemical shifts to study molecular interactions



Application: modulation of binding affinity between RAR and vinexin by RAR phosphorylation



Assignment problem

Journal of Biomolecular NMR (2005) 31: 67–68

Letter to the Editor: ^1H , ^{15}N and ^{13}C Backbone resonance assignments of the 37 kDa surface antigen protein Bd37 from *Babesia divergens*

Yin-Shan Yang^a, Stephane Delbecq^b, Marie-Paule Strub^a, Frank Löhre^c, Theo Schettler^d, André Gorenflot^b, Eric Precigout^b & Christian Roumestand^{a,*}

294 residues
37 kDa
293 peaks in ^{15}N -HSQC

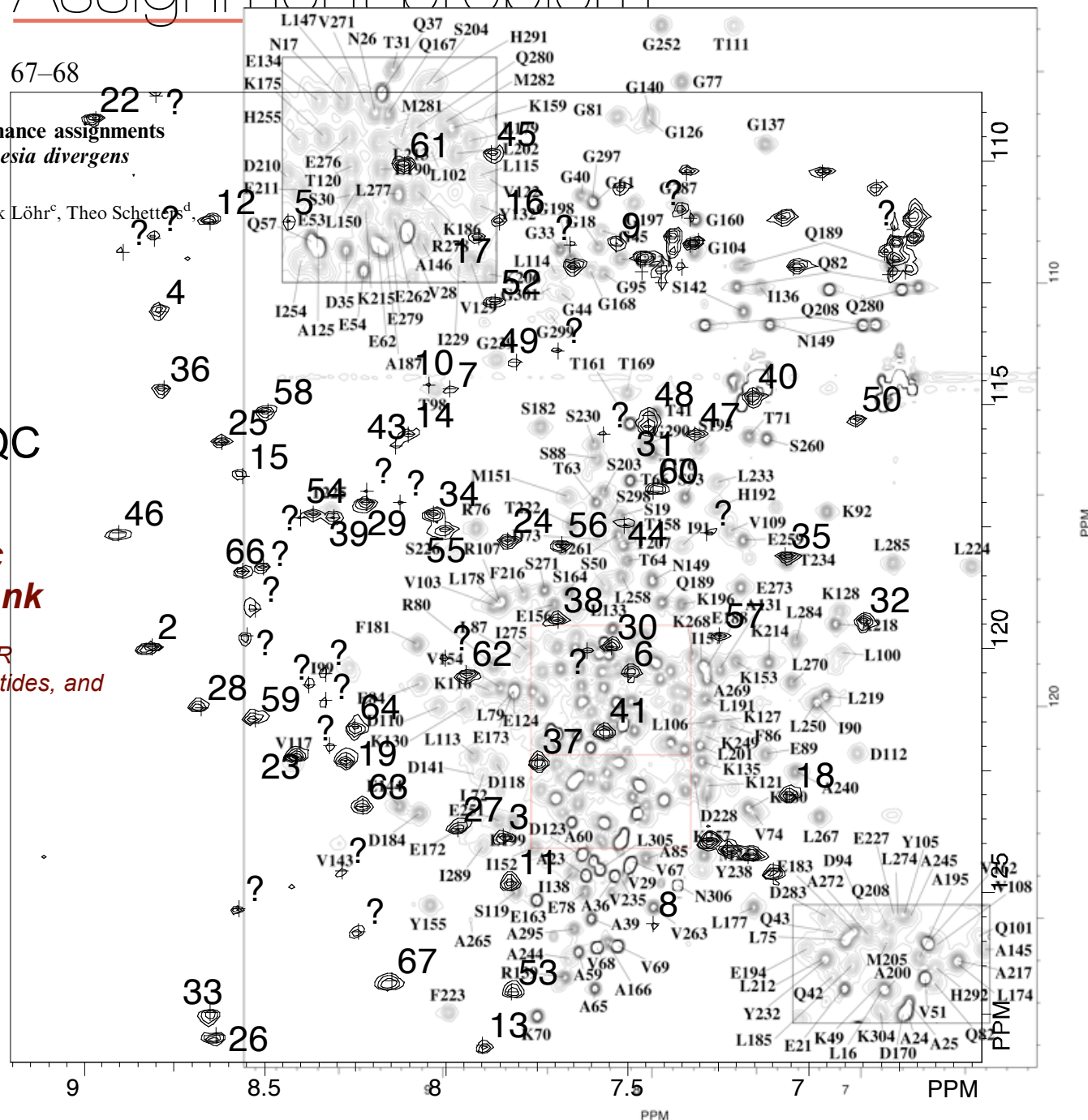


Biological Magnetic Resonance Data Bank

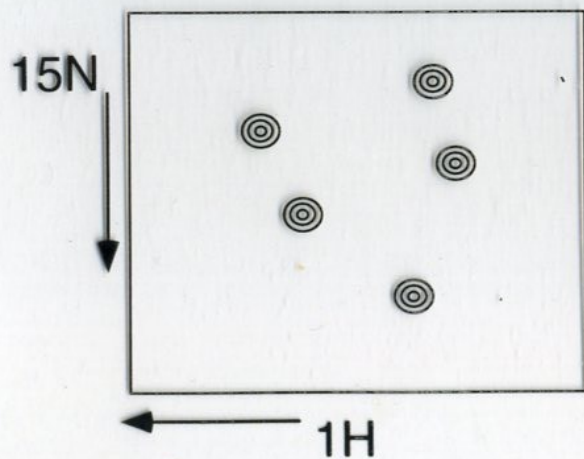
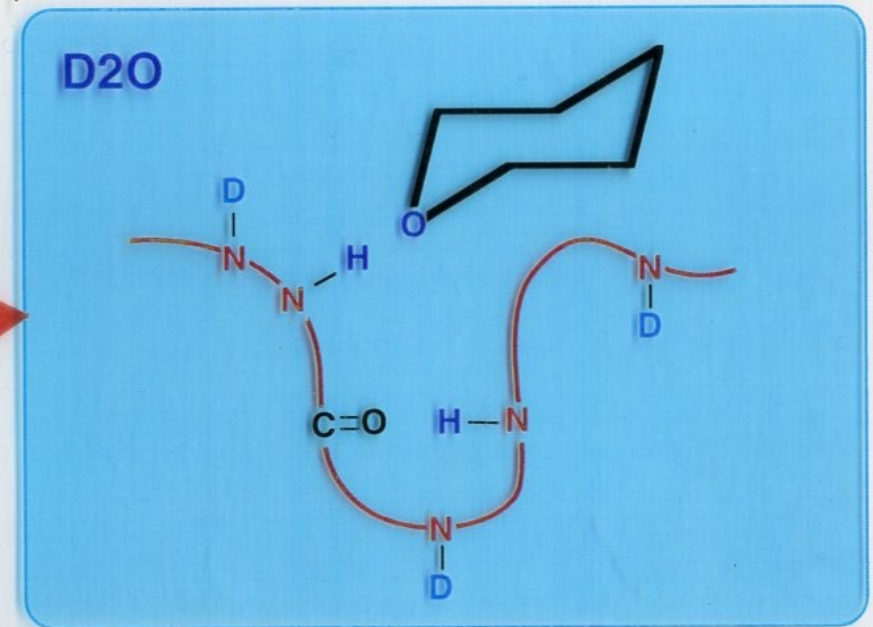
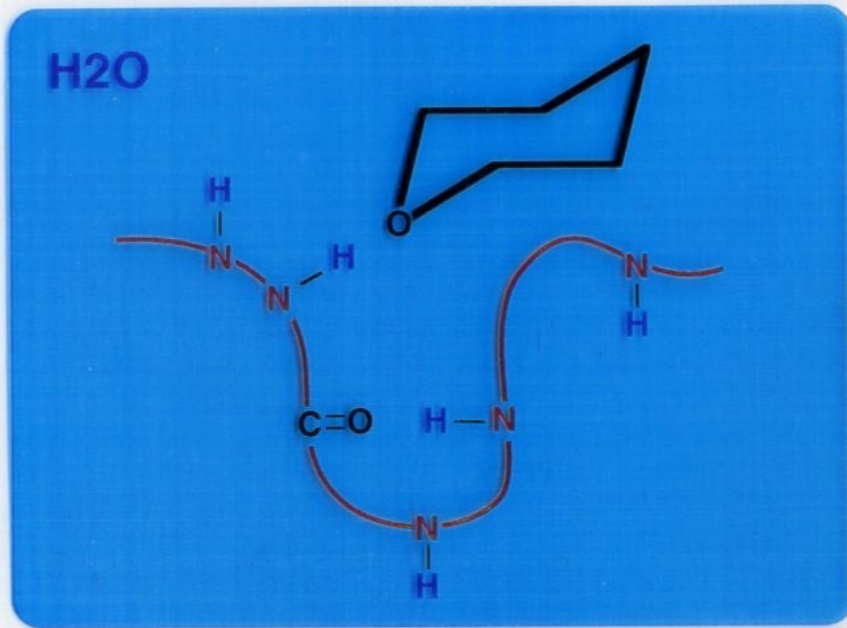
A Repository for Data from NMR Spectroscopy on Proteins, Peptides, and Nucleic Acids

Experimental Data:

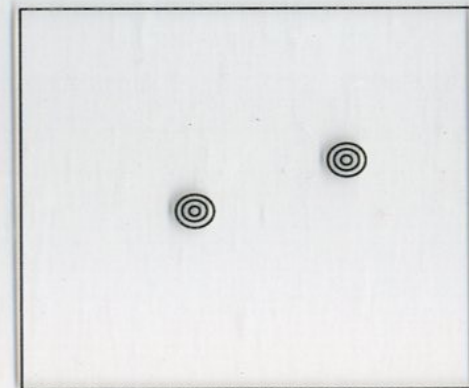
Type	Number of: Values Sets
Assigned Chemical Shifts	1
- ^1H Chemical Shifts	557
- ^{15}N Chemical Shifts	278
- ^{13}C Chemical Shifts	829



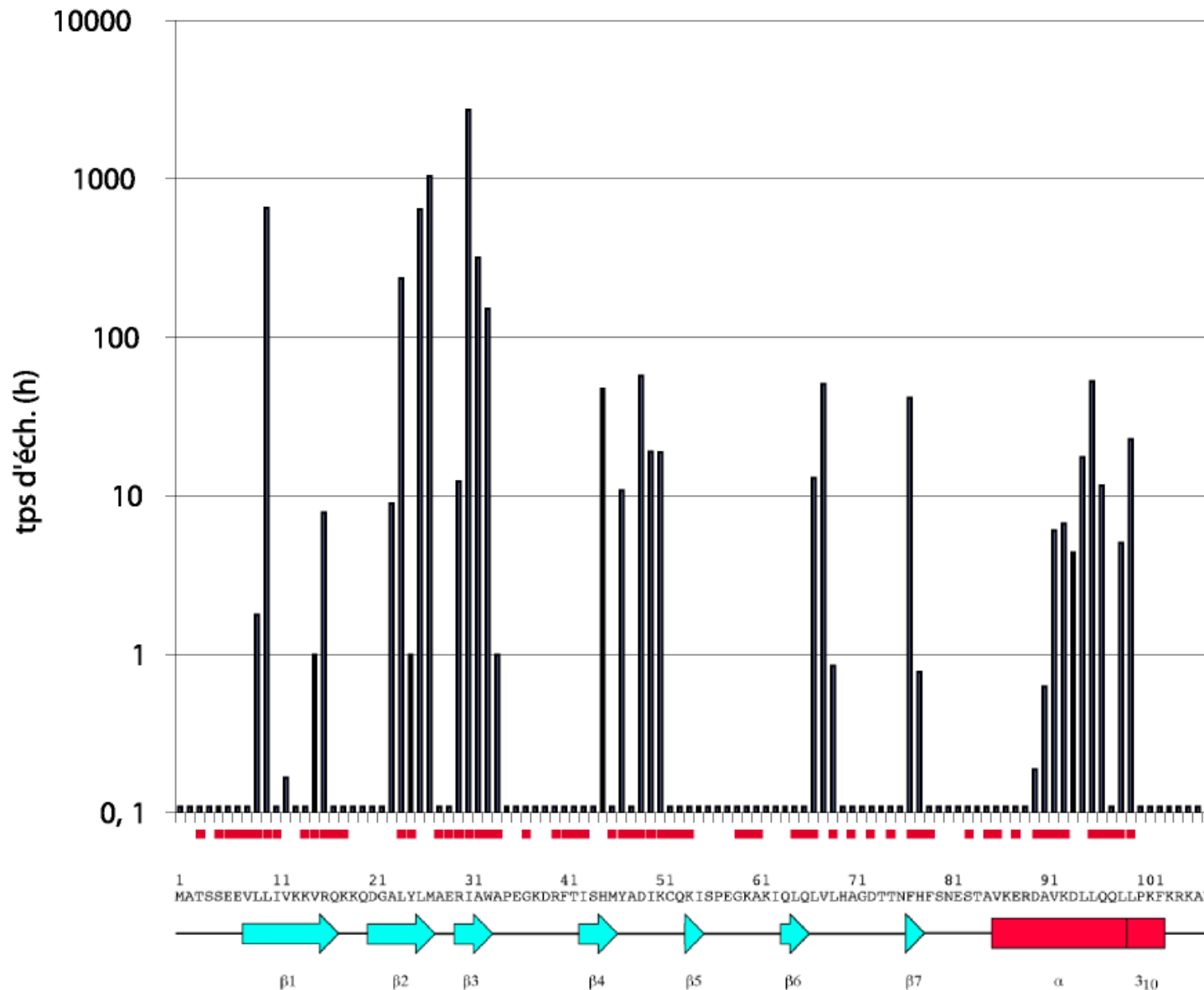
Real-time solvent exchange kinetic experiment



HSQC 15N



The exchangeable protons



Measure of proton exchange rates of amide protons of the PH domain of TFIIF P62 subunit

Gervais et al.
Nat struct biol 2004

3D Structure Determination

THE JOURNAL OF BIOLOGICAL CHEMISTRY
© 2003 by The American Society for Biochemistry and Molecular Biology, Inc.

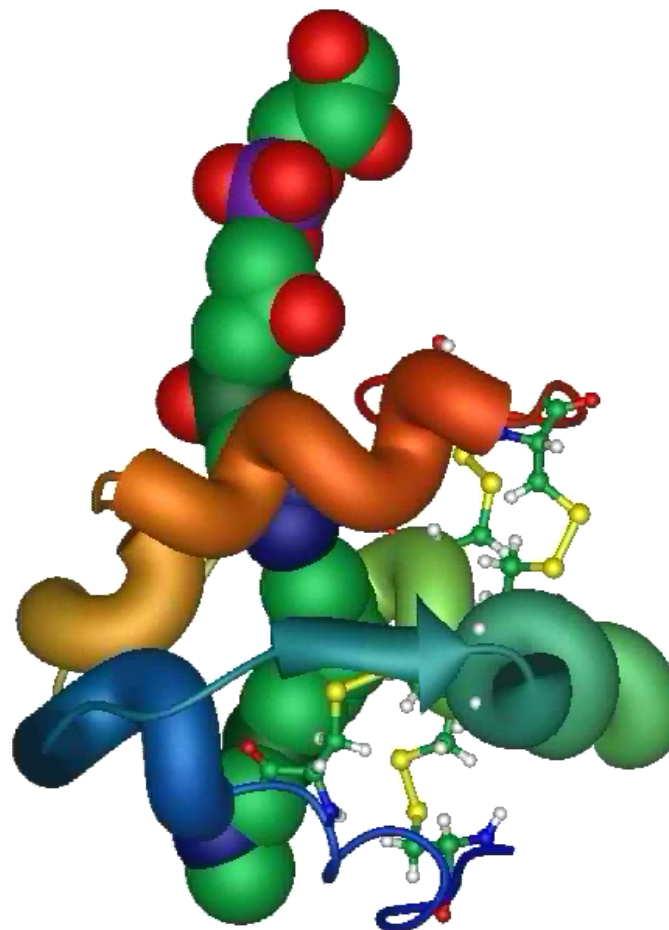
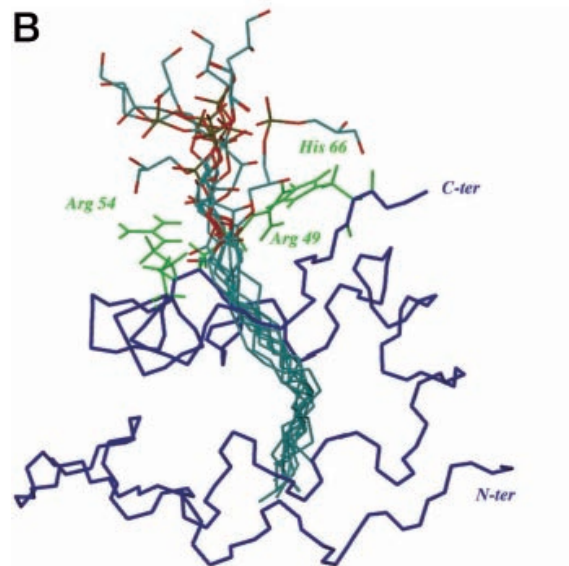
Vol. 278, No. 16, Issue of April 18, pp. 14249–14256, 2003
Printed in U.S.A.

Refined Solution Structure of a Liganded Type 2 Wheat Nonspecific Lipid Transfer Protein*

Received for publication, November 15, 2002, and in revised form, January 10, 2003
Published, JBC Papers in Press, January 13, 2003, DOI 10.1074/jbc.M211683200

Jean-Luc Pons[‡], Frédéric de Lamotte[§], Marie-Françoise Gautier[§], and Marc-André Delsuc^{‡¶}

jbc

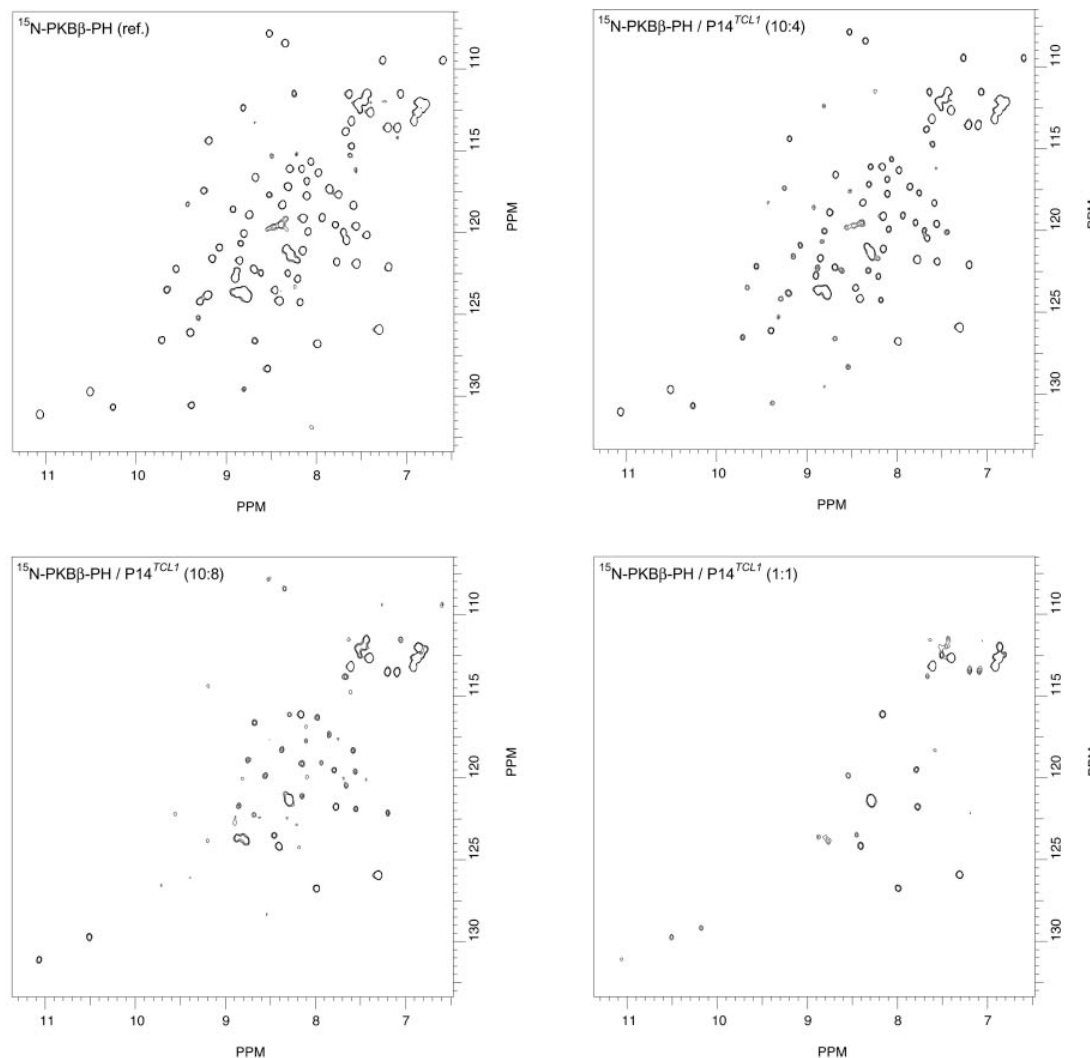


from NOE measures,
⇒ local proximities
between hydrogens
through space

obtained by MolMod

Structural Basis for the Co-activation of Protein Kinase B by T-cell Leukemia-1 (TCL1) Family Proto-oncoproteins*[§]

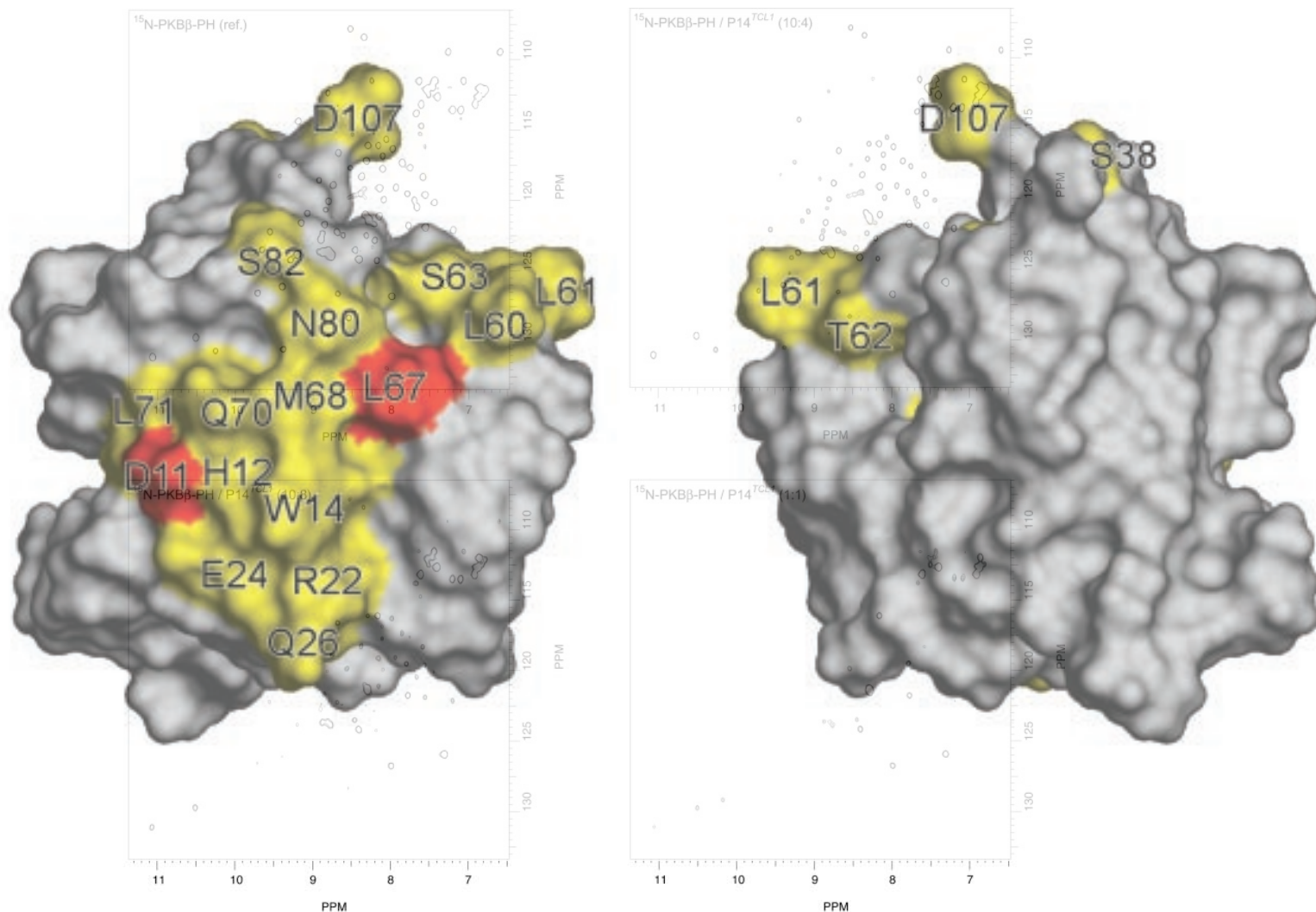
Daniel Auguin[‡], Philippe Barthe[‡], Catherine Royer[‡], Marc-Henri Stern[§], Masayuki Noguchi[¶], Stefan T. Arold^{‡||}, and Christian Roumestand^{‡||}



titration de PKB (Akt) par l'oncoprotéine P14^{TCL1}

Structural Basis for the Co-activation of Protein Kinase B by T-cell Leukemia-1 (TCL1) Family Proto-oncoproteins*[§]

Daniel Auguin[‡], Philippe Barthe[‡], Catherine Royer[‡], Marc-Henri Stern[§], Masayuki Noguchi[¶], Stefan T. Arold^{‡||}, and Christian Roumestand^{‡||}



titration de PKB (Akt) par l'oncoprotéine P14^{TCL1}

Structural Basis for the Co-activation of Protein Kinase B by T-cell Leukemia-1 (TCL1) Family Proto-oncoproteins*[§]

Daniel Auguin[‡], Philippe Barthe[‡], Catherine Royer[‡], Marc-Henri Stern[§], Masayuki Noguchi[¶], Stefan T. Arold^{‡||}, and Christian Roumestand^{‡||}

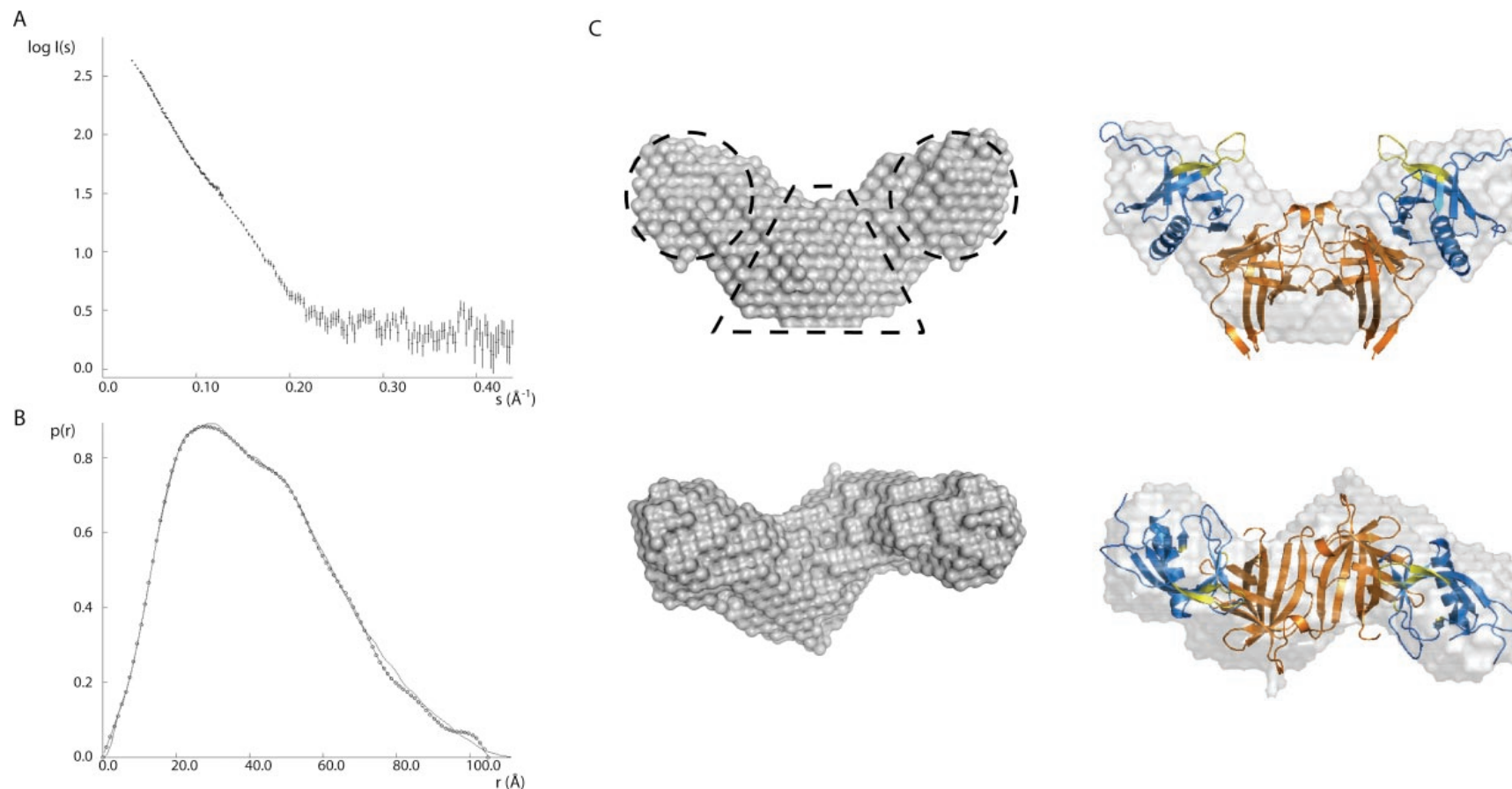
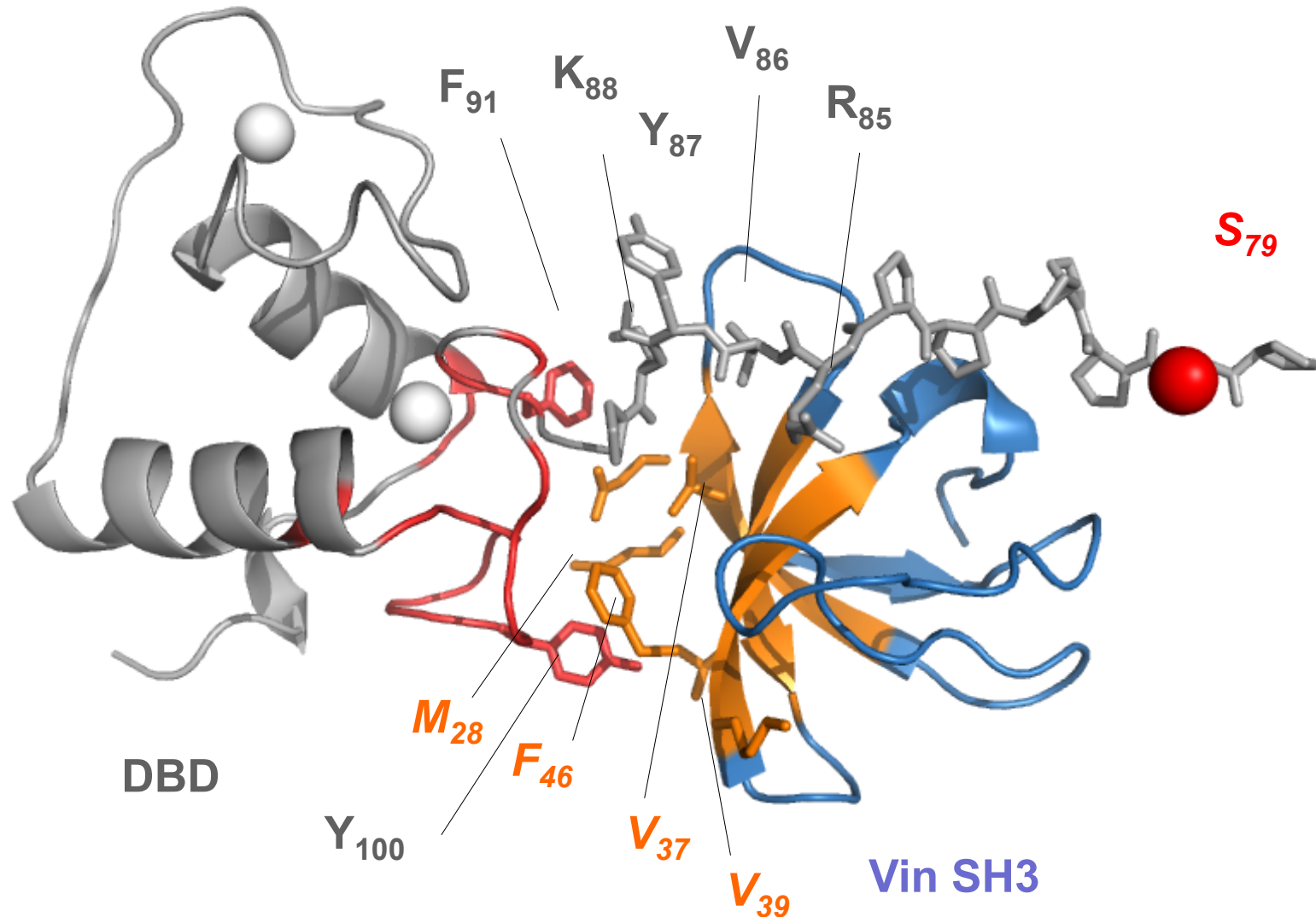


FIG. 6. SAXS analysis of the PKBβ-PH-p14^{TCL1} complex. *A*, experimental scattering data. Error bars are indicated by vertical lines. *B*, pair distribution function $p(r)$ for the PKBβ-PH-p14^{TCL1} complex. Open circles, experimental curve; solid line, calculated curve for a typical *ab initio* model. *C*, side and top views of the molecular envelope of the PKBβ-PH-p14^{TCL1} complex obtained by averaging 10 individual *ab initio* models. Proposed position of PKBβ-PH domains (circles) and the p14^{TCL1} dimer (trapeze) within the SAXS envelope are indicated in the side view.

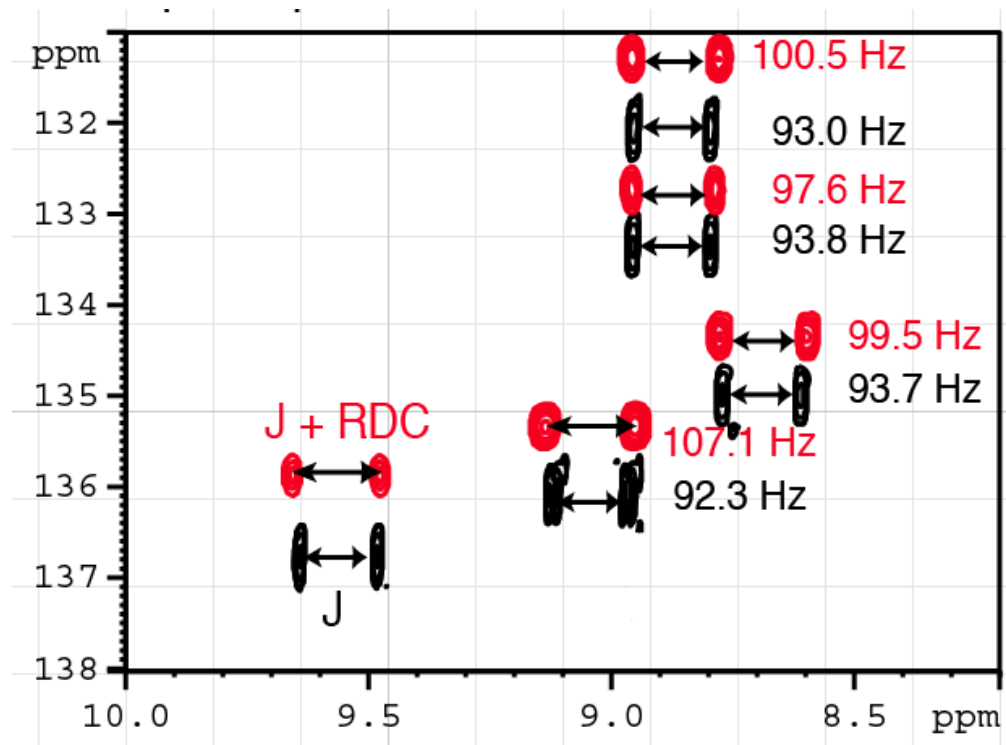
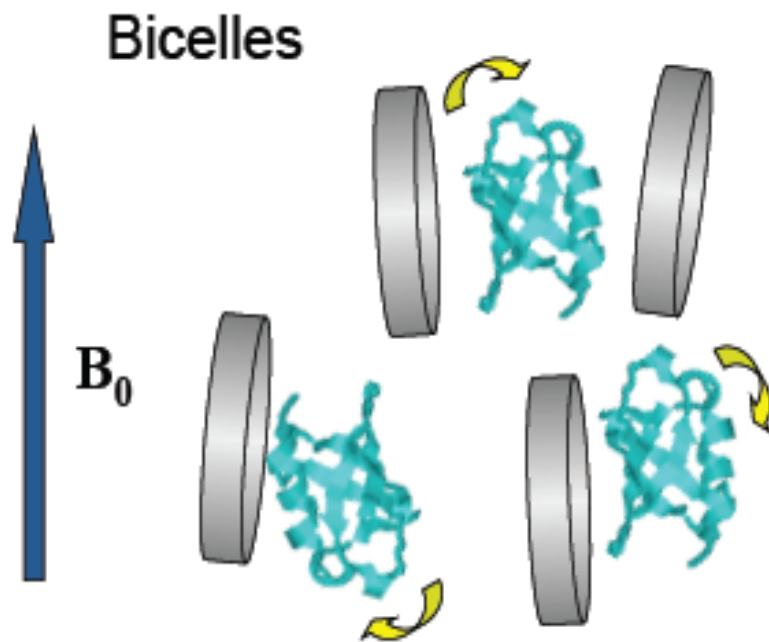
Protein-Protein interaction

3D model of the Vin SH3.3 / RAR γ DBD complex using HADDOCK



Residual dipolar couplings (RDC)

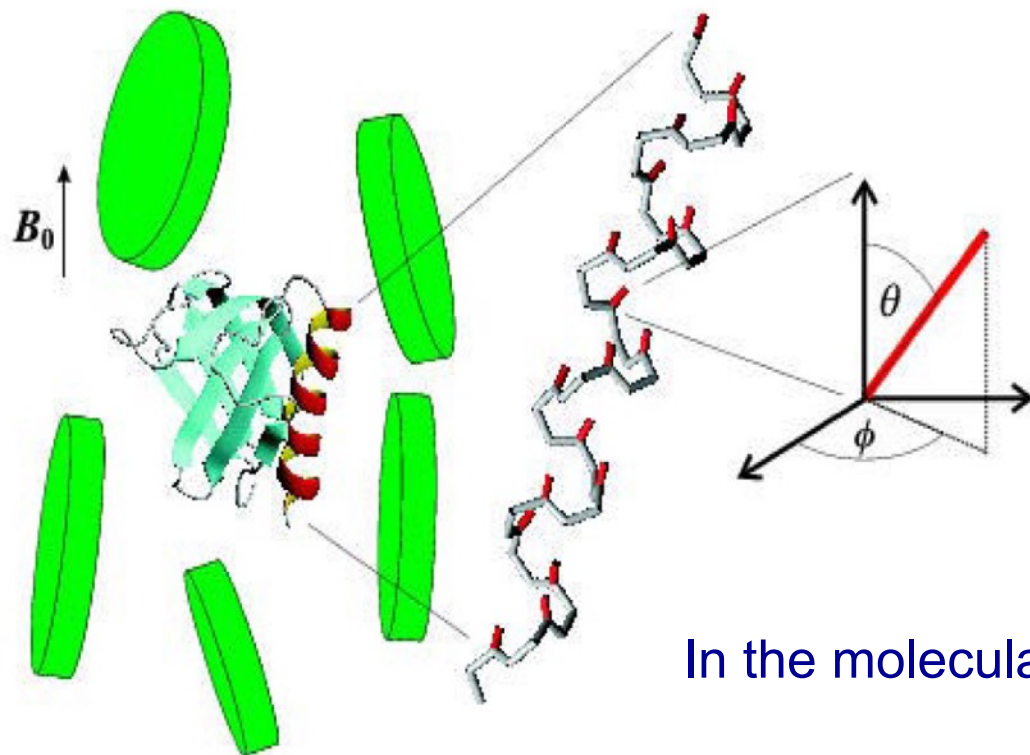
- Principle: the sample is diluted in an anisotropic medium
- This introduces a very small bias in the molecular orientations
- That leads to dipolar couplings that depends on the orientation of the internuclei vectors of the molecules



Partially oriented molecule

Isotropic phase

Modeling RDC data

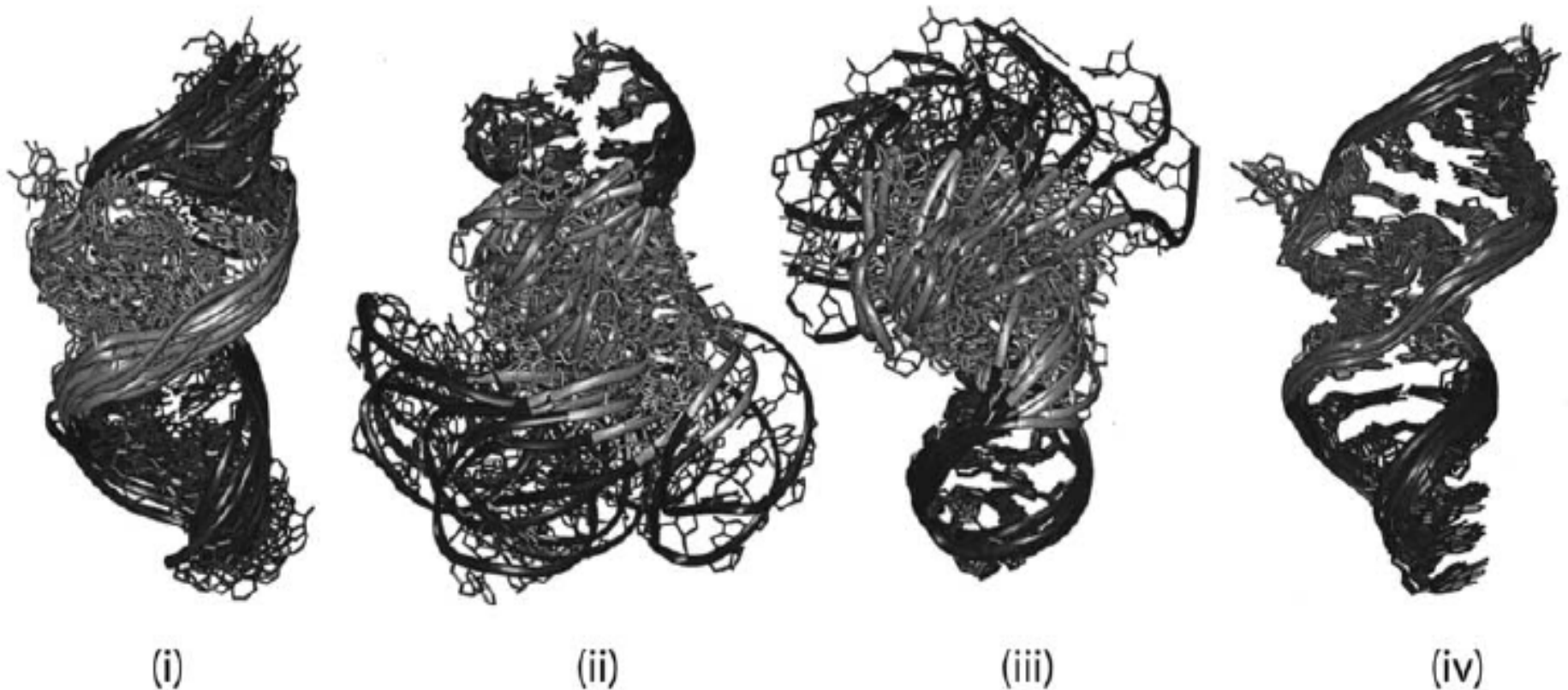


In the molecular frame:

$$RDC = D_a \left\{ (3 \cos^2 \theta - 1) + \frac{3}{2} R \sin^2 \theta \cos 2\phi \right\}$$

At least 5 RDC values are needed to define the molecular frame

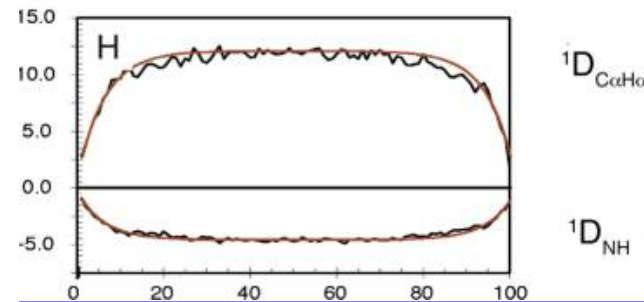
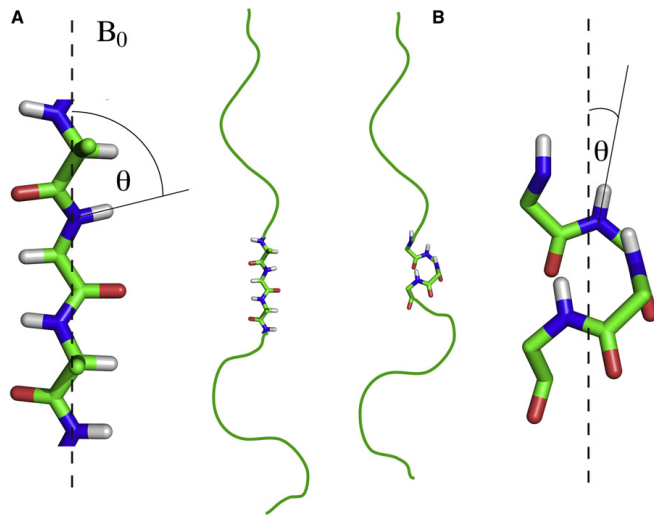
Application of RDC to RNA structure



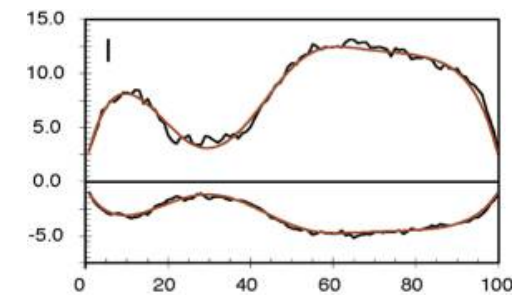
Calculation of the structure of the theophylline-binding RNA aptamer using ^{13}C – ^1H residual dipolar couplings and restrained molecular dynamics.

by adding the angular dependence : (non local)
to NOE constraints (local)

RDC of IDP



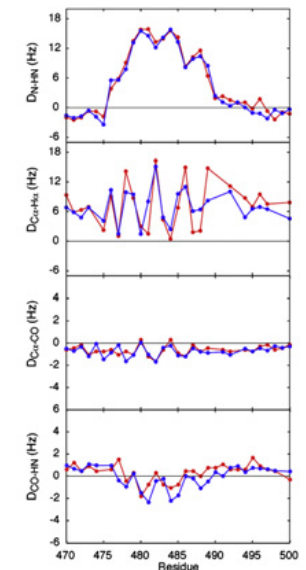
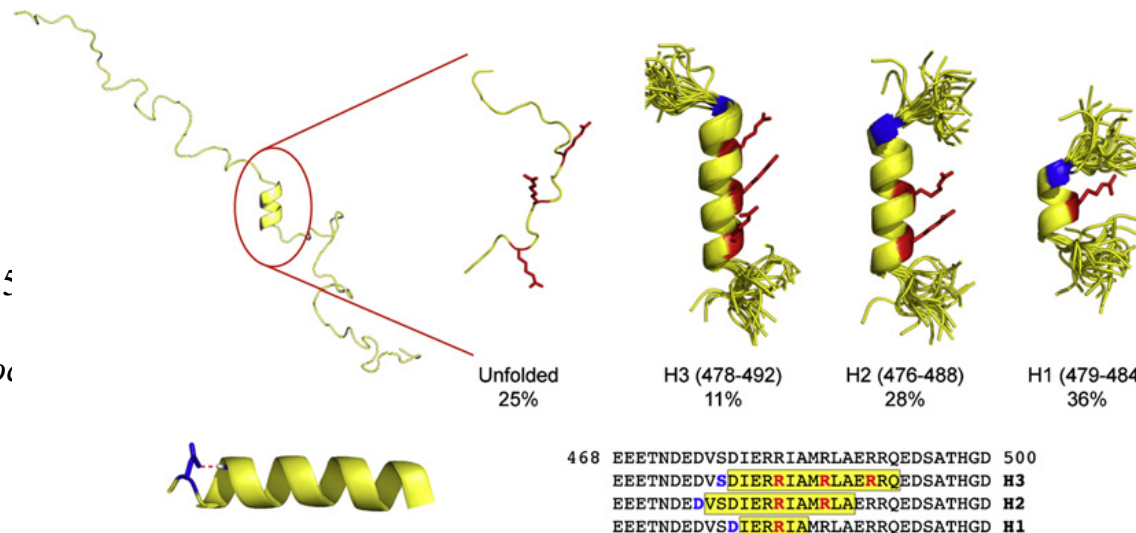
no LR contact



with LR contacts

Jensen, M. R., .. M. Blackledge (2009). *Structure* 17(9), 1169–1185

Jensen, M. R., Blackledge, M. *Proc Natl. Acad. Sci. U.S.A.* 2011, 108, 9839



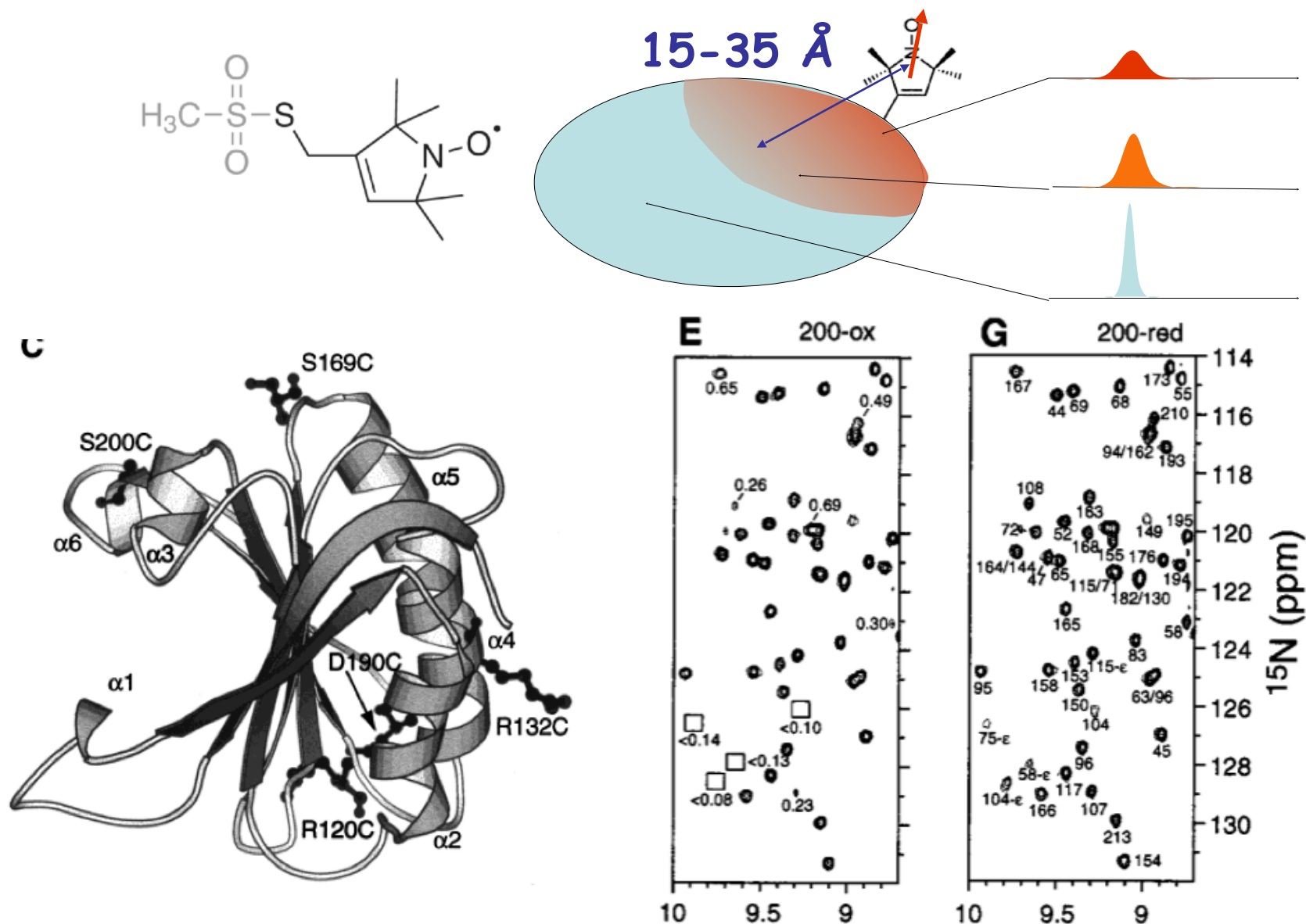
Paramagnetic Relaxation Enhancement

- ◆ The presence of an electronic spin in the vicinity of nuclear spins increases their relaxation rates
- ◆ If the electronic spin is characterized by an isotropic g tensor, the effect depends only on the distance between the nucleus and electronic spins

$$R_2^{PRE} = \frac{1}{15} \left(\frac{\mu_0}{4\pi} \right)^2 \gamma_I^2 g^2 \mu_B^2 S(S+1) \left(\frac{1}{r_{IS}^6} \right) \left\{ 4\tau_c + \frac{3\tau_c}{1 + (\omega_I \tau_c)^2} \right\}$$

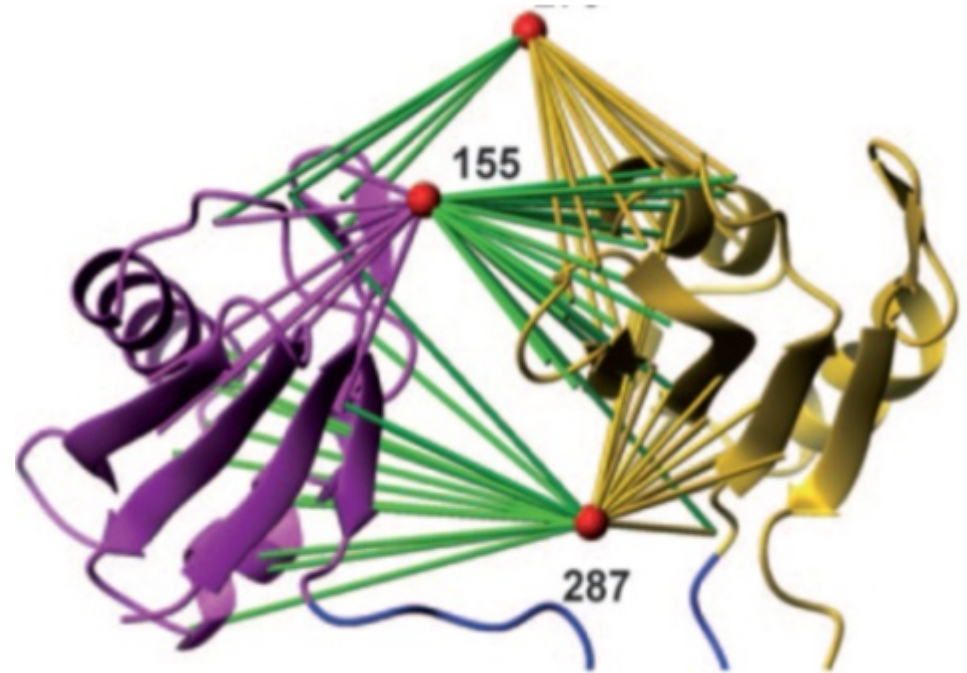
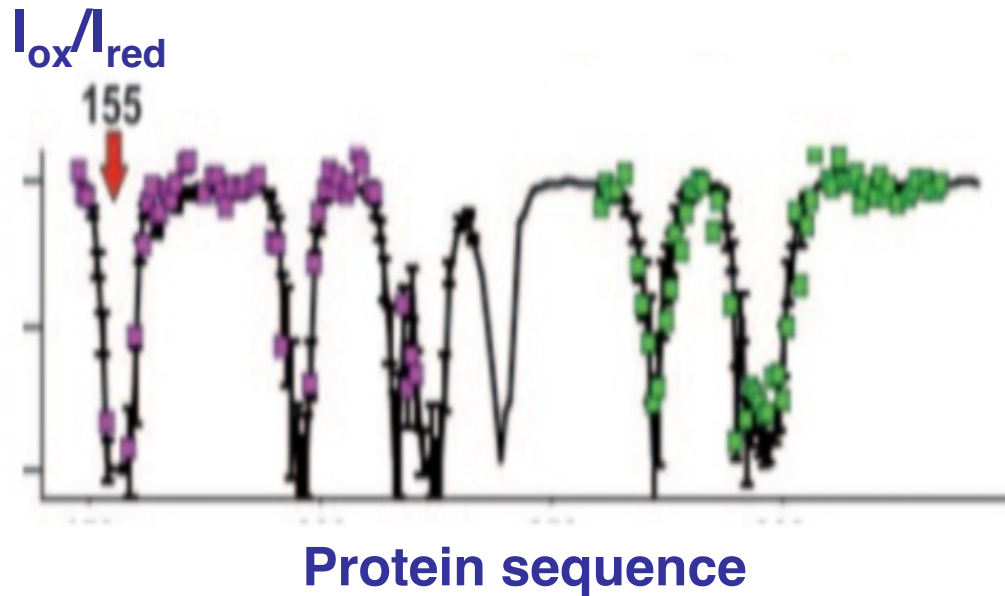
$$R_1^{PRE} = \frac{2}{5} \left(\frac{\mu_0}{4\pi} \right)^2 \gamma_I^2 g^2 \mu_B^2 S(S+1) \left(\frac{1}{r_{IS}^6} \right) \left\{ \frac{\tau_c}{1 + (\omega_I \tau_c)^2} \right\}$$

Introducing spin label to protein surface

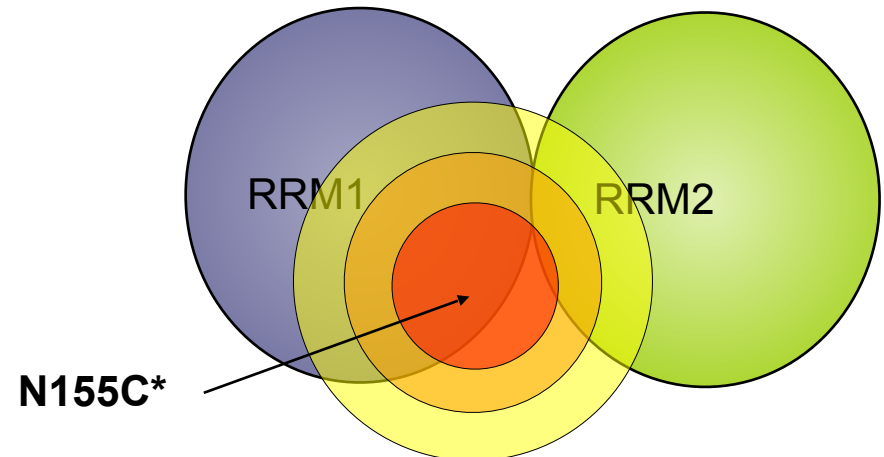


Battiste et Wagner Biochemistry V39, p5355 (2000)

Application to multiple domain proteins

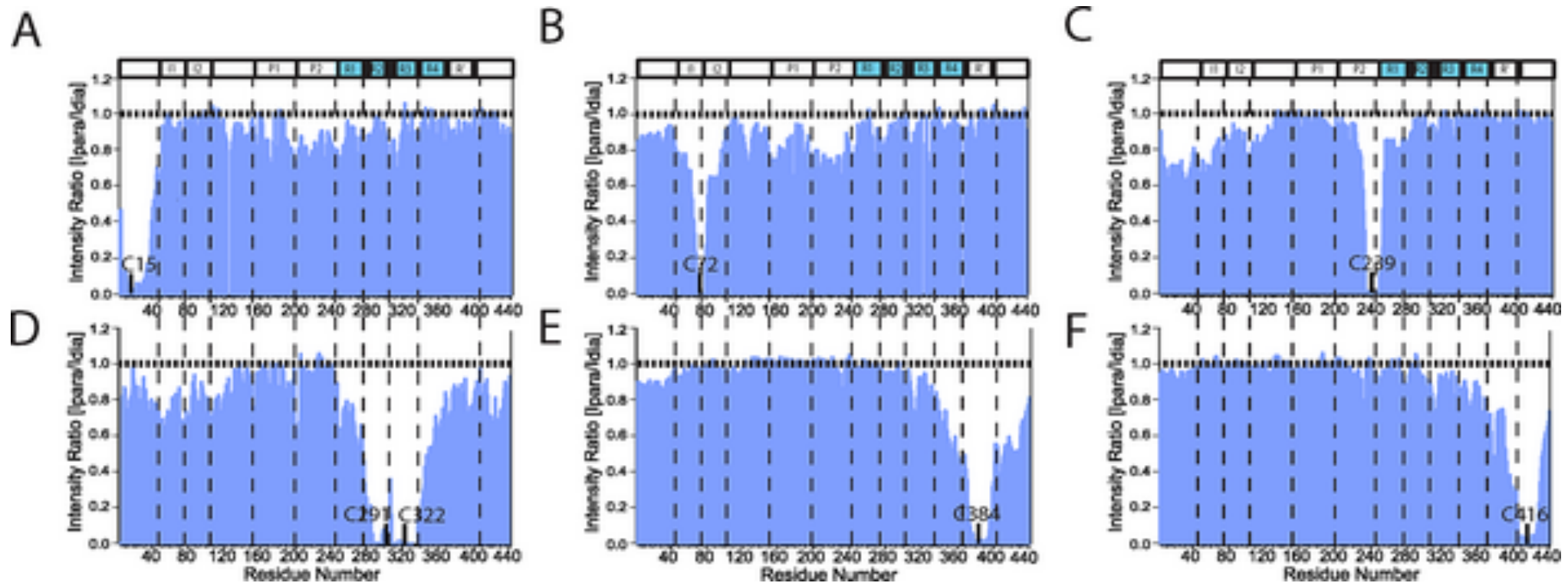


- >12 Å (not bleached)
- <20 Å (25% reduction)
- <15 Å (50% reduction)
- <10 Å (heavy bleaching)



Applied to IDP (Tau)

Figure 7. PRE of Amide Protons in Spin-Labelled Tau

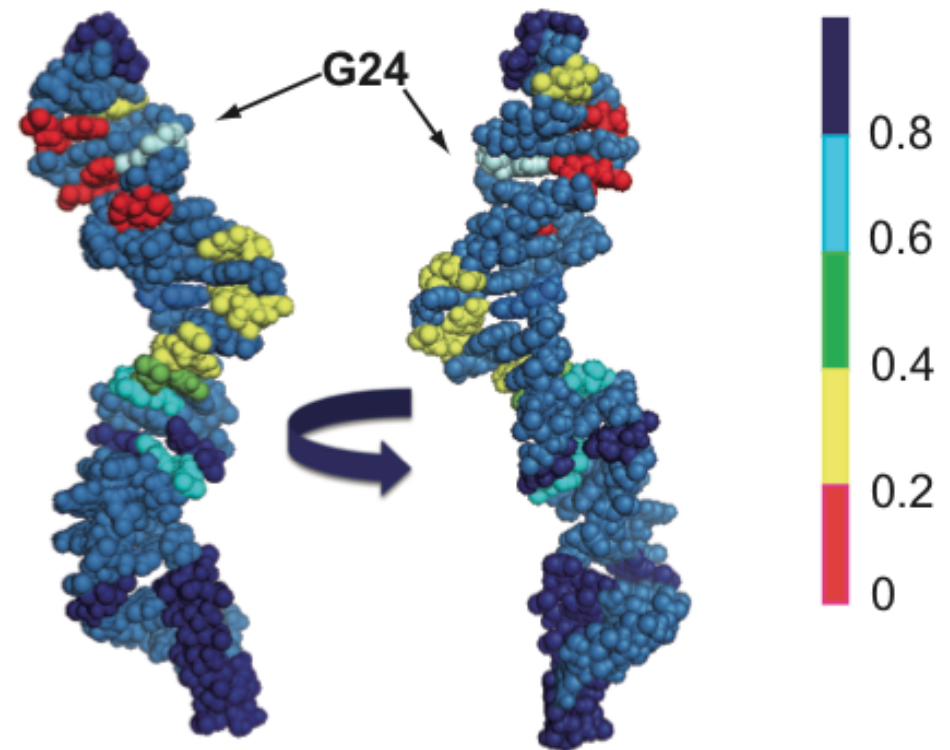
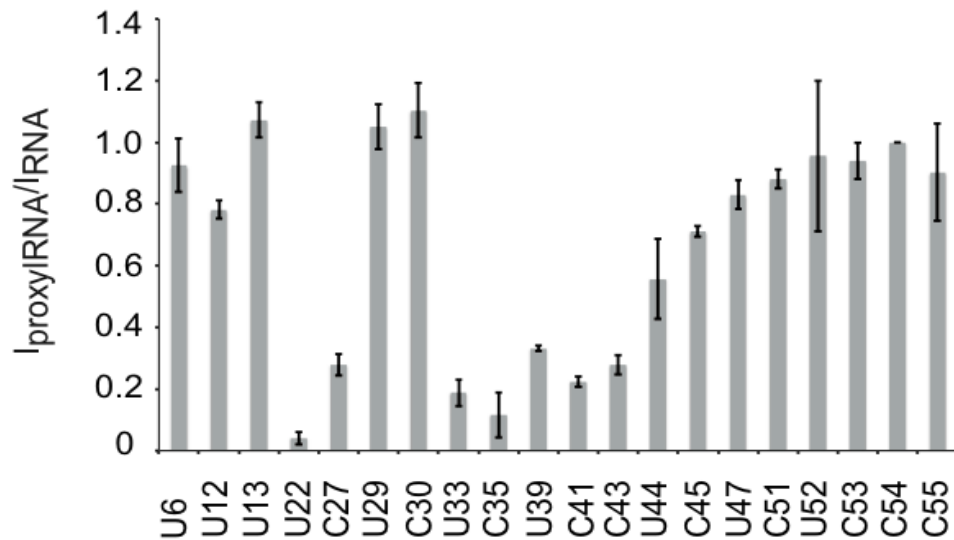
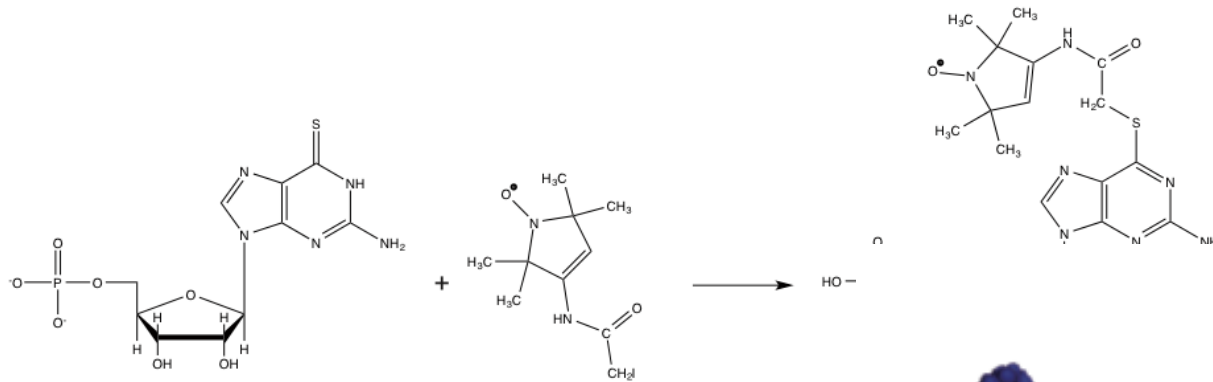


Mukrasch MD, Bibow S, Korukottu J, Jeganathan S, et al. (2009) Structural Polymorphism of 441-Residue Tau at Single Residue Resolution. PLoS Biol 7(2): e1000034. doi:10.1371/journal.pbio.1000034
<http://www.plosbiology.org/article/info:doi/10.1371/journal.pbio.1000034>

RNA spin labelling

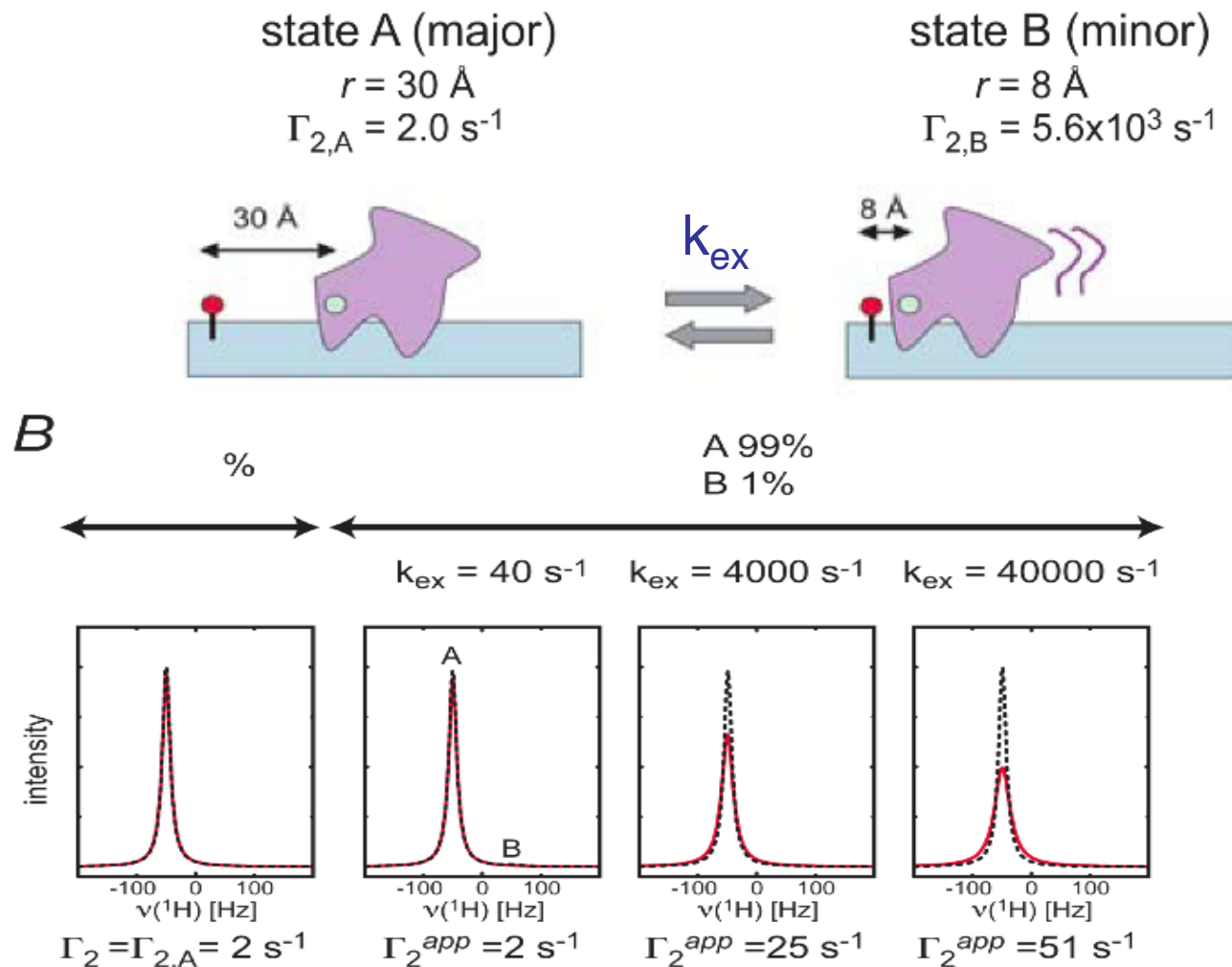
Lebars I.*, Vileno B., Bourbigot S., Turek P., Wolff P. & Kieffer B. (2014)

"A fully enzymatic method for site-directed spin-labeling of long RNA", *Nucleic Acids Res.*, 42(15), e117,



PRE based amplification of low population states

- ◆ Due to the r^{-6} distance dependance of the PRE, small distances in low populated states may be revealed



Iwahara & Clore (2006)
Nature 440, p 1227

Phenomenon

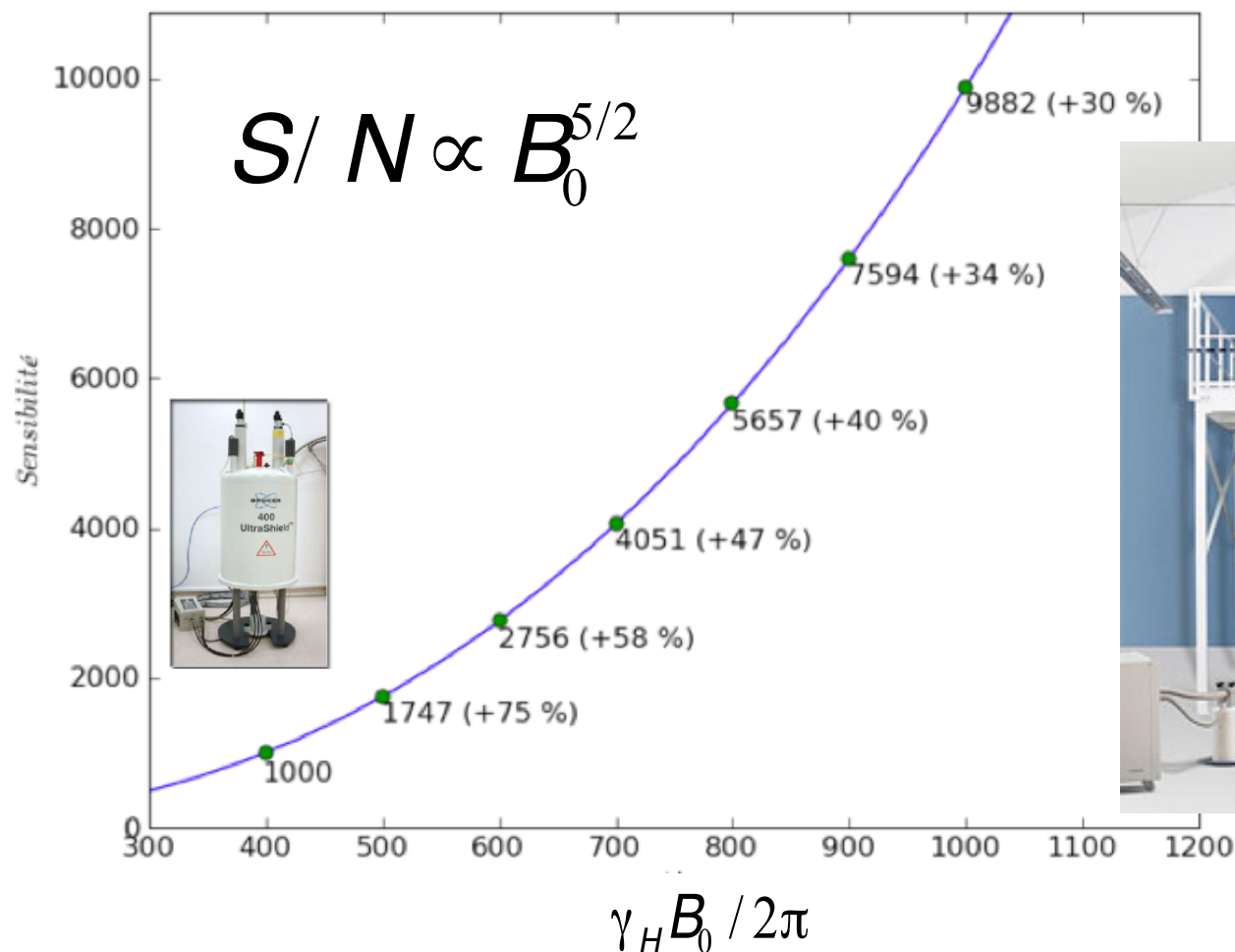
- Chemical-Shift \equiv position in the spectrum
- Spin-Spin coupling
 - “Dipolar” coupling - depends on spin-spin geometry
 - “Scalar” coupling - depends on electronic orbital
- Relaxation
 - *decoherence* of the quantum states
- NOE
 - relaxation due to spin-spin \Rightarrow information on atomic distances
- RDC: Reduced Dipolar Coupling
 - information on angular geometry
- PRE: Paramagnetic Relaxation Experiment
 - relaxation due to electronic spin-spin \Rightarrow information on molecular contacts

final remarks

- sensitivity aspects
- protein size aspects
- signal aspects
- more than structure

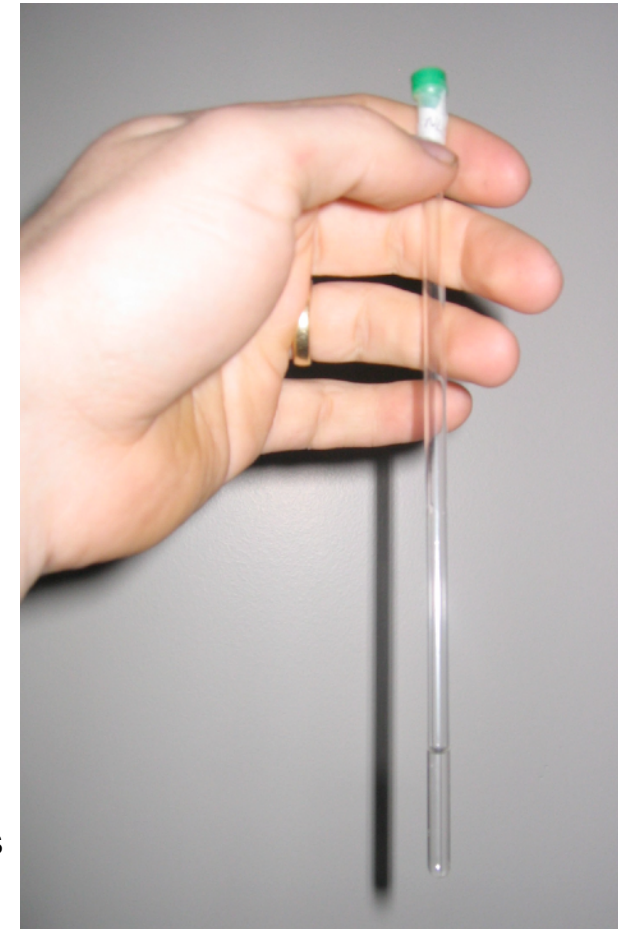
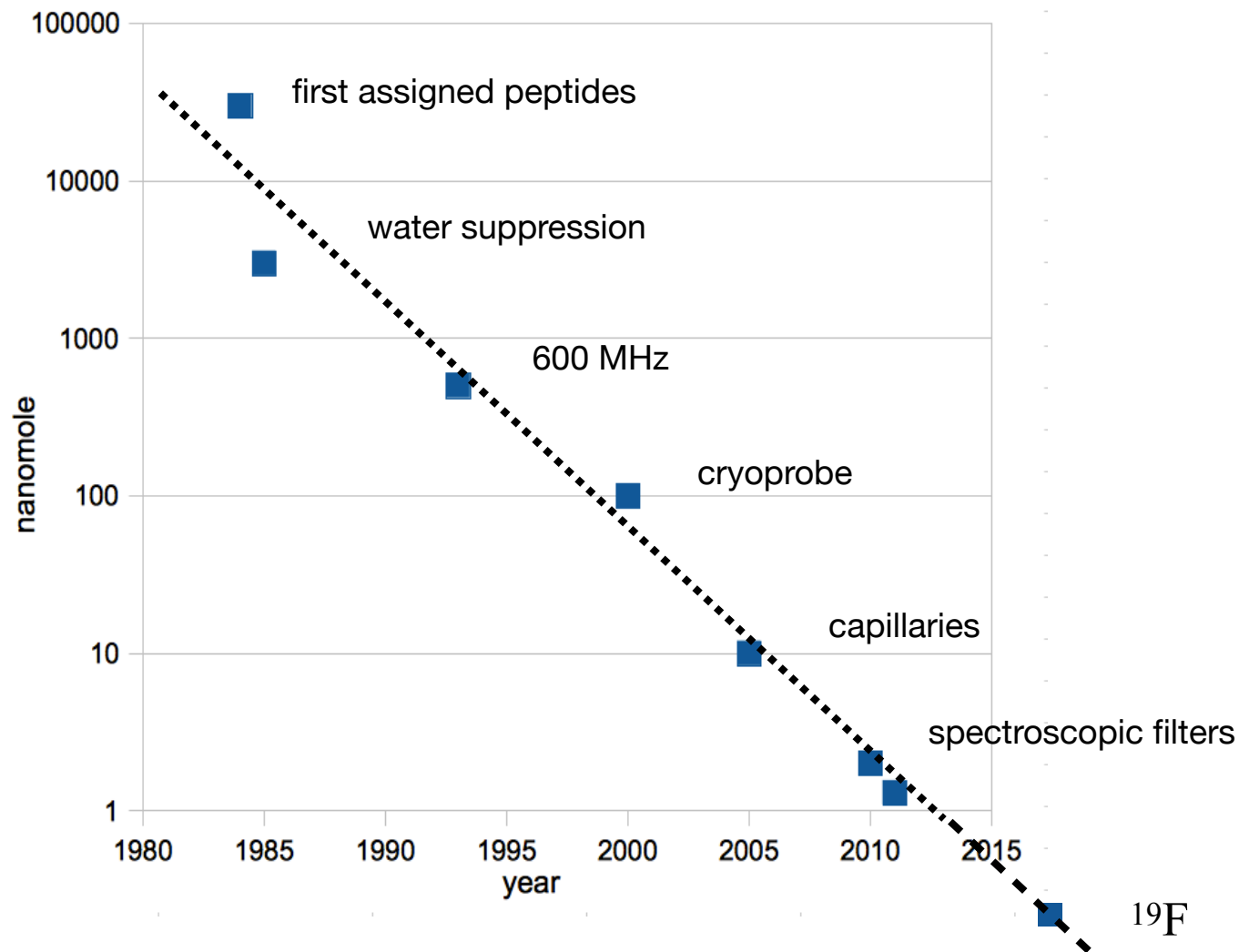
Recent advance in NMR instruments

- The Signal/Noise ratio depends on the applied magnetic field



Sensitivity increase over my carrier

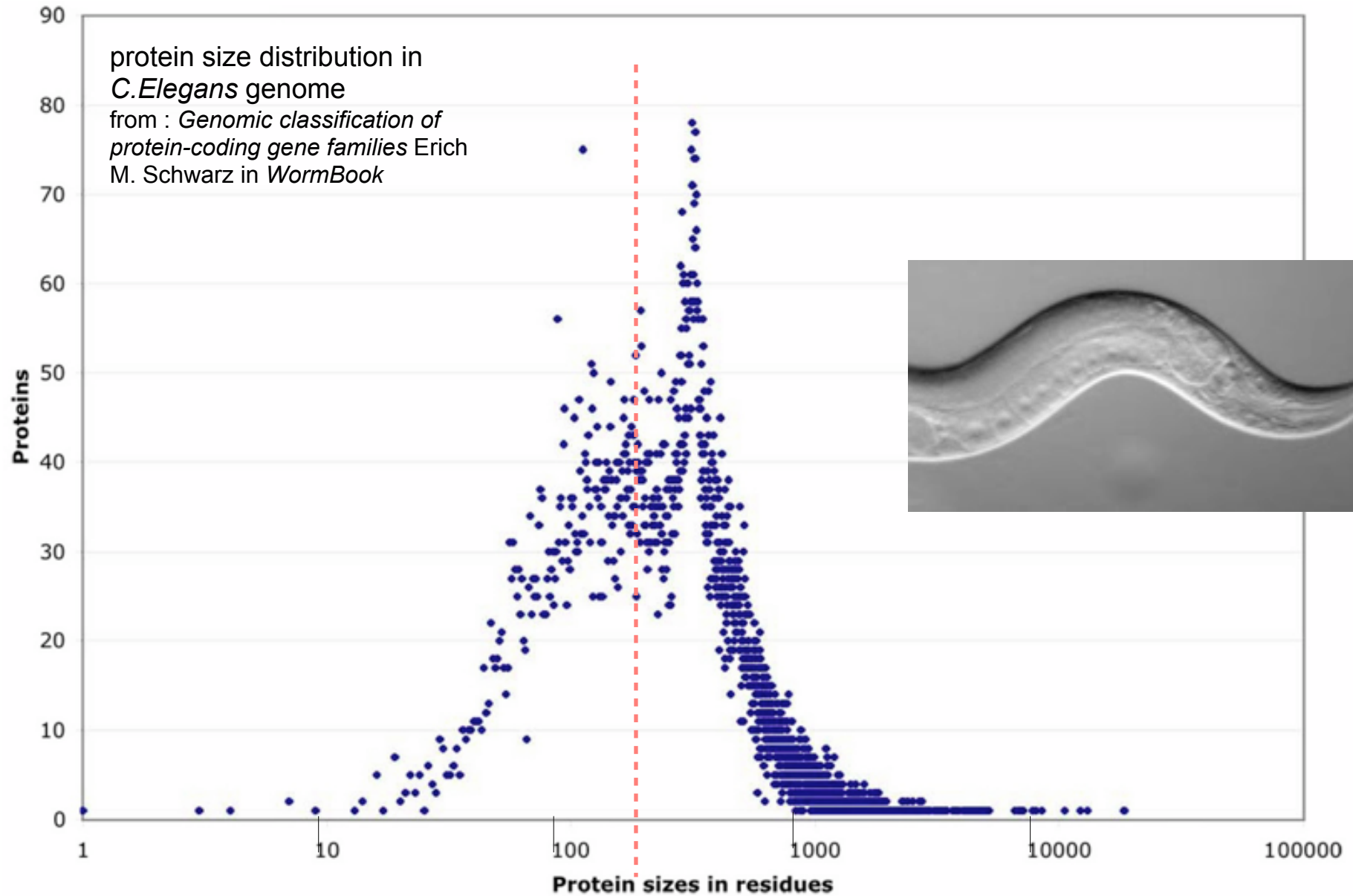
Protein quantity \sim Moore law
/2 every 2 years /1000 in 20 years



Strategy related to size

- tiny proteins $M < 6 \text{ kD}$
 - ▶ very easy to study
 - ▶ peptides !
- small proteins $M < 12\text{-}15 \text{ kD}$
 - ▶ easy -
 - ▶ ^{15}N labelling might be enough
- larger proteins $M < 40 \text{ kD}$
 - ▶ ^{15}N and ^{13}C required - ^2H to be considered
- very large proteins $M > 50 \text{ kD}$
 - ▶ ^2H labelling and ^{15}N / ^{13}C labelled specific incorporation
- beware of “hidden” oligomers
 - Glutathion-S-Transferase 2x50kD
 - Insuline : 6x6kD

Distribution de taille



Overview of cell free isotopic labeling



Specific amino acids labeling

CECF

Val, Thr ^{15}N , ^{13}C

+ 18 aa unlabeled

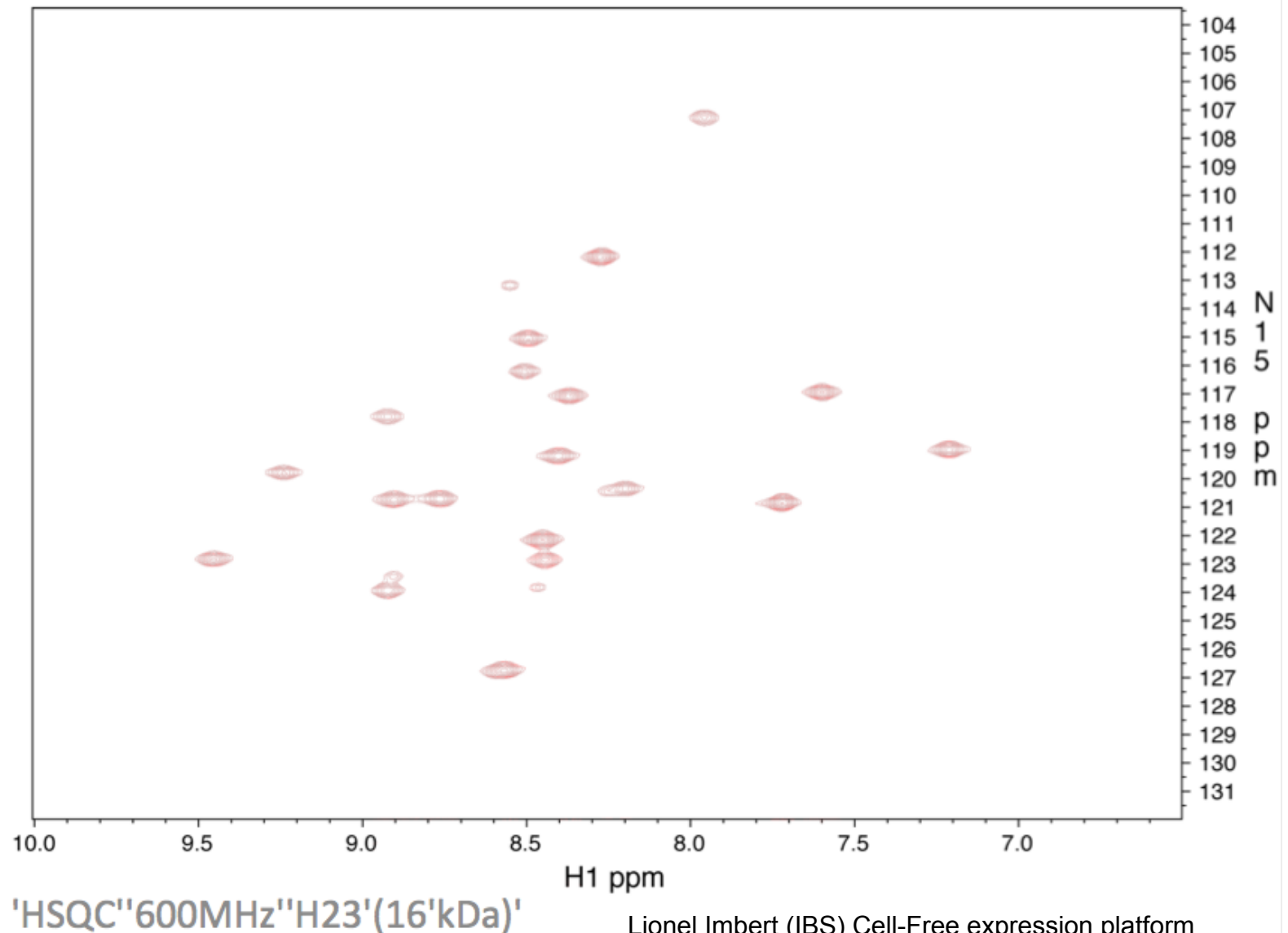
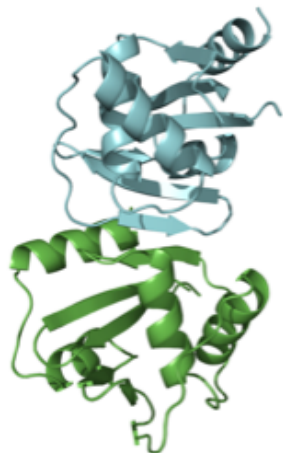
Expected peaks: 21

^{13}C Val

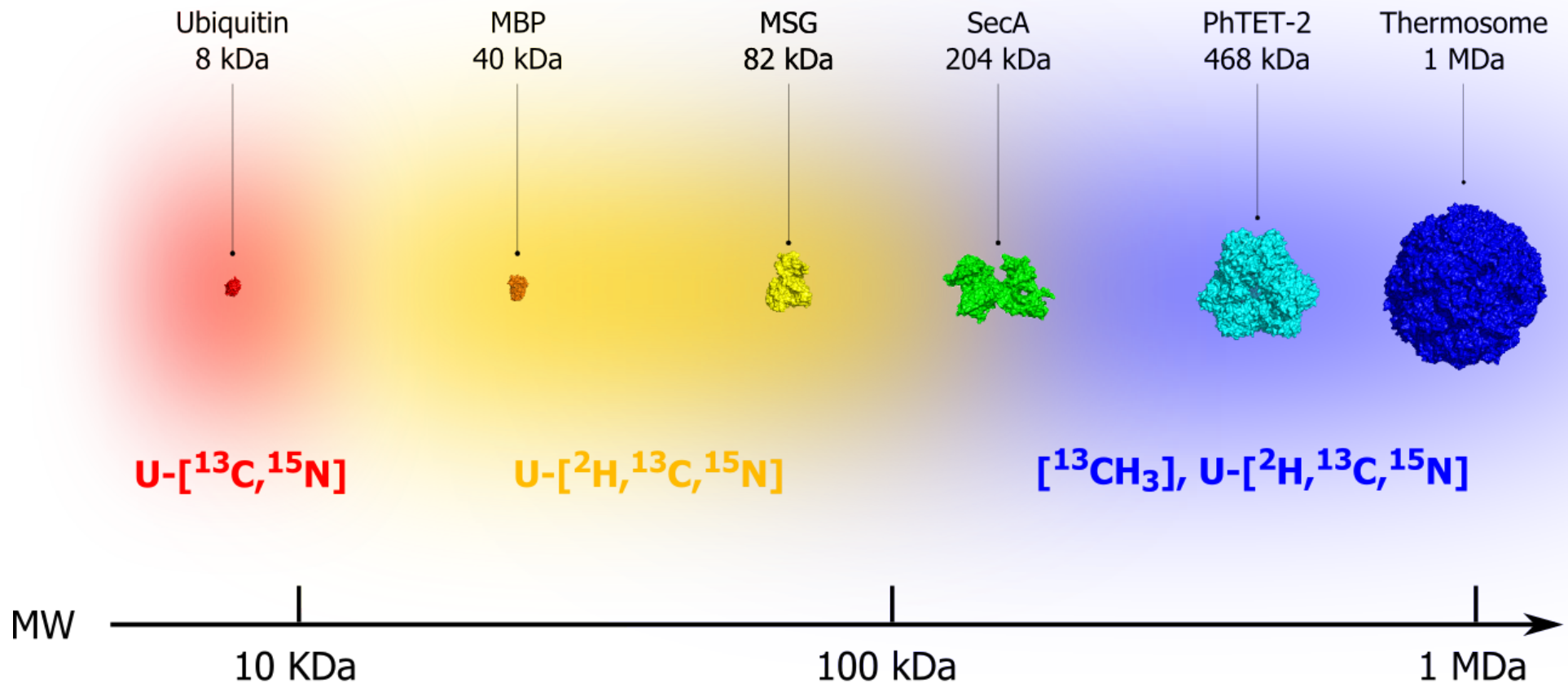
8 Thr

Observed: 22

Yield 4mg/ml



Is NMR spectroscopy only limited to small molecules?

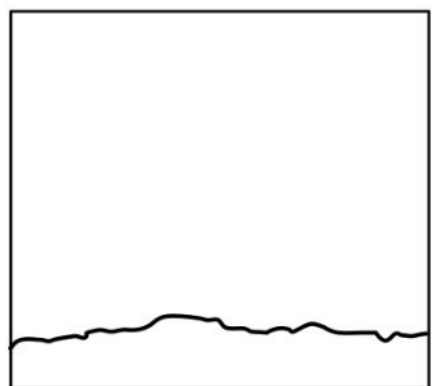
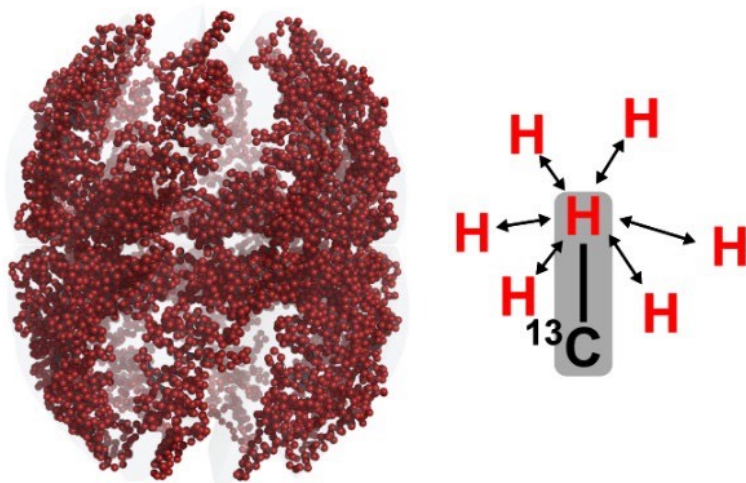


Courtesy of J Boisbouvier et al.

Solution NMR Spectroscopy

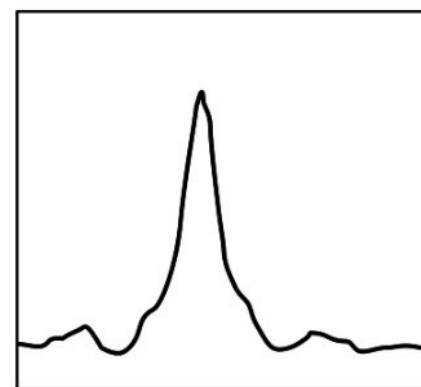
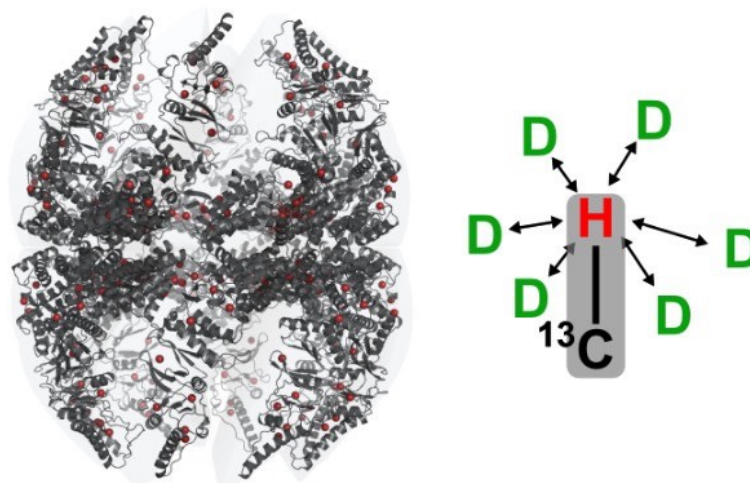
Specific protonation of methyl groups

Uniformly
[^1H , ^{13}C , ^{15}N]



1.00 1H (ppm) 0.80

Methyl groups

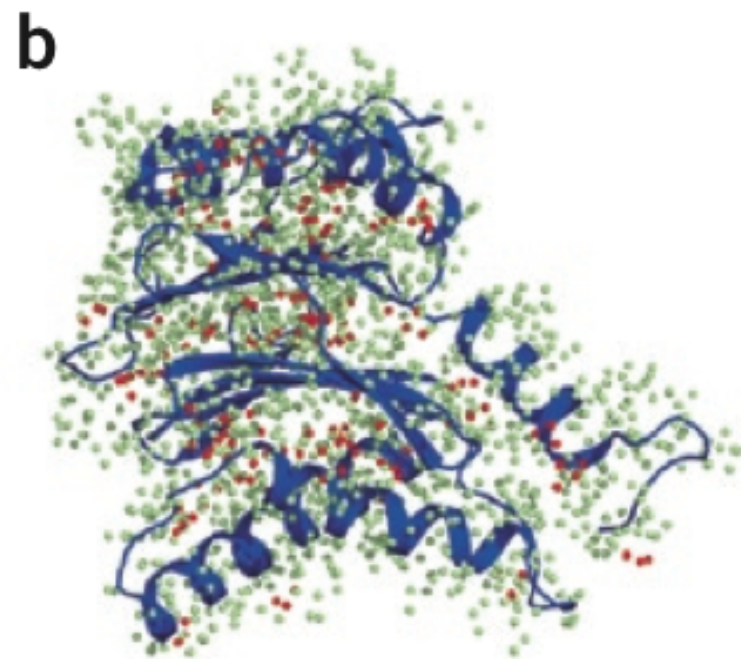
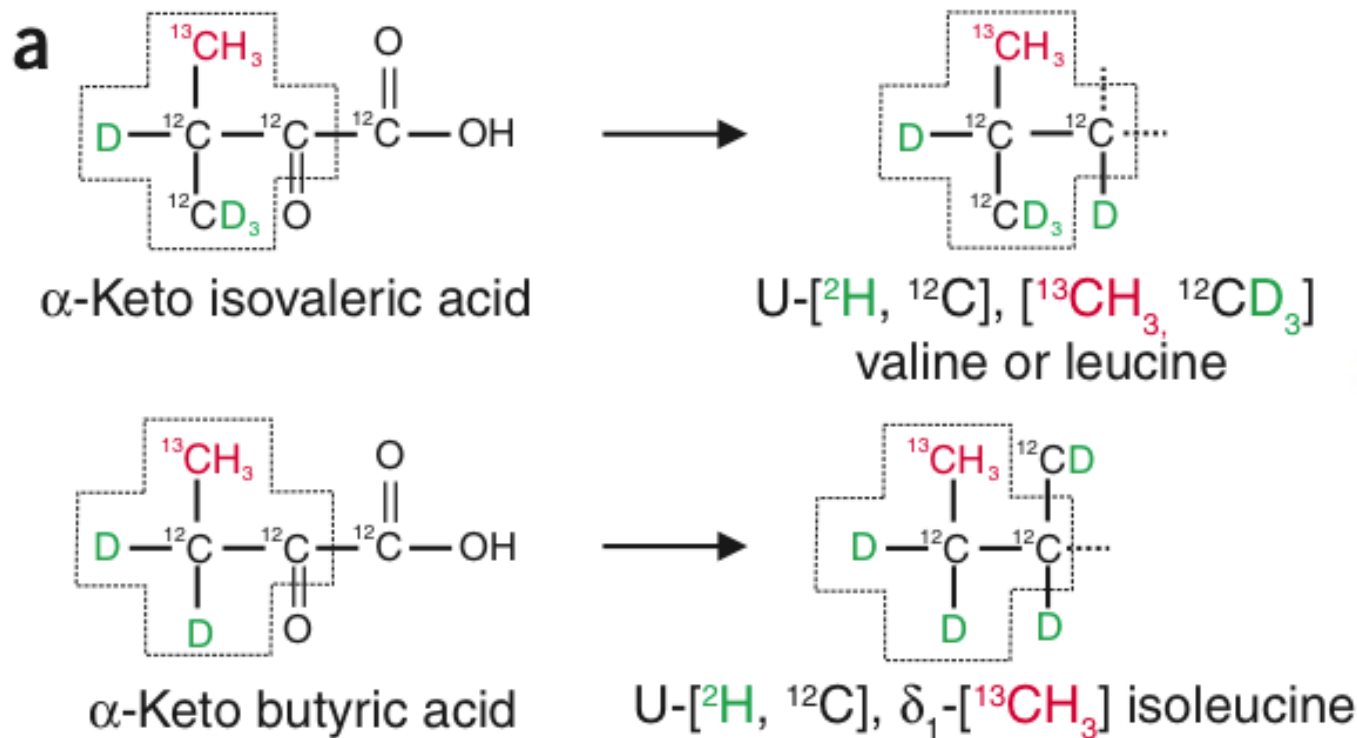


1.00 1H (ppm) 0.80

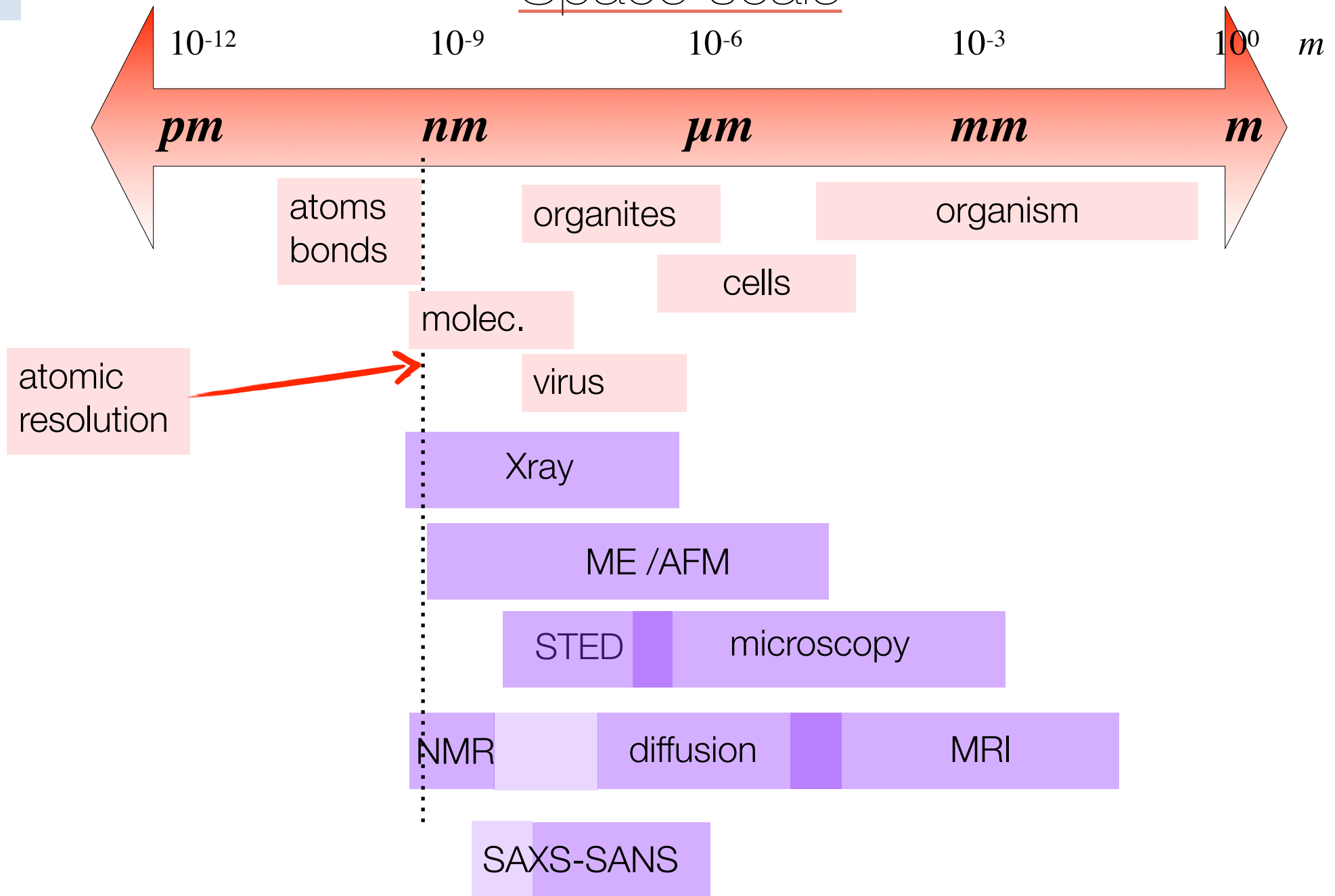
Solution NMR of supramolecular complexes: providing new insights into function

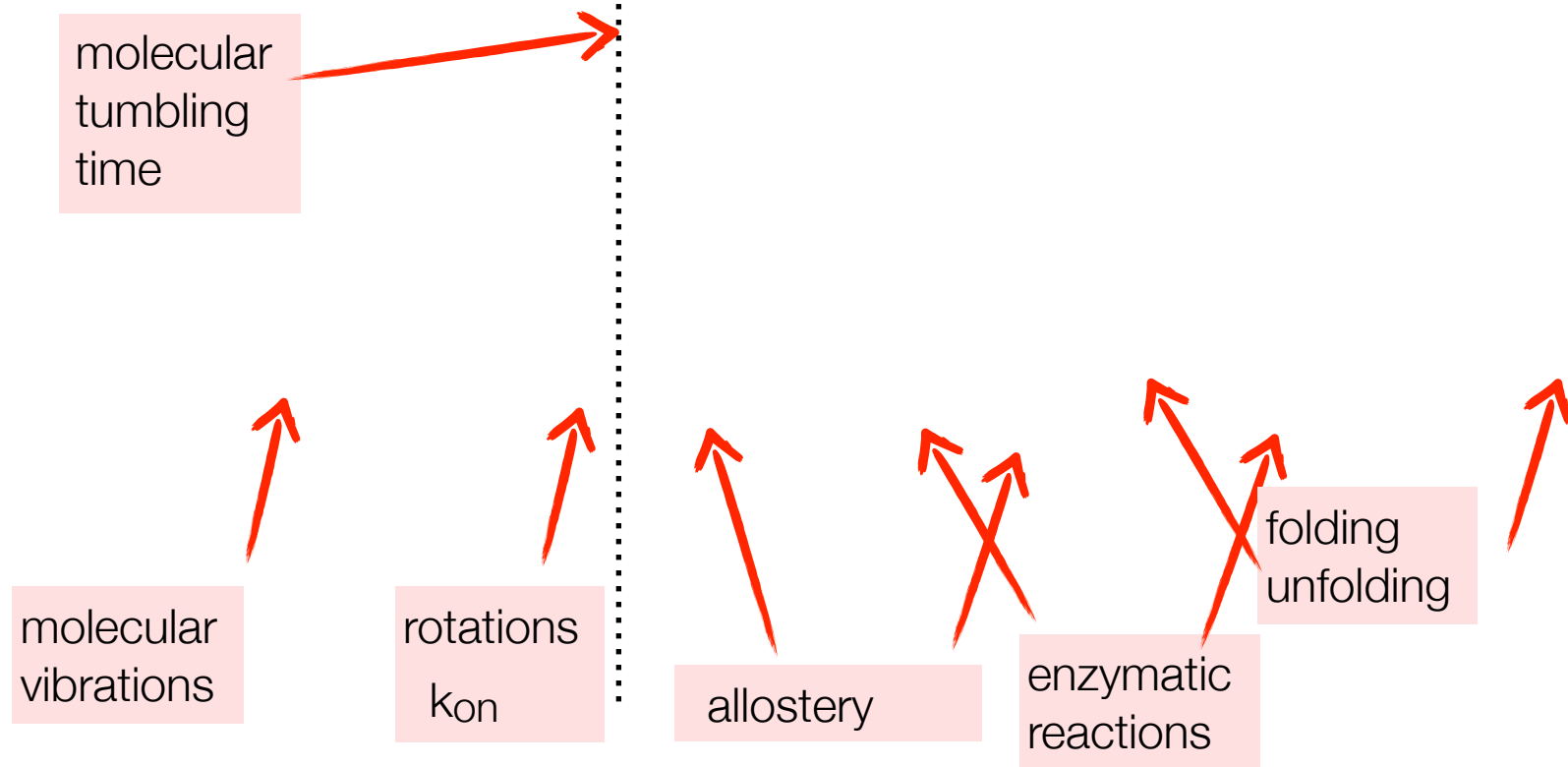
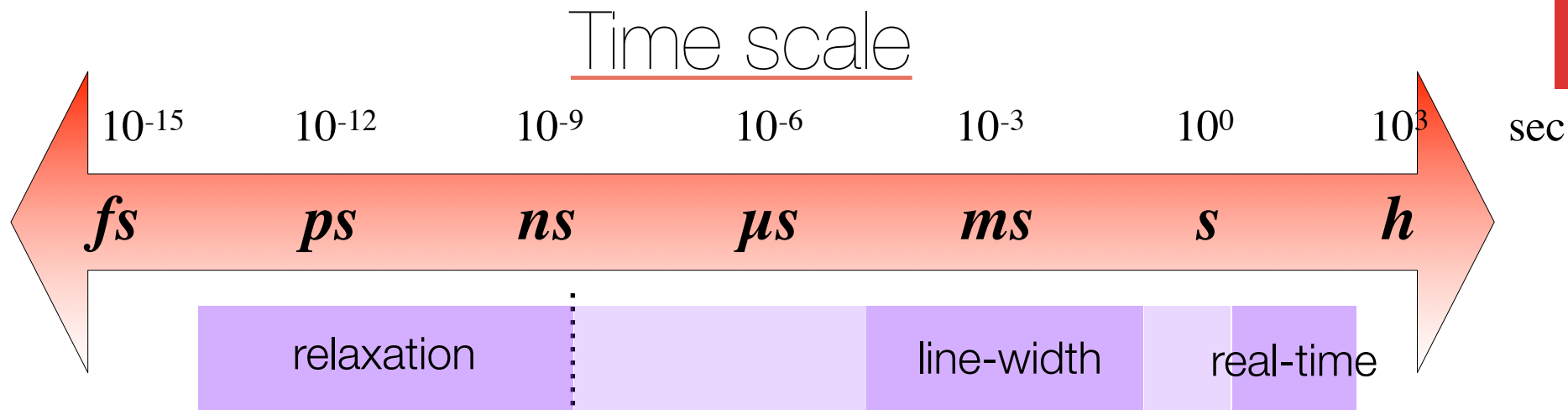
Remco Sprangers, Algirdas Velyvis & Lewis E Kay

Nature Methods 2007

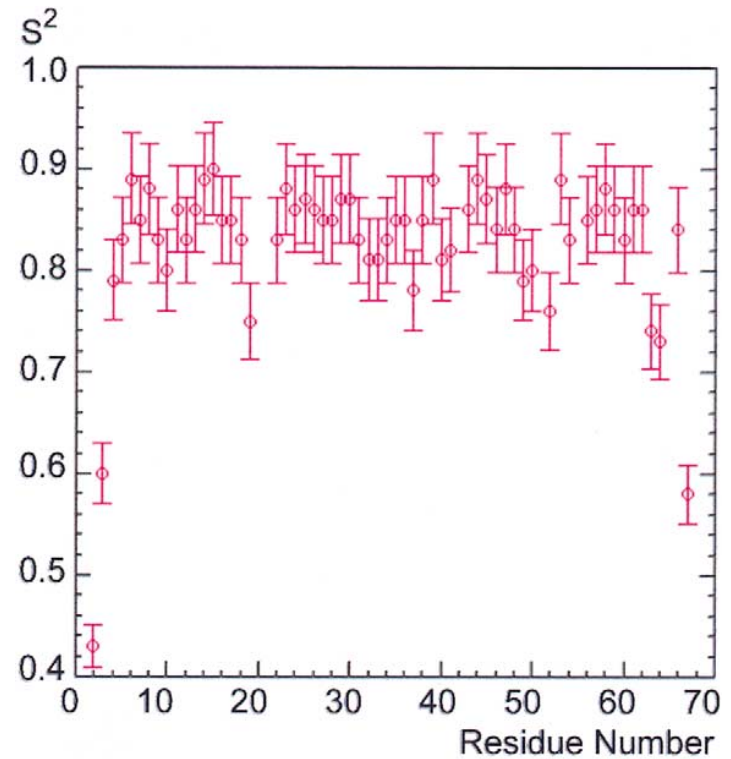
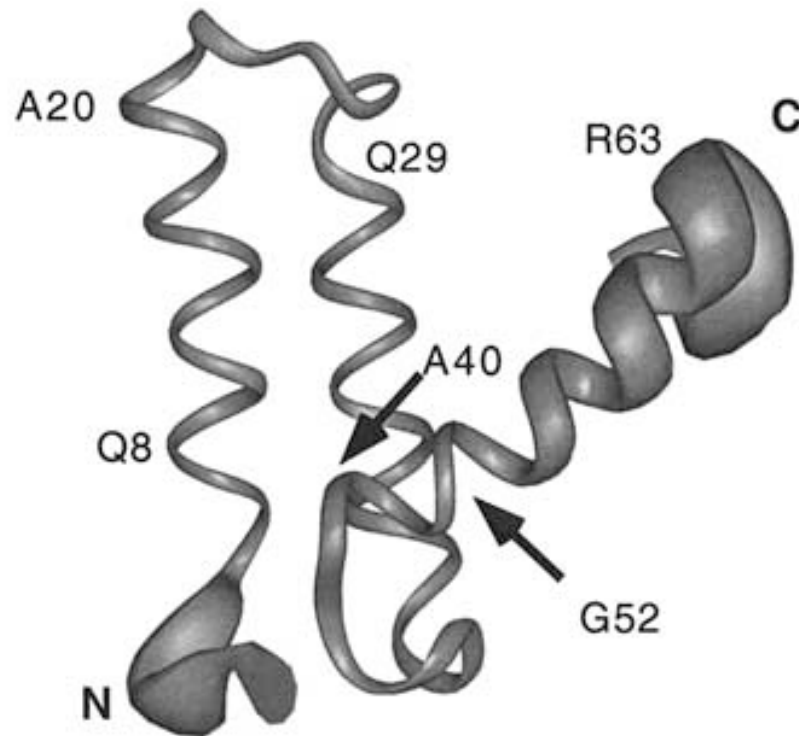


Space scale





dynamic measurements



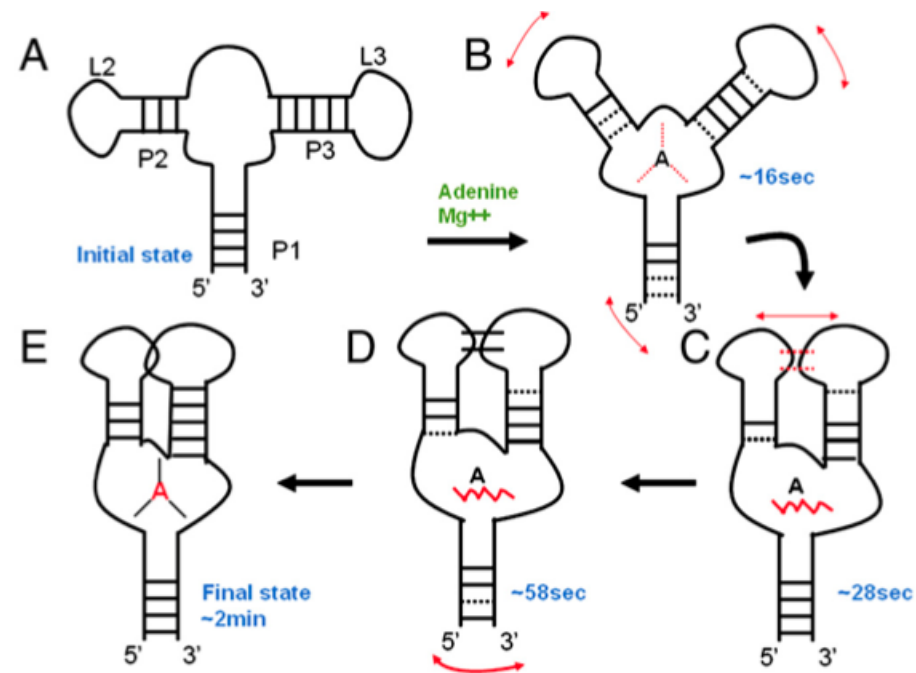
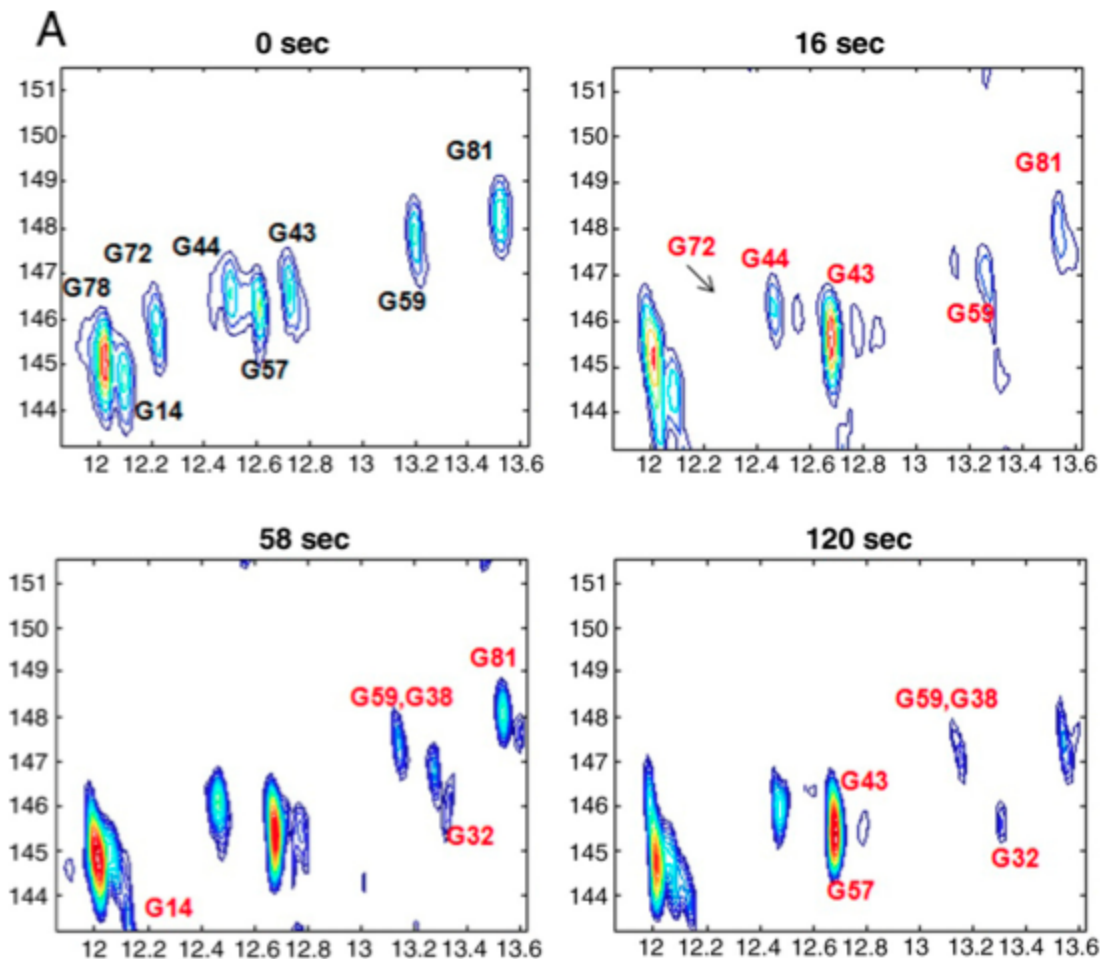
Déméné, H., Ducat, T., Barthe, P., Delsuc, M.-A., & Roumestand, C. (2002). Structure refinement of flexible proteins using dipolar couplings: application to the protein p8MTCP1. *Journal of Biomolecular NMR*, 22(1), 47–56.

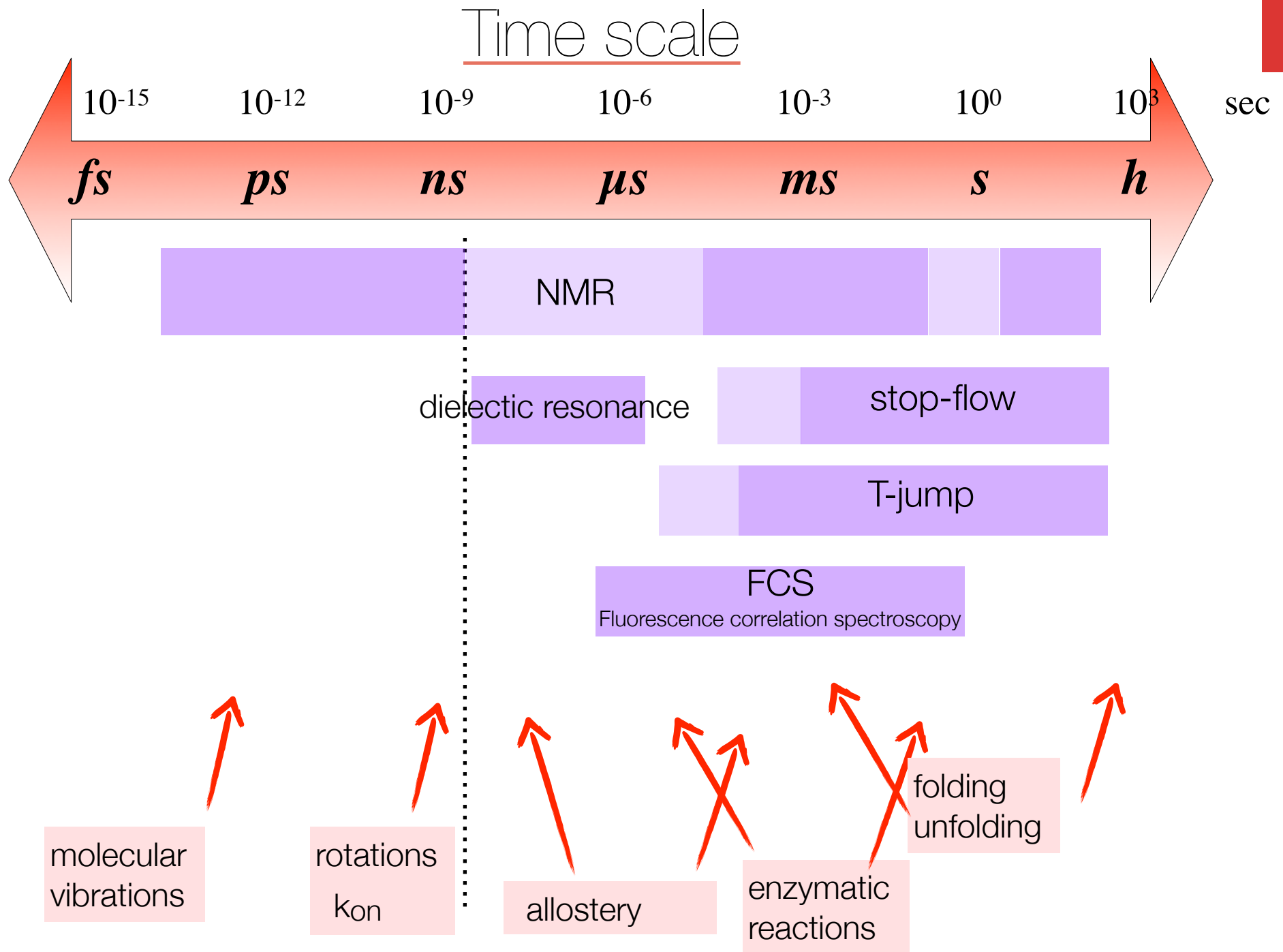
Application: Real-time follow-up of a folding

Real-time multidimensional NMR follows RNA folding with second resolution

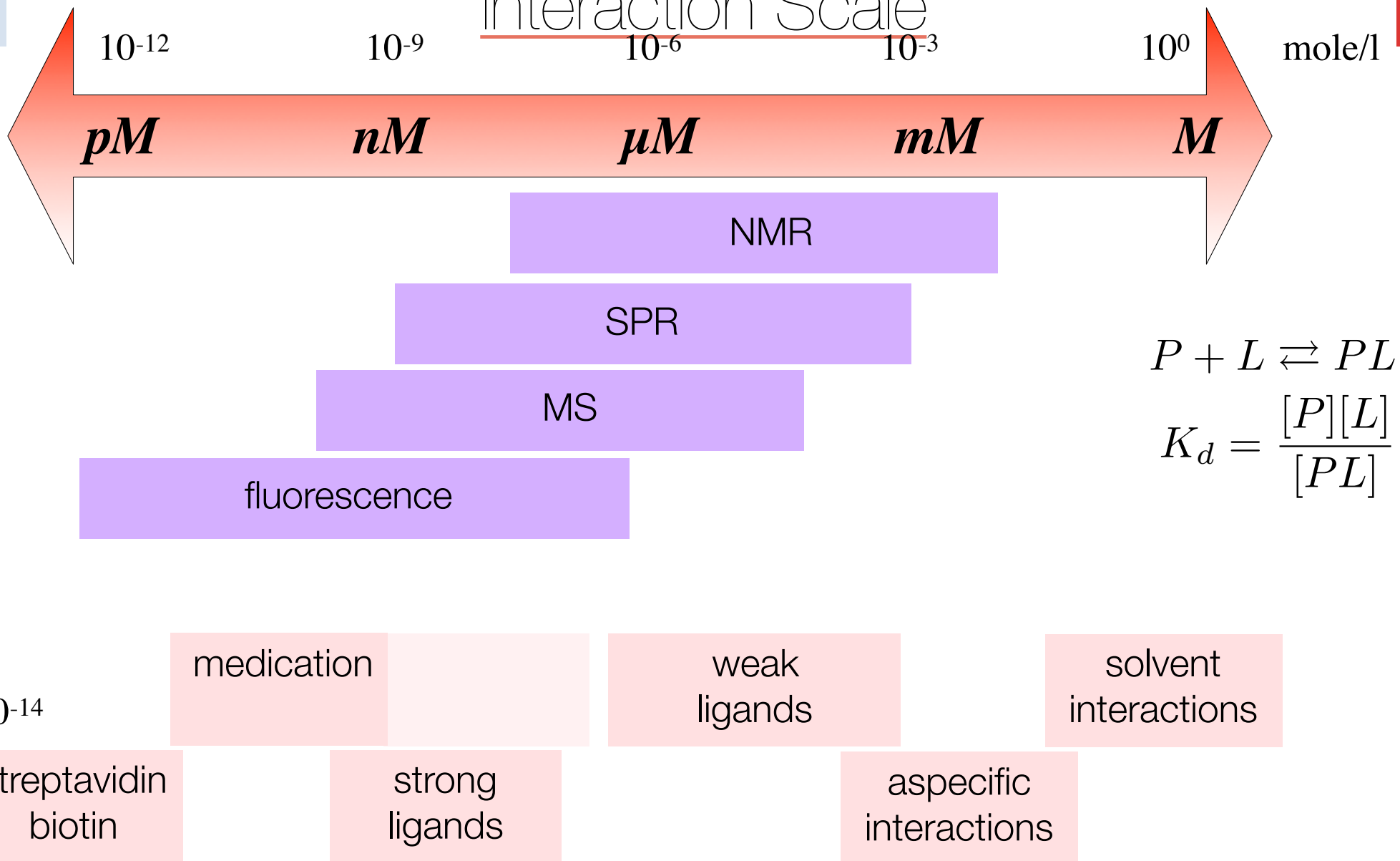
Mi-Kyung Lee^{a,1}, Maayan Gal^{b,1}, Lucio Frydman^{b,2}, and Gabriele Varani^{a,c,2}

PNAS 2010





Interaction Scale

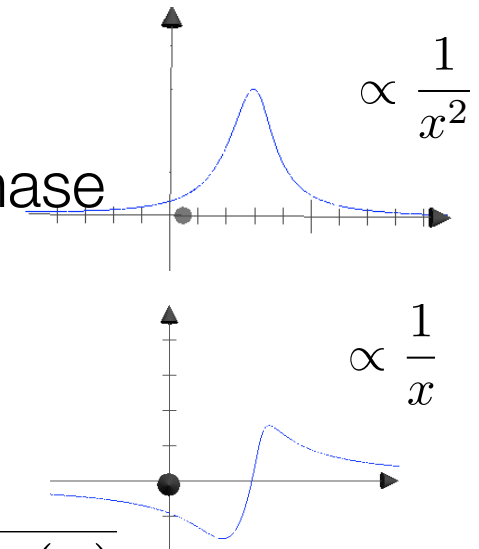
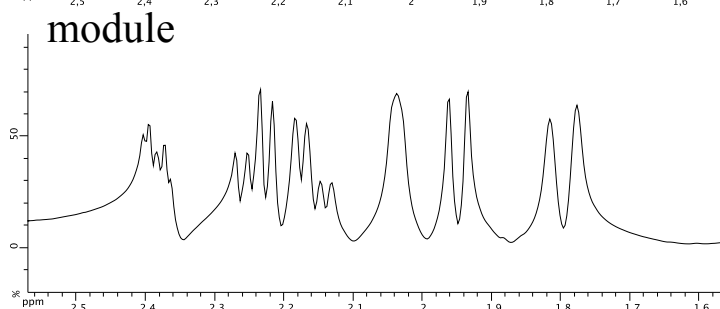
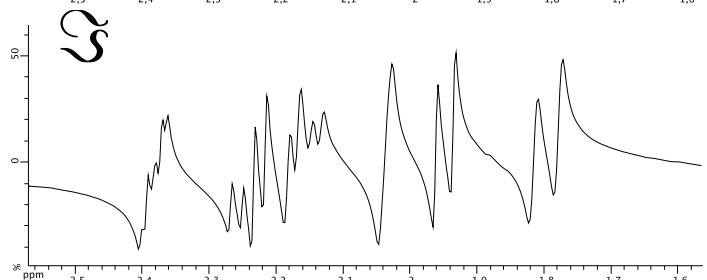
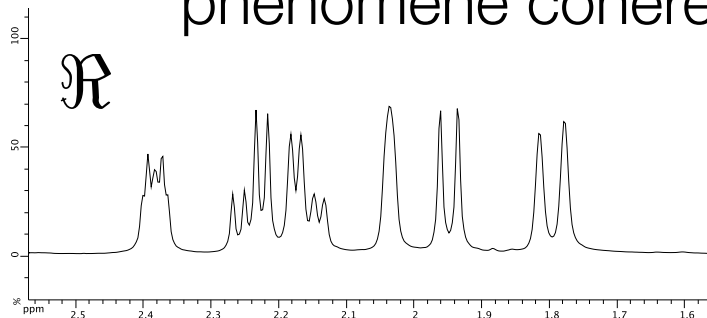


aspect signal

- Transformée de Fourier
- spectre complexe

$$F(\nu) = \int_{-\infty}^{\infty} f(t) e^{-2i\pi\nu t} dt$$

- calcul en module
phénomène cohérent = calcul sensible à la phase

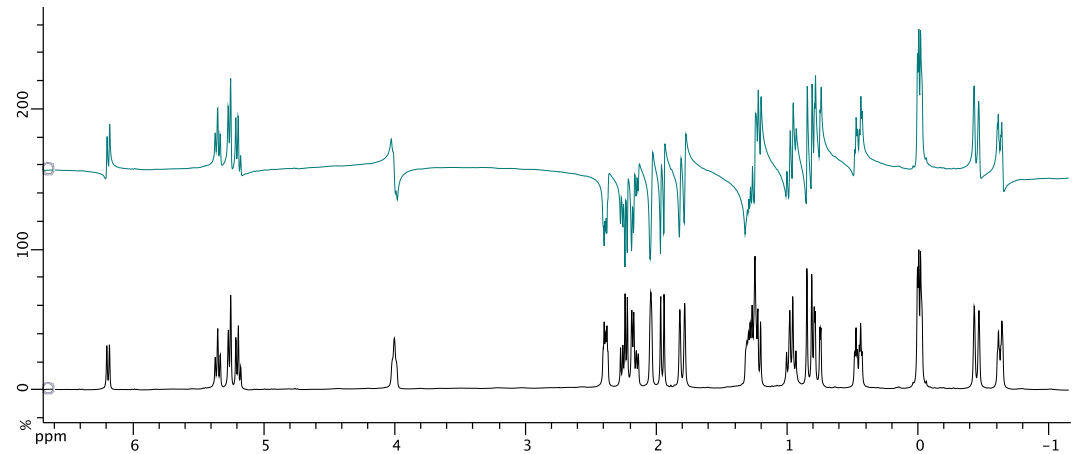
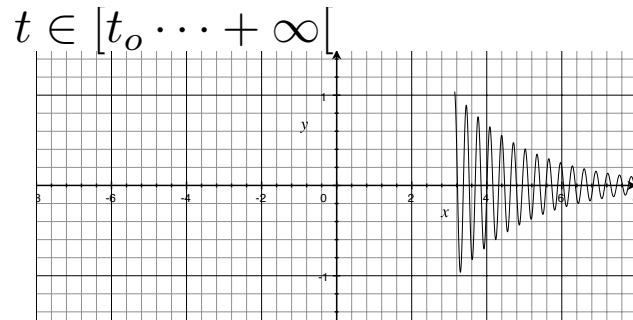


$$\|S(\nu)\| = \sqrt{S(\nu)S^*(\nu)}$$

- calcul de la densité spectrale de puissance
- adapté aux signaux stationnaires
- mal adaptés aux FID

quelques remarques (2)

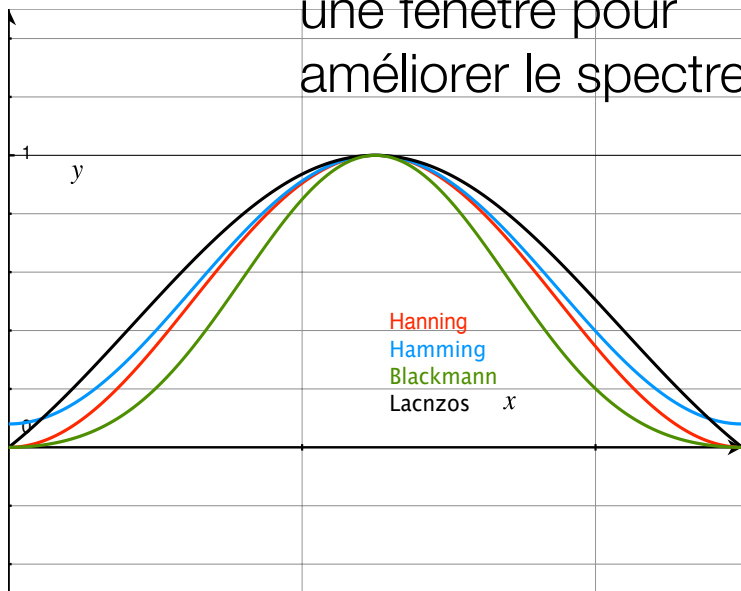
- Erreur sur t_0
 - \Rightarrow convolution du spectre par $e^{i\nu t_0}$
 - rotation de la phase proportionnel à la fréquence
 - correction de phase



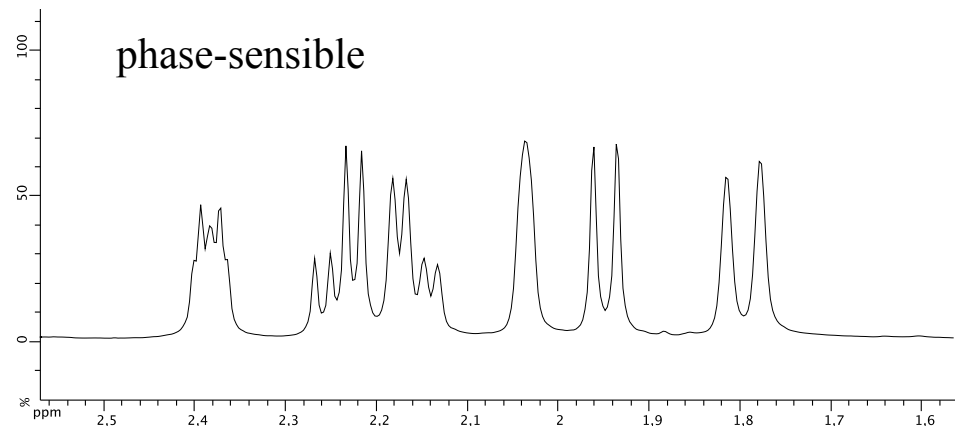
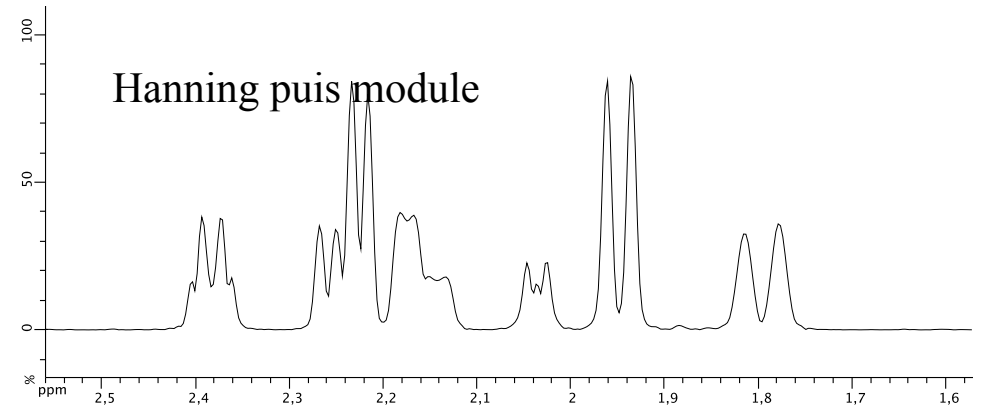
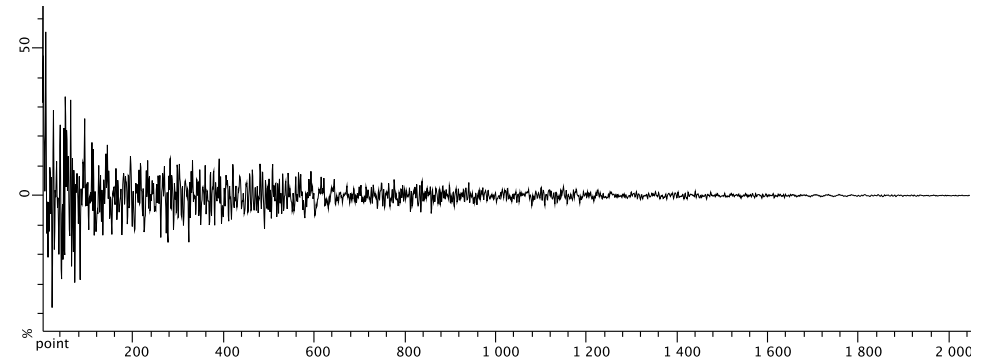
Mise en œuvre (2)

- Apodisation

- multiplier les données par une fenêtre pour améliorer le spectre

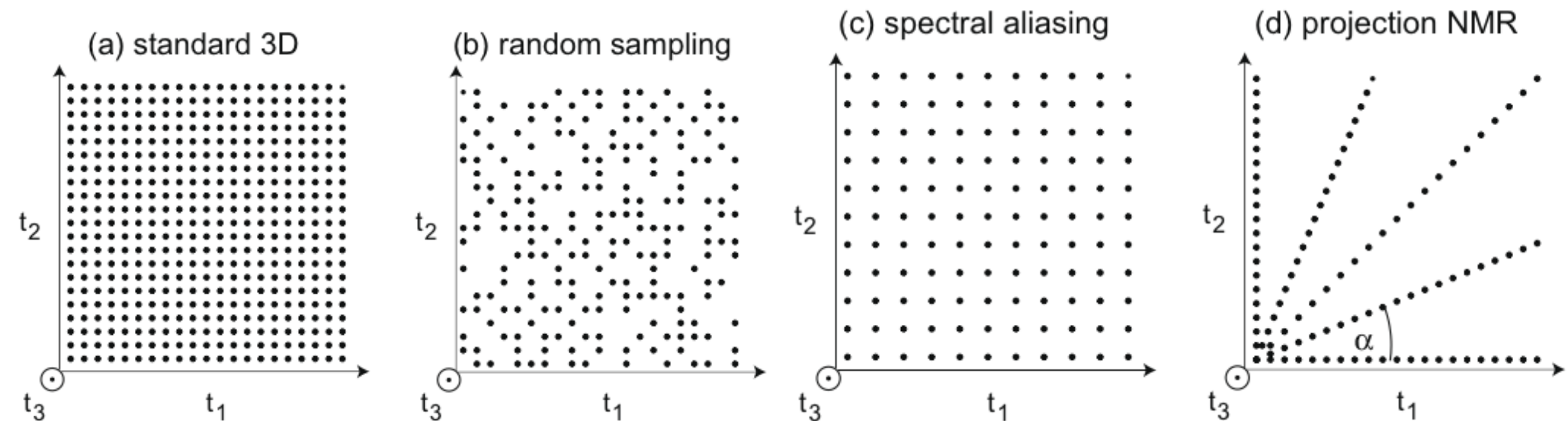


- artefacts
- forte de perte de signal dans certains cas
- modification du signal mesuré !



Working on sampling methods

- FFT : Fast Fourier Transform $n \log n$ vs n^2
- The use of FFT imposes a linear sampling
- Non Uniform Sampling (NUS) are currently being developed allowing considerable gain of time



2005-2018

- Study of Intrinsically Disordered Proteins (IDP)
- Study of Molecular Recognition fundamental mechanisms
- Description of Protein and Nucleic Acid excited states
- Visualizing Large complexe's motions
- Monitoring protein's states within the cell

Characterization and molecular basis of the oligomeric structure of HIV-1 Nef protein

STEFAN AROLD,^{1,3} FRANÇOIS HOH,¹ STEPHANIE DOMERGUE,¹ CATHERINE BIRCK,²
MARC-ANDRÉ DELSUC,¹ MAGALI JULLIEN,¹ AND CHRISTIAN DUMAS¹

¹Centre de Biochimie Structurale, UMR C5048 CNRS, U414 INSERM, Université Montpellier I,
Avenue C. Flahault, 34060 Montpellier, France

²Groupe de Cristallographie Biologique, IPBS-CNRS, 31077 Toulouse, France

(RECEIVED November 3, 1999; FINAL REVISION March 6, 2000; ACCEPTED April 21, 2000)

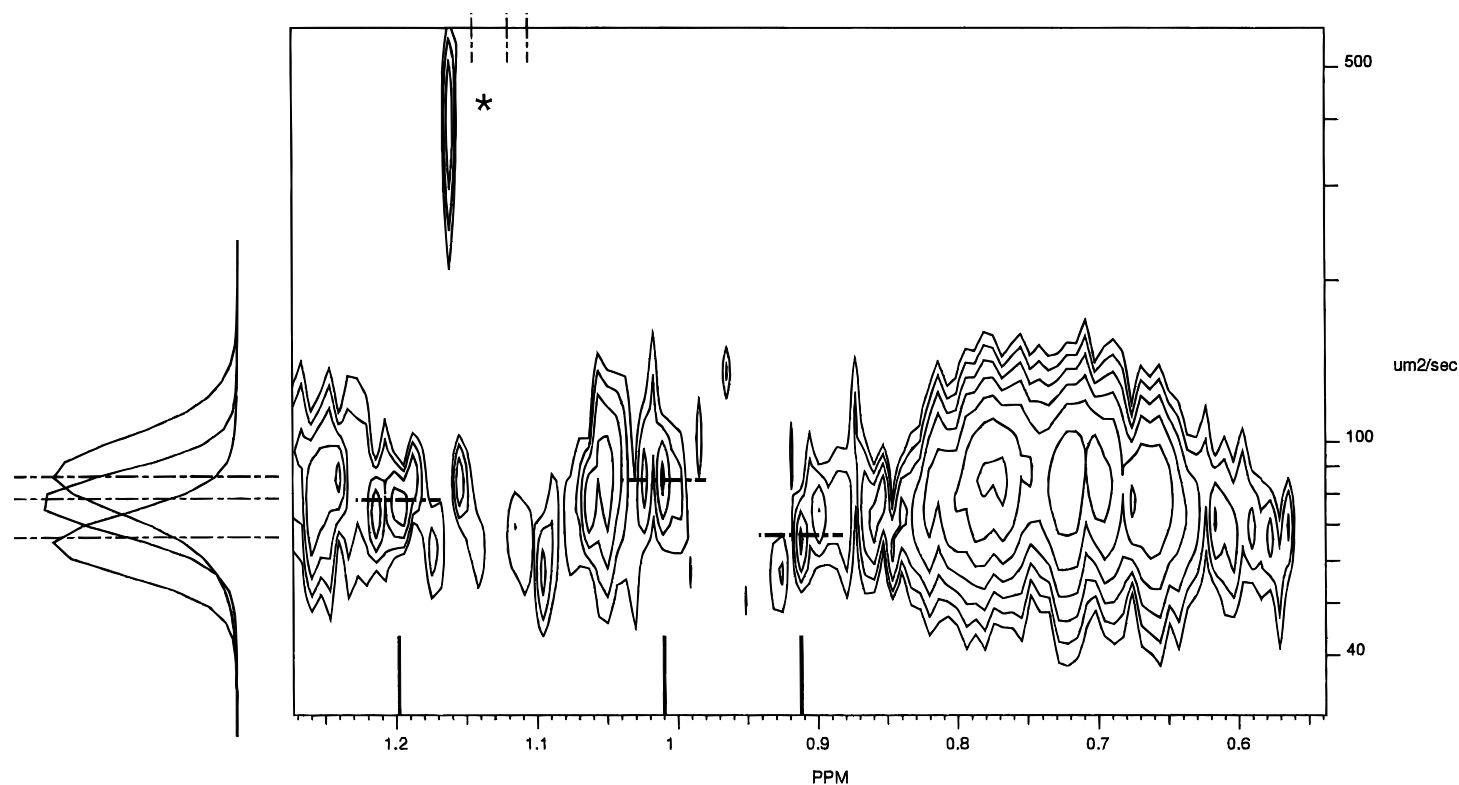


Fig. 4. Analysis of the oligomeric state based on NMR DOSY data: the methyl region of the DOSY spectrum of Nef _{Δ 1–56, Δ 206} at 140 μM is shown. Three columns have been extracted at 0.91, 1.01, and 1.20 ppm and are reported to the left. The corresponding diffusion coefficients, materialized by hatched axes, are 66, 84, and 77 mm^2/s , respectively. The star indicates an impurity, with a much faster diffusion coefficient.